How star cluster evolution shapes protoplanetary disc sizes

I n a u g u r a l - D i s s e r t a t i o n

zur
Erlangung des Doktorgrades
der Mathematisch-Naturwissenschaftlichen Fakultät
der Universität zu Köln

vorgelegt von
Kirsten Vincke
aus Arnsberg

Köln
2019

Berichterstatter/in: Prof. Dr. Susanne Pfalzner .....

Prof. Dr. Peter Schilke .....

Tag der mündlichen Prüfung: 23.07.2018

Zusammenfassung

Die meisten Sterne entstehen nicht in Isolation, sondern als Teil von Gruppen, die zwischen einigen zehn bis mehreren hunderttausend Mitglieder enthalten können. Die Sterne entstehen durch den Kollaps einer kalten Riesenmolekülwolke, wobei ein Anteil des Gases in der Molekülwolke in Sterne umgewandelt wird, während der Rest spätestens einige Millionen Jahre nach Beginn der Sternentstehung aus der Sterngruppe ausgestoßen wird. Wurde weniger als 30% der Molekülwolkenmasse in Sterne umgewandelt, so wird hierbei ein Teil der Sterngruppe ungebunden. Entstehen allerdings Sterne aus mehr als 60% der Masse, bleibt die Sterngruppe größtenteils gebunden. Im ersten Fall spricht man von kurzlebigen *Assoziationen*, in letzterem von langlebigen *Sternhaufen*, die sich zu *Offenen Sternhaufen* mit Lebensdauern von vielen Milliarden Jahren entwickeln können. Die beiden Typen von Sterngruppen unterscheiden sich sehr in ihren Eigenschaften und ihrer Entwicklung im Bezug auf Dichte und Größe.

Jeder Stern, unabhängig von der Art seiner Sterngruppe, ist von einer *protoplanetaren Scheibe* umgeben, aus der sich potentiell Planeten bilden können. Bis heute wurden mehr als 3 700 Planeten entdeckt, die andere Sterne umkreisen. Viele dieser Planetensysteme unterscheiden sich allerdings stark von unserem Sonnensystem. In dieser Arbeit wird untersucht, inwieweit die Art der Sterngruppe, in der ein Stern entstanden ist, Einfluss auf die Größe eines sich formenden Planetensystems haben kann. Zwei Prozesse, welche maßgeblich die Größe der protoplanetaren Scheibe verkleinern oder sie gar komplett zerstören, sind (1) die externe *Photoevaporation* durch Winde der massiven Sterne und (2) gravitative Wechselwirkungen zwischen den Sterngruppenmitgliedern (*Vorbeiflüge*). Die Wirksamkeit dieser Prozesse hängt direkt vom Abstand der beiden involvierten Sterne und damit von der Dichte der Sterngruppe ab. Mit Hilfe von Computersimulationen wird der Einfluss der gravitativen Wechselwirkungen auf die Größe von protoplanetaren Scheiben in verschiedenen Assoziationen und Sternhaufen untersucht.

Die Ergebnisse zeigen, dass in Assoziationen die gravitativen Wechselwirkungen nur in den ersten 3 Millionen Jahren der Sterngruppenentwicklung eine Rolle spielen; danach ist die stellare Dichte zu gering. Typischerweise werden nur wenige Scheiben auf Größen unter 100 Astronomische Einheiten (AE) reduziert. Im Gegensatz dazu werden die Scheiben in langlebigen Sternhaufen im Mittel auf 20 AE reduziert und ein beträchtlicher Anteil

ist wesentlich kleiner. Daraus folgt, dass Scheiben aus verschiedenen Systemen eine sehr unterschiedliche Größe und Struktur haben – und somit auch die entstehenden Planetensysteme.

Es gibt viele Hinweise darauf, dass auch unser Sonnensystem als Teil einer Sterngruppe entstanden ist, welche sich entweder aufgelöst hat oder aus welcher die Sonne herausgeschleudert wurde. In unserem Sonnensystem fällt die Massendichte jenseits 30 AE dramatisch ab, was potentiell durch den Vorbeiflug eines Mitgliedes des Ursprungssternhaufens herbeigeführt worden sein kann. Die Simulationen zeigen, dass unser Sonnensystem vermutlich Teil einer sehr massiven Assoziation, wie zum Beispiel NGC 6611, gewesen ist, oder sogar in einem Sternhaufen wie dem Arches-Sternhaufen entstanden ist.

Abstract

The majority of stars form from cold, collapsing *Giant Molecular Clouds (GMCs)*, which not only yield single stars, but groups of a few up to many hundreds of thousands of stars. The gas and dust which was not transformed into stars is expelled at the end of the star formation process. Stellar groups react very differently to this mass removal, depending on their virial state and on the fraction of gas which is transformed into stars, called *star-formation efficiency (SFE)*. In one type of group, called *associations*, the SFE is rather low (≤ 0.3) and the gas removal leaves the stellar members (largely) unbound. On the other hand, if the SFE is higher, observations and theory find that the stellar accumulations largely remain bound and can survive many billions of years in this state, which makes them *stellar clusters*. These two types of stellar groups evolve on very distinct tracks concerning their density, size, and mass.

It is probable that most – if not all – stars are initially surrounded by a protoplanetary disc, the formation site of planets. In the last decades – and especially since the launch of *Kepler* in 2009 – observations were able to find more than 3 700 planets orbiting other stars. Many of these *extrasolar planets (exoplanets)* are part of planetary systems, which differ significantly from our own solar system. External processes in the stellar birth environments like gravitational interactions between the cluster members (*fly-bys*) and *external photoevaporation* are possible reasons for these differences. The strength of such processes is directly connected to the dynamical and density evolution of the environments.

Simulations of different associations and clusters were performed and the influence of fly-bys on protoplanetary discs was investigated. In associations, the most fly-bys happen in the phase, where they are still embedded in their natal gas. After gas expulsion, most members of the associations become unbound and thus the effect of stellar fly-bys becomes less important. In systems comparable to the *Orion Nebular Cluster (ONC)*, the discs in the simulations are cut down to a few hundreds of AU, which fits observational findings very well. By contrast, stellar clusters, like for example the *Arches*, retain their high stellar density even after gas expulsion. In such dense clusters, fly-bys play an important role in shaping disc properties at later evolutionary stages as well, cutting down discs to much smaller sizes of ≈ 20 AU.

For a long time, such very dense systems were considered to be too hostile to yield, for

example, a planetary system like our own solar system. However, under the assumption that the steep drop in mass density at 30 AU in our solar system was caused by a fly-by, the results presented in this thesis show that the solar system was most probably part of a very massive association, like for example NGC 6611, or a stellar cluster, like Arches.

Contents

1 Introduction

A remarkable feature of our solar system is that all planets orbit in a plane on nearly circular orbits around the Sun. Based on this observation, theories of how the solar system formed have been developed for hundreds of years. The so-called *nebula hypothesis* was already proposed in 1734 by Swedenborg (1734) and later expanded by Kant (1755). At almost the same time as Kant, Pierre-Simon Laplace postulated a similar theory (see for example See, 1909). It stated that the Sun and the planets all formed from the same nebula. This theory is still the basis of solar system – and in general planet – formation.

Soon afterwards, it was speculated that not only the Sun but also other stars are surrounded by planetary systems. This was confirmed in 1995, when the first planet outside our solar system – extrasolar planet or *exoplanet* – was found around a main-sequence star (Mayor & Queloz, 1995).

Planetary systems are formed from the material present in the protoplanetary disc surrounding a star after its formation. Therefore, the properties of the planets is strongly influenced by the properties of the disc.

On the one hand, the discs are shaped by their host's magnetic fields and stellar winds. On the other hand, most stars are born not in isolation but as part of a stellar group (Lada & Lada, 2003). This environment can influence the discs through external photoevaporation by the most massive stars (Johnstone et al., 1998; Störzer & Hollenbach, 1999; Scally & Clarke, 2001; Clarke et al., 2001; Matsuyama et al., 2003; Johnstone et al., 2004; Alexander et al., 2005; Adams et al., 2006; Alexander et al., 2006; Ercolano et al., 2008; Drake et al., 2009; Gorti & Hollenbach, 2009; Winter et al., 2018b), and through gravitational interactions between its members (see e.g. Clarke & Pringle, 1993; Hall, 1997; Scally & Clarke, 2001; Olczak et al., 2006; Pfalzner et al., 2006; Pfalzner & Olczak, 2007; Olczak et al., 2010; de Juan Ovelar et al., 2012; Breslau et al., 2014; Rosotti et al., 2014; Steinhausen & Pfalzner, 2014; Vincke et al., 2015; Portegies Zwart, 2016; Vincke & Pfalzner, 2016; Breslau et al., 2017; Winter et al., 2018a,b). Therefore, the environment can alter the protoplanetary disc significantly and strongly influence the shape of a planetary system.

Stellar groups themselves are dynamical entities, which evolve drastically over the first several million years and can live up to many hundreds of millions of years. Their development and properties can influence the formation and shape of protoplanetary discs, which

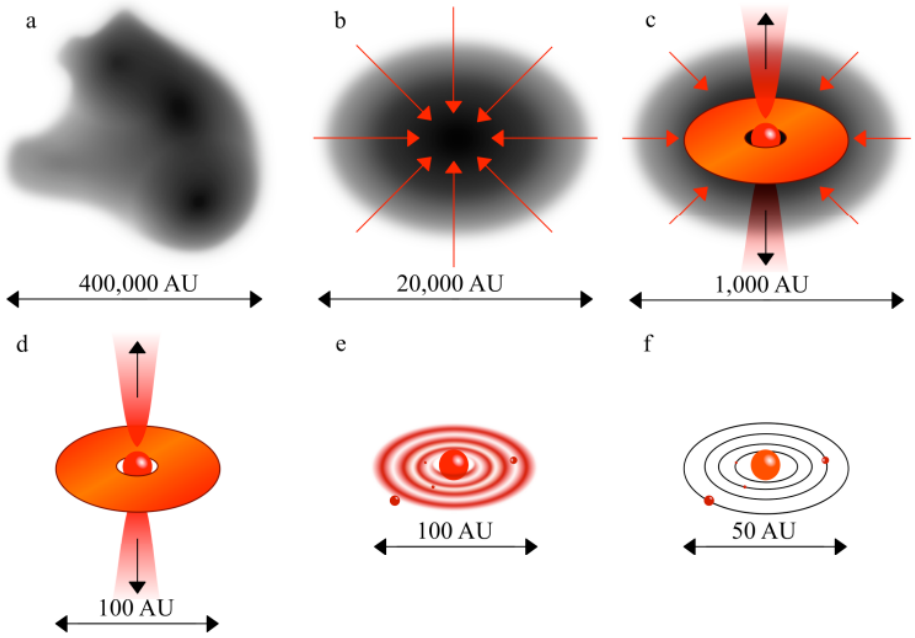

FIGURE 1.1: Schematic depiction of star formation: from GMCs to stars with planetary systems. Taken from Braiding (2011).

has an impact on the structure of eventually forming planetary systems.

1.1 Associations and stellar clusters

Observations found that the majority of stars ($70-90\%$) form in stellar groups with >100 stars (Lada & Lada, 2003). However, most of these groups in the solar neighbourhood seem to dissolve with time, as their birthrate is much larger than the observed number of groups would suggest. On the other hand, open clusters like for example Praesepe (Beehive Cluster, M44) or Hyades are 790 ± 60 Myr and 750 ± 100 Myr old, respectively, (Brandt & Huang, 2015b,a) and still bound.

A distinction between the precursors of solar neighbourhood clusters and of clusters like Praesepe and Hyades can be made when looking at their formation and dynamical evolution.

1.1.1 Star formation in associations and clusters

Stellar clusters form from *Giant Molecular Clouds (GMCs)* consisting of gas and dust with masses of $10^2 - 10^6$ $M_\odot$, temperatures of $10-20$ K, and sizes of $10-100$ pc (Fig. 1.1a).

Typically, the density in GMCs is low, between 20 $M_\odot$ pc^{-2} and of the order of 100 $M_\odot$ pc^{-2} (Elmegreen, 1985, 1993; Larson, 2003), so gravitational instabilities are necessary to trig-

ger star formation (Fig. 1.1b). The GMCs may also have filamentary or clumpy structures (Williams et al., 2000), which – if they are massive and large enough – may form stellar groups. The minimum mass needed to get gravitational instabilities, and thus trigger star formation, is the *Jeans mass* M_J:

$$M_J = \left(\frac{\pi}{6}\right) \frac{c_s^3}{G^{2/3}\rho^{1/2}}, \tag{1.1}$$

where c_s is the isothermal sound speed, G the gravitational constant, and ρ the density (see also Binney & Tremaine, 1987).

The collapsing gas forms *protostars*, which are surrounded by a dust envelope from which they accrete material (Dunham et al., 2014). Their temperature is too low to trigger hydrogen burning and radiation emitted from such stars usually stems from the accreted envelope, not from the core directly (1.1c). At first, the energy produced through the gravitational collapse can directly be transported away from the protostar's surface by infra-red radiation. As more material is accreted, the system becomes opaque and the radiation cannot penetrate the dust envelope. Therefore, the core temperature increases further and the resulting pressure counteracts the gravitational in-fall of material (Larson, 1969). Eventually, the protostar blows away the remaining envelope, becoming optically visible and developing into a *pre-main-sequence star* (*PMS star*, Fig. 1.1d). The core further contracts until the *hydrogen burning* sets in once a temperature of 10^7 K is reached. A balance between gravitational collapse and pressure from nucleosynthesis stabilises the core, yielding a *main-sequence star (MS star)*. The mass distribution of the newly formed stars within a stellar group is usually described by a so-called *initial mass function (IMF)*, (cf. for example IMFs by Salpeter, 1955; Kroupa, 2002). For an overview of star formation and the involved processes, see for example Larson (2003); McKee & Ostriker (2007); Dunham et al. (2014) and Scilla (2016).

During protostar formation, a circumstellar disc forms around them due to angular momentum conservation (Fig. 1.1c, see e.g. Cassen & Moosman (1981)). When the protostar turns into a PMS star, the disc can already show signs of structures, like spiral arms (Fig. 1.1e). If the protoplanetary disc is massive enough, a planetary system might form around the star (Fig. 1.1f).

During this process, even though up to several tens of thousands of stars can form together in a stellar cluster, only a portion of the gas of the GMC is transformed into stars. This portion is quantified by the *star-formation efficiency* (SFE):

$$SFE = \frac{M_{stars}}{M_{stars} + M_{gas}}, \tag{1.2}$$

where M_{stars} is the total stellar mass of the cluster and M_{gas} the mass of the left-over gas at the end of the star formation process.

With time, gas which is not already transformed into stars is driven outwards by a number of processes, for example, bipolar stellar outflows (Matzner & McKee, 2000), stellar winds of the most massive stars, or super-nova explosions (Zwicky, 1953; Pelupessy & Portegies Zwart, 2012).

The duration of this gas expulsion and the SFE mainly determine whether a group of stars disperses or remains bound (see e.g. Lada et al., 1984; Adams, 2000). Short-lived groups are referred to as *associations*, whereas long-lived stellar systems are called *stellar clusters*. It is important to note that there is no consistent nomenclature within the community, for example the term cluster might be used for all stellar aggregates, whose density is much higher than that of the stellar field, even if they are not necessarily bound in the long term (e.g. Fall & Chandar, 2012; Craig & Krumholz, 2013). In this thesis, as well as in the publications attached, the nomenclature *associations* for short-lived and *clusters* for long-lived stellar groups will be used.

Figure 1.2 shows the observed density and radius of a number of young and massive ($> 10^3$ $M_\odot$) associations (bottom) and clusters (top). The association/cluster ages are colour coded: very young systems are shown in red, systems between $4 - 10$ Myr in green, and older systems (> 10 Myr) in blue. It is evident, that the sizes and masses of clusters and associations evolve along two separate, well defined time tracks (Pfalzner & Kaczmarek, 2013b). [1]

The distinction of two types of stellar groups is not only visible in the Milky Way, also extragalactic clusters in the local group show this bimodal development (Da Costa et al., 2009).

It is important to note that there are studies claiming that the "gap" in the half-mass radius mass plane between open clusters in the Milky Way and old globular clusters is filled by young, massive clusters like the Orion Nebula Cluster (ONC) (Portegies Zwart et al., 2010). However, it is questionable if systems like, for example, the ONC are massive enough to evolve into old, open or globular clusters. Currently it is unknown why stellar groups appear as either associations or clusters. Studies of globular clusters in the outer halo of the Galaxy indicate that the cluster formation process yields a bimodal distribution (Elmegreen, 2008; Baumgardt et al., 2010).

The two cluster types represent very distinct (birth) environments of protoplanetary discs and planetary systems, therefore, their properties and evolution are discussed in more detail in the following section.

[1] Note that Pfalzner (2009) uses the term *leaky cluster* for associations and *starburst cluster* for clusters.

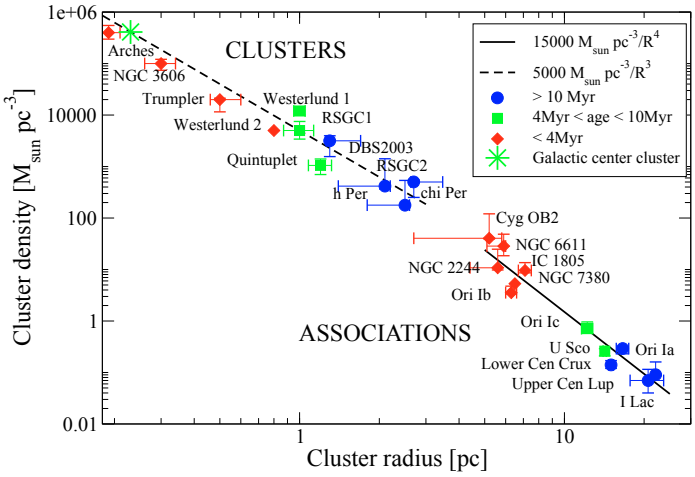

FIGURE 1.2: Observed densities and radii for clusters (top) and associations (bottom). The age of the systems is shown by colour: very young (< 4 Myr) in red, $4 - 10$ Myr in green, and old (> 10 Myr) blue. Taken from Pfalzner (2009). The labels for cluster types were changed according to nomenclature used in this work.

1.1.2 Associations

Observations found that, in the solar neighbourhood, most associations disperse rather quickly (< 10 Myr) and their members become part of the *field star population* (Lada & Lada, 2003; Porras et al., 2003). Lamers & Gieles (2008) compared the star-formation rate in the solar neighbourhood and the surface density of open clusters – including effects like stellar evolution, tidal stripping, perturbations by spiral arms, and encounters with other GMCs – and estimated an *infant mortality*, that is the dispersion of very young systems, of $50 - 95\%$.

This high infant mortality cannot be explained by two-body dispersion of the clusters alone. Two-body relaxation becomes important after a timespan of $t_{tbr} = 10N \ \ln(N) * t_{cross}$, where N is the number of stars, $t_{cross} = R/V$ the crossing time, R the cluster radius, and V the average velocity (Binney & Tremaine, 1987). Even for a cluster with 1 000 stars, this yields $t_{tbr} = 10 - 100$ Myr, which cannot account for the short dispersion timescale of < 10 Myr found by observations (Krumholz et al., 2014).

One theory which can explain the fast dispersal is that these associations already formed from gravitationally unbound GMCs (e.g. Clark et al., 2005). However, this kind of simulations did not include stellar feedback, such that even unbound GMCs might form bound stellar clusters (Krumholz et al., 2014).

Gas expulsion

Another explanation for the short lifetimes of associations in the solar neighbourhood is the effect of gas expulsion due to stellar feedback. Most of them have a rather low SFE of 30% at most (Lada & Lada, 2003), so when the remaining gas is expelled at the end of the star formation process, they lose 70% of their mass. As a result, they expand quickly and most – if not all – stars become unbound (Baumgardt & Kroupa, 2007).

Gas expulsion and its effect on associations and stellar clusters has been studied thoroughly in the past, focussing on the conditions under which a bound remnant survives the gas expulsion (Tutukov, 1978; Hills, 1980; Lada et al., 1984; Goodwin, 1997a,b; Kroupa et al., 1999; Adams, 2000; Geyer & Burkert, 2001; Kroupa et al., 2001; Boily & Kroupa, 2003a,b; Fellhauer & Kroupa, 2005; Bastian & Goodwin, 2006; Baumgardt & Kroupa, 2007; Goodwin, 2009; Lüghausen et al., 2012; Pfalzner & Kaczmarek, 2013a,b).

Figure 1.3 shows the percentage of bound mass as a function of the SFE for associations ("loose massive clusters") and star clusters ("compact massive clusters"). The higher the SFE, the more mass in associations remains bound. In the more compact clusters, however, the bound mass does not exceed $\approx 82\%$ in the simulated models. They are less susceptible to gas expulsion, but they continuously lose stars due to gravitational interactions between the cluster members (Pfalzner & Kaczmarek, 2013b).

Star formation within a clump is not homogeneous. Observations found that the local surface density of *young stellar objects (YSOs)* depends on the local column density of the gas within the cloud (Gutermuth et al., 2011). This local dependence can be described by the *star formation efficiency per free-fall time* ϵ_{ff} (Krumholz & McKee, 2005; Parmentier & Pfalzner, 2013). Even systems with a low overall SFE of 10% can thus form systems which leave a bound remnant after gas expulsion, because the SFE in the system centre is higher. In summary, recent studies found that an SFE between 10% and 35% is needed to form a bound association.

However, the bound fraction is not only a function of the SFE, but also of the timescale on which the gas is expelled. The *gas-expulsion timescale* is considered to be of the order of, or smaller than, the *dynamical timescale* of the association/cluster, which describes the time a typical star needs to cross the system:

$$t_{dyn} = \left(\frac{G M_{cl}}{r_{hm}^3} \right)^{-1/2}, \tag{1.3}$$

where G is the gravitational constant, M_{cl} is the total association/cluster mass, and r_{hm} the half-mass radius (Geyer & Burkert, 2001; Melioli & de Gouveia dal Pino, 2006; Portegies Zwart et al., 2010). Typical dynamical timescales of associations can be between a few Myr up to several tens of Myr, whereas for clusters they are of the order of 1 Myr or less.

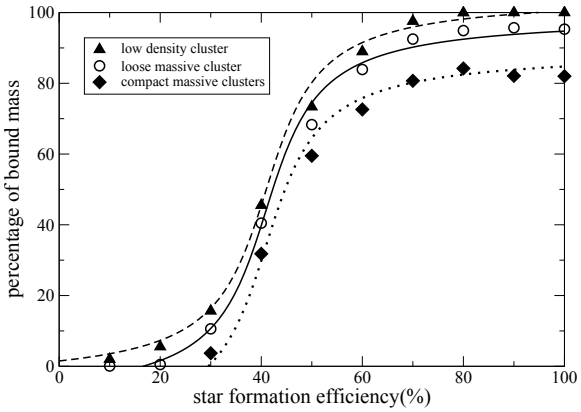

FIGURE 1.3: Simulated percentage of bound mass as a function of the SFE after a simulation time of 20 Myr for low-density clusters (dashed line, triangles), association (drawn line, circles), and clusters (dotted line, diamonds); taken from Pfalzner & Kaczmarek (2013a). Note that associations are called loose clusters and clusters are called massive clusters here.

A compilation can be found in (Portegies Zwart et al., 2010).

If the gas expulsion is slow, i.e. adiabatically, even associations with a relatively low SFE can remain bound, because they have enough time to adjust to the mass loss. On the other hand, if the expulsion happens fast, a high SFE is required to yield a bound remnant. In addition, the more substructure an association/a cluster shows, the more probable it is to remain bound (see e.g. Smith et al., 2011). It is important to note that even if a remnant remains bound, its surface density might be so low that it would not be detected by observations which are based on searches for stellar surface densities (Pfalzner et al., 2015b).

Another key parameter for association/cluster survivability is the virial ratio $Q = -T/U$, which is the ratio between kinetic and potential energy (see also Goodwin, 2009). An association or a cluster in virial equilibrium ($Q = 0.5$) is dynamically stable, whereas so-called *hot* systems ($Q > 0.5$) are bound less strongly and expand; in *cold* systems ($Q < 0.5$) the gravitational energy dominates and the systems contract. As a result, hot systems are more prone to destruction compared to systems which are in virial equilibrium or cold (see e.g. Goodwin, 2009). After gas expulsion, the system is out of virial equilibrium, which it regains within a few crossing times, if a bound remnant remains.

In summary, four parameters determine whether an association/a cluster is destroyed or a bound cluster remains: the SFE, the duration of the gas expulsion itself, the stellar distribution within the association/cluster, and the virial ratio Q.

The Orion Nebula Cluster

One of the most studied associations is the Orion Nebula Cluster, because it is the closest dense stellar group in which stars are still formed. It contains about 4 000 stars, is roughly 1 Myr old and has a half-mass radius of about 1 pc (Hillenbrand & Hartmann, 1998). It still contains some of its gas and is therefore used as a model for young, massive, embedded clusters in many numerical studies concerning protoplanetary discs and their evolution (see e.g. Scally & Clarke, 2001; Olczak et al., 2006; Pfalzner & Olczak, 2007; Steinhausen et al., 2012; Portegies Zwart, 2016).

Observations of today's ONC suggest an approximately isothermal density profile in the outer parts of the cluster (McCaughrean & Stauffer, 1994; Hillenbrand & Hartmann, 1998) and a flatter profile in the core (Scally et al., 2005). Olczak et al. (2010) provide a three-dimensional density distribution which, after 1 Myr of evolution, yields the current density distribution of the ONC:

$$\rho_0(r) = \begin{cases} \rho_0 \left(r/R_{0.2}\right)^{-2.3}, r \in (0, R_{0.2}] \\ \rho_0 \left(r/R_{0.2}\right)^{-2.0}, r \in (R_{0.2}, R] \\ 0, r \in (R, \infty], \end{cases} \tag{1.4}$$

where $\rho_0 = 3.1 \times 10^3$ stars pc^{-3} is the density, $R_{0.2} = 0.2$ pc the core radius, and $R = 2.5$ pc the cluster radius.

Associations in general cover a wide density range, for example the ones presented in Figure 1.2 have densities between $0.07 - 40$ M$_\odot$ pc^{-3} (Pfalzner, 2009, and references therein). The initial conditions in the simulations discussed in the papers included are chosen in such a way as to cover this wide range of densities. They all have the same density profile and, as such, can be regarded density-scaled versions of the ONC, meaning that the half-mass radius and the density distribution are the same as for the ONC. However, the number of stars was varied: models with 1 000, 2 000, 4 000 (ONC model), 8 000, 16 000, and 32 000 stars were simulated.

1.1.3 Compact clusters

In contrast to associations, young, massive stellar clusters are much denser and eventually develop into open clusters, which can become several hundreds of millions of years old. Clusters – also called compact clusters or starburst clusters – are preferably located in the Galactic centre and in the spiral arms. Estimates predict that only about 10% of all stars in the Milky Way are born in such long-lived clusters (Schweizer, 2006).

The major difference in the formation process between clusters and associations are the

much higher SFE (Bastian, 2011; Pfalzner & Kaczmarek, 2013a,b), and the smaller half-mass radius at the end of star formation (Stolte et al., 2010). Observations of young, massive clusters find rather low velocity dispersions in the systems, making it likely that they are in or close to virial equilibrium (see e.g. Mengel & Tacconi-Garman, 2007; Clarkson et al., 2012; Hénault-Brunet et al., 2012). As the observed clusters are still young, this could indicate that their SFE was high. Comparing observations to numerical simulations of clusters, Pfalzner & Kaczmarek (2013b) found that the evolution of clusters with an SFE of $60 - 70\%$ is in accordance with the observed increase in cluster size during the first 20 Myr. This high SFE renders them less prone to disruption due to gas expulsion. However, clusters lose mass and expand as well, see Figure 1.3 (dotted line, diamonds). The reason for this are stellar interactions, which lead to ejections of stars from the clusters and, consequently, to expansion (Pfalzner & Kaczmarek, 2013b).

Two of the most well observed young, massive clusters are Arches and Westerlund 2. Both are between $1.5 - 2.5$ Myr old, have a mass of the order of 10^4 $M_\odot$ and densities of $4 \cdot 10^5$ $M_\odot$ pc^{-3} and $5 \cdot 10^3$ $M_\odot$ pc^{-3}, respectively (Figer, 2008, and references therein). They will most probably develop into open clusters like the Hyades or Praesepe (790 ± 60 Myr and 750 ± 100 Myr, respectively, see Brandt & Huang, 2015b,a).

Arches was taken as a model for the simulations of clusters in this theses, assuming an initial half-mass radius of 0.2 pc (core radius of current Arches, see Stolte et al., 2010) and a stellar population of 32 000 stars, analogue to the most massive association and in accordance with Arches' current mass (Figer, 2008, and references therein). To date, no gas-embedded precursor of clusters has been detected, thus, the embedded phase is most probably very short, as is the gas expulsion itself. Therefore, two different types of cluster simulations were performed. The first type was embedded for 1 Myr, which is an upper limit for the embedded timescale. In the second type of clusters, the gas was expelled at the beginning of the simulations ($t_{emb} = 0$ Myr), mimicking a very short embedded time of $t_{emb} \ll 1$ Myr.

1.2 Protoplanetary discs and extrasolar planets

Protoplanetary discs form as a consequence of angular-momentum conservation around most – if not all – stars. The launch of the *Hubble Space Telescope (HST)* made it possible to directly detect discs, for example, around young stars in the ONC (O'dell et al., 1993). Since then, a large number of protoplanetary discs around field stars, as well as around association and cluster members has been found. Together with theoretical models and

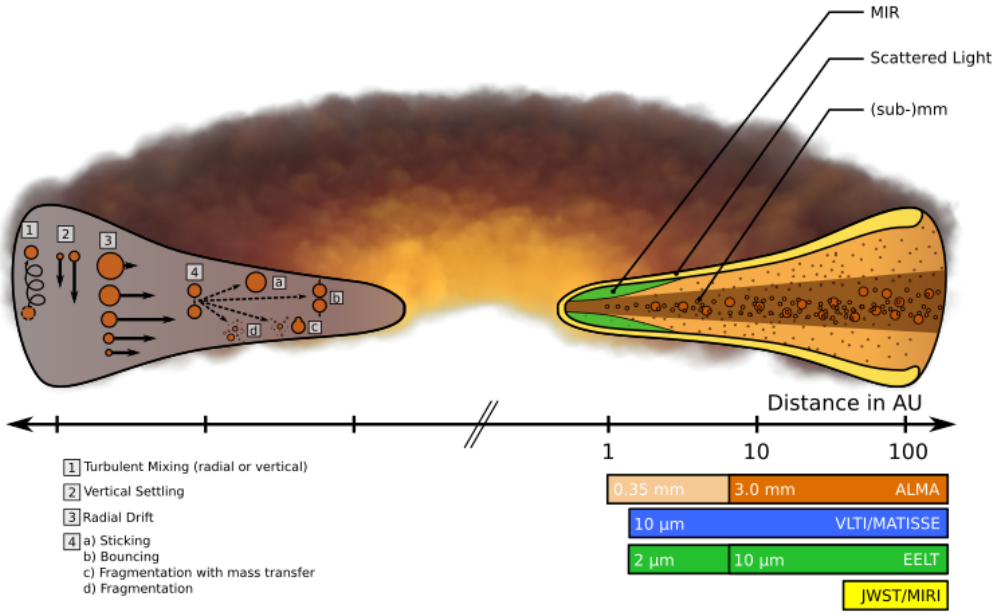

FIGURE 1.4: Schematic depiction of a protoplanetary disc. The physical grain-growth processes are depicted on the left of the plot. On the bottom right, different telescopes are listed: the *Atacama Large Millimeter/submillimeter Array (ALMA)*, the *Very Large Telescope Interferometer (VLTI)* with the *Multi Aperture Mid-Infrared Spectroscopic Experiment (MATISSE)*, the *European Extremely Large Telescope (EELT)*, and the *James Webb Space Telescope (JWST)* with the *Mid-Infrared Instrument (MIRI)*. The colours depict the areas within the disc which they oberve with their given rage of wavelengths. The axis shows the logarithmic radial distance from the central star in AU. Taken from Testi et al. (2014).

simulations, the evolution of discs and eventually forming planetary systems has been studied thoroughly.

Here, only a brief overview of disc evolution, dust growth, and planet formation will be given. For a comprehensive review see, for example, Testi et al. (2014).

At birth, a protoplanetary disc consists of gas and dust from the GMC. The dust particles are micrometer-sized and thus coupled to the gas. Larger dust particles sink to the mid-plane of the disc (*vertical settling*) and are transported inwards (*radial drift*), whereas small particles are mixed vertically by turbulences and are transported outwards. Drag forces (Whipple, 1972; Weidenschilling, 1977), radial drift (Whipple, 1972; Adachi et al., 1976; Weidenschilling, 1977), dust trapping, and radial mixing lead to collisions of dust particles and therefore grain growth, as long as their relative velocities are low. Additionally, condensation of gaseous material or the sublimation of solids can form small particles, but these effects are less important for larger dust grains (see Testi et al., 2014).

Due to the partial sorting of the particles by size within the disc, its different areas can be observed with specific wavelengths. This is important to keep in mind when it comes to the measurement of the disc size, as the observational techniques may otherwise limit or bias the resulting size. Figure 1.4 depicts a simplified protoplanetary and its internal

structure (right). The areas within the disc are colour coded, the corresponding wavelengths and telescopes, with which the different areas can be observed, are presented below. The grain-growth mechanisms are shown on the left hand side of the picture.

1.2.1 Protoplanetary-disc lifetimes and destruction processes

If the discs are massive and dense enough, planets or planetary systems might form. Therefore, the lifetime of protoplanetary discs constrains the formation and evolution time of planets significantly. It is not straightforward to determine the age of young stars and their protoplanetary disc. Especially around field stars this is rather difficult and prone to significant errors. The age of stellar clusters and associations can be constrained to a certain degree with the help of their *Hertzsprung-Russel diagram (HRD)*, which depicts the luminosity and the effective temperature of the cluster members. When stars have turned most of their hydrogen in the core to Helium, they turn into red giants, and leave the main sequence in the HRD. This point is called the *Main-Sequence turn-off* and quantifies the cluster age, assuming that all stars formed at the same time. Multiple Main-Sequence turn-offs can be either a sign of a stellar age spread within the cluster or of cluster-rotation (see Yang et al., 2013, and references therein). Therefore, it is preferable to observe discs in associations or clusters to constrain the formation, evolution, and (possibly) destruction timescales more accurately. However, a dense environment leads to observational difficulties, for example, due to the high luminosity in the centre.

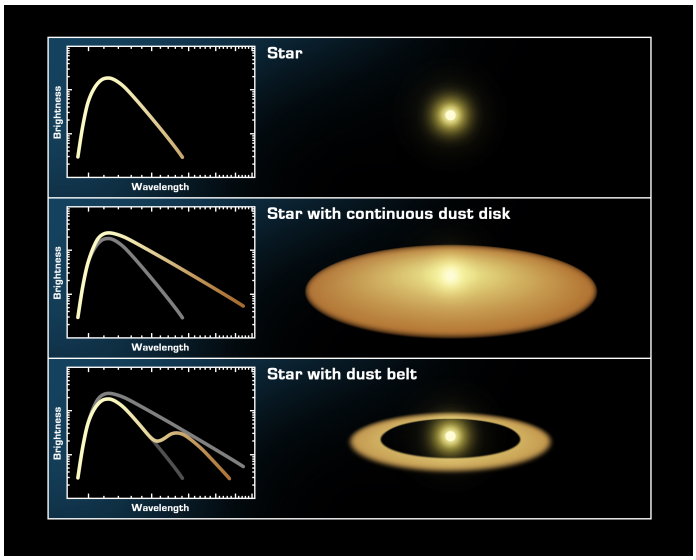

FIGURE 1.5: SED of a star without a disc (black body, top), of a star with a smooth dusty disc (mid), and of a star with a dust belt (disc with gap, bottom). Credit: NASA/JPL-Caltech/T. Pyle (SSC), http://www.spitzer.caltech.edu/images/2632-sig05-026-The-Invisible-Disk.

A disc surrounding a star can not only be discovered directly, but also indirectly through the infra-red excess in the stellar *spectral energy distribution (SED)*. If a disc is present, the SED shows characteristic deviations (Figure 1.5 mid and bottom) from the one of a black body (Figure 1.5 top).

If the membership of an association/a cluster is well determined, the *disc fraction*, i.e. the fraction of stars in the stellar group, which is surrounded by a protoplanetary disc, can be obtained. With the help of the disc fraction of many associations/clusters and the systems' age, the timescales of disc formation and of the influence of external effects by the environment can be constrained.

The disc fraction has been determined by observations in a variety of associations and clusters, and seems to decline with association/cluster age, see Figure 1.6. Haisch et al. (2001) concluded from their investigation of clusters (black points) that almost all stars lose their disc within the first 5 Myr. Taking more clusters into account, Mamajek (2009) revised the linear fit by Haisch et al. (2001) by fitting an exponential function of the disc fraction to the data and found a half-life time of $2 - 3$ Myr.

However, recently, there have been cautious remarks concerning these disc lifetimes (Pfalzner et al., 2014), as selection effects might bias the data above. Firstly, the depicted clusters with ages of > 3 Myr (after gas expulsion) are rather large and massive. Younger systems, which are still forming stars, will not necessarily evolve in the same way, because they do not contain enough gas to reach such masses. Thus, the sample of clusters is inhomogeneous.

Secondly, the systems lose stellar members due to gas expulsion and stellar interactions. Especially associations respond very strongly to gas expulsion, as a result, they usually cover several tens of parsecs in radius. However, observations focus on the inner few parsecs, where the stellar density is highest. This means that the plot depicts only the stars which still reside within a few parsecs from core after gas expulsion took place, which might not be representative for the cluster as a whole.

Thirdly, clusters as well as associations expand, which means that the stars which initially resided in the innermost, densest part of the system now cover the inner few parsecs. Observations therefore pick out discs which are most likely already influenced or destroyed by fly-bys, external photoevaporation, and other effects.

Summarising, the data in the above mentioned work depicts the discs around stars

1. in massive clusters,
2. which reside within a few parsecs of the cluster after gas expulsion,
3. and originated from the very dense system centre.

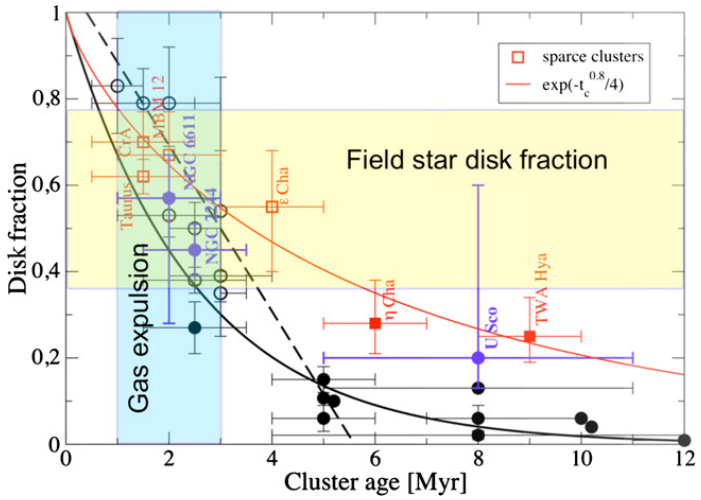

FIGURE 1.6: Disc fraction as a function of system age. Open symbols represent embedded associations/clusters, filled symbols associations/clusters after gas expulsion. The red symbols depict very low-density associations. The purple symbols indicate associations where the disc fraction was observed outside the cluster core. Taken from Pfalzner et al. (2014), based on Haisch et al. (2001) (linear fit, dashed), Mamajek (2009) (exponential fit, solid), and values from Fang et al. (2013) (low-density associations, red).

Therefore, according to these new findings, the lifetimes of discs in very low-density associations, for example, are much longer than predicted before (red squares in Fig. 1.6, see also Pfalzner et al. (2014)).

This poses a crucial question: **Are protoplanetary discs and planetary systems in associations and clusters similar, or is there a systematic influence of the environment on their shape?**
To investigate this, the different processes involved in protoplanetary disc destruction or manipulation will be discussed in more detail in the following.

Internal disc-dispersal mechanisms

There are a number of processes which can alter or completely destroy a protoplanetary disc, for example viscous torques (Shu et al., 1987), turbulent effects (Klahr & Bodenheimer, 2003), magnetic fields (Balbus & Hawley, 2002), and viscous accretion (Lynden-Bell & Pringle, 1974).

Currently, one favoured disc-dispersal process is *internal photoevaporation*, meaning that strong stellar winds of the disc-hosting star can heat up and/or blow away material from the disc (Hollenbach et al., 1994). The strength of the internal photoevaporation is affected by the radiative transfer within the disc, hydrodynamics, and thermodynamics. In addition, optically thick discs are affected differently than optically thin discs (Alexander et al., 2014).

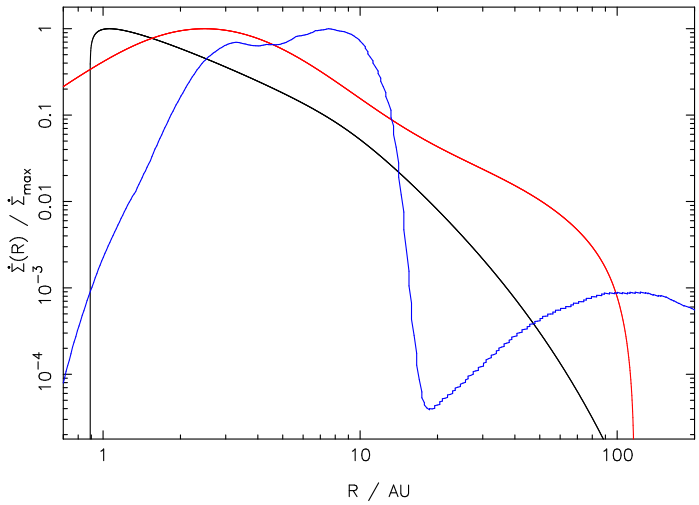

FIGURE 1.7: Normalised mass-loss profile, i.e. the mass loss at radius R, $\dot{\Sigma}(R)$, devided by the maximum mass loss $\dot{\Sigma}_{max}$, due to photoevaporation by EUV radiation (black, Font et al. (2004)), X-rays (red, Owen et al. (2012)), and FUV radiation (blue, Gorti et al. (2009)), as a function of the disc radius R. Taken from Alexander et al. (2014).

To date, it is computationally not possible to include all the above effects in an all-encompassing simulation, therefore, separate numerical simulations are performed to study the effects and the strength of the photoevaporation. One way of classifying different wavelength regimes in the simulations is to distinguish between *far-ultraviolet* radiation (*FUV*, 6-13.6 eV), *extreme ultraviolet* radiation (*EUV*, 13.6-100 eV), and *X-rays* (100 eV-10 keV), see Alexander et al. (2014). 13.6 eV is the ionization energy of atomic hydrogen. Below this energy, mainly neutral dissociation of molecules takes place. The different types of radiation are most effective in different parts of the disc. They will be discussed in more detail the following, an overview of the areas where they are most effective is given in Figure 1.7.

EUV radiation ionises hydrogen atoms in the disc, such that an ionised atmosphere forms. Close to the star, the material is still bound, but beyond the critical radius $R_{c,EUV} = 1.8 \cdot (M_{star}/1\ \mathrm{M}_{\odot})$ AU it becomes unbound in form of ionised wind (Alexander et al., 2014).

X-rays are capable of inner-shell ionising heavy elements, for example oxygen, carbon, and iron. The resulting photoelectrons heat up the hydrogen atoms/molecules, creating a smooth transition from a very hot corona close to the star, to an ionised atmosphere, and down to a cold disc. The mass loss due to X-rays is larger than the one caused by EUV (Owen et al., 2012).

Finally, in photoevaporation simulations, FUV radiation is usually assumed to be non-ionising and H_2 dissociating. It is mostly absorbed by dust grains and then re-emitted

as IR continuum. In contrast to EUV radiation and X-rays, FUV radiation is capable of depleting the disc mass at large radii ($\geq$ 100 AU, see also Gorti & Hollenbach (2009)). However, its effectiveness strongly depends on the incident flux and the density of the disc. There is still much ongoing work in order to constrain the heating/cooling rates in the discs and thus the importance of FUV radiation.

External disc dispersal mechanisms

In addition to internal photoevaporation, massive stars in the vicinity of a disc-hosting star influence the outer parts of the disc (*external photoevaporation*, see e.g. Johnstone et al. (1998); Störzer & Hollenbach (1999); Scally & Clarke (2001); Clarke et al. (2001); Matsuyama et al. (2003); Johnstone et al. (2004); Alexander et al. (2005, 2006); Ercolano et al. (2008); Drake et al. (2009); Gorti & Hollenbach (2009); Winter et al. (2018b)).

The timescales on which external photoevaporation can destroy discs are still under discussion. Simulation results vary between $t_{photo} \approx 0.1$ Myr up to ≈ 10 Myr (numerical simulations by Scally & Clarke, 2001; Gorti & Hollenbach, 2009; Adams et al., 2006; Winter et al., 2018b). A recent study argues that photoevaporation within a cluster with a number density of $n_c \approx 10^4$ (comparable to the models presented above) is the main mechanism shaping and destroying protoplanetary discs within 3 Myr (Winter et al., 2018b). They estimate that even the gas in the clusters is not capable of preventing disc destruction due to photoevaporation. However, they did not model the gas explicitly, instead, they took a Monte Carlo approach to obtain the fly-by history of the stars and the disc sizes after fly-bys. The stars remain in a "fixed stellar environment" for the whole simulation time, exposed to constant FUV radiation with $G_0 = 3000$ (Winter et al., 2018b). However, associations react strongly to gas expulsion after 2 Myr and stars move outwards, away from each other and the most massive association members. Therefore, the effect might be overestimated for those discs. If a disc-hosting star resides far away from the most massive cluster members, or becomes unbound as a result of gas expulsion, its disc will most probably not be influenced significantly by external photoevaporation. Discs which reside sufficiently close to or pass by massive stars are most probably destroyed by either mechanism, fly-bys or photoevaporation. For a detailed overview of the theoretical basis of internal and external photoevaporation and their effects, see e.g. Alexander et al. (2014).

Stellar interactions

The external process which is investigated in detail in this work is *stellar interactions*.[2] Associations and stellar clusters are highly dynamical environments and stellar fly-bys can

[2] In the publications attached, these interactions are called *encounters* or *fly-bys*.

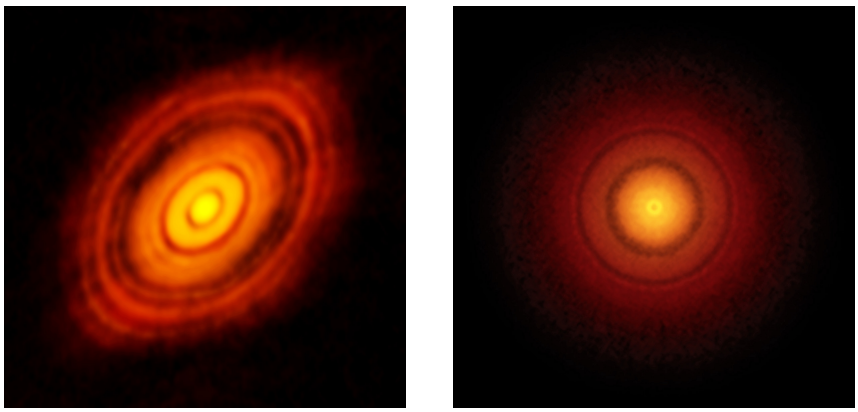

FIGURE 1.8: Pictures of the protoplanetary discs around HL Tauri (left) and TW Hydrae (right) taken with the Atacama Large Millimeter/submillimeter Array (ALMA). Credit left: ALMA (ESO/NAOJ/NRAO), http://www.eso.org/public/images/eso1436a/. Credit right: S. Andrews (Harvard-Smithsonian CfA); B. Saxton (NRAO/AUI/NSF); ALMA (ESO/NAOJ/NRAO), http://www.eso.org/public/images/eso1611a/.

change the angular momentum, the mass, and the size of the discs (see e.g. Clarke & Pringle, 1993; Hall, 1997; Scally & Clarke, 2001; Olczak et al., 2006; Pfalzner et al., 2006; Pfalzner & Olczak, 2007; Olczak et al., 2010; de Juan Ovelar et al., 2012; Breslau et al., 2014; Rosotti et al., 2014; Steinhausen & Pfalzner, 2014; Vincke et al., 2015; Portegies Zwart, 2016; Vincke & Pfalzner, 2016; Breslau et al., 2017; Winter et al., 2018a).

The size is most sensitive to changes due to stellar interactions, because fly-bys can push material inwards without removing it, thus shrinking the disc without changing its mass (Hall, 1997; Rosotti et al., 2014; Vincke et al., 2015). Together with the disc mass, the disc size pre-defines the position and mass of eventually forming planets.

There are two main methods of disc observation: direct and indirect detection. Connected with this, there are also two ways of determining the sizes of protoplanetary disc sizes. Two very famous examples of direct detection are shown in Fig. 1.8, namely the discs HL Tauri and TW Hydrae, which show signs of structure (rings). The size of such discs is usually determined by taking the outer luminosity drop as the disc radius (O'dell, 1998; Vicente & Alves, 2005). Large, luminous discs in the vicinity of the Sun are the best candidates for direct detection, as they are bright enough to be around their host star. Smaller discs which are less luminous and/or too far away can be detected indirectly by analysing the SED of a star, looking for infra-red access. The disc size is then assumed to be the truncation radius of the disc (see e.g. Andrews & Williams, 2007).

A number of protoplanetary discs have been found in associations like, for example, Taurus, the ONC, and Ophiuchus (McCaughrean & O'dell, 1996; Vicente & Alves, 2005; An-

drews & Williams, 2007; Eisner et al., 2008; Andrews et al., 2009, 2010; Brinch & Jørgensen, 2013; Harsono et al., 2014). Their radii range from about 10 AU up to ≈ 500 AU in the ONC (McCaughrean & O'dell, 1996) to up to 700 AU in Ophiuchus (Andrews & Williams, 2007). However, even in these low-stellar-density environments, it is questionable whether the discs are pristine or already shaped by, for example, fly-bys of other association members.

To study the effect of fly-bys on protoplanetary discs in more detail, a variety of theoretical models and numerical simulations have been developed and performed in the last decades. Most of them have modelled isolated star-disc fly-bys, where one star – surrounded by a disc – is passed by another star without a disc. They found a very simple connection between the disc size after the fly-by and the periastron distance of the passing star: the disc is truncated to 1/2 (Clarke & Owen, 2015) or 1/3 (Hall et al., 1996; Kobayashi & Ida, 2001) of the fly-by's periastron distance (e.g. Adams et al., 2006; Brasser et al., 2006; Adams, 2010; Malmberg et al., 2011; Jiménez-Torres et al., 2011; Pfalzner, 2013). However, these disc-size limits were obtained only considering *equal-mass fly-bys*, meaning that the disc-hosting star and the perturbing star have the same mass. However, the stellar masses in associations and clusters cover a broad parameter space, therefore, the mass ratio between two interacting stars is, in most cases, not unity.

In principle, it would be preferable not to model such star-disc interactions in isolation, but to accurately model protoplanetary discs within an association or a stellar cluster, and then to determine their size after each stellar fly-by. Rosotti et al. (2014) performed such simulations, combining *smooth-particle hydrodynamics (SPH)* simulations of discs and NBody simulations of an association of 100 equal-mass stars, and evolving the association for 0.5 Myr. They found that discs can indeed be strongly influenced by stellar fly-bys. The difficulty with such combined simulations is that they are computationally very costly. Stellar clusters, which are much more massive and much denser than the association studied by Rosotti et al. (2014), can therefore not be studied with a realistic initial mass function (see Sect. 1.4.1) with these kinds of simulations.

Therefore, a two-step approach is taken here, separating the simulation of young, massive associations/clusters with NBody from the disc simulations, which are described in more detail in Sect. 1.4.

Breslau et al. (2014) defined a disc-size limit which mimics the disc sizes as they would be found by observations: they took the steepest point in the disc's density distribution as

the outer disc rim. With this criterion, they performed an extensive parameter study of star-disc fly-bys, with different periastron distances and stellar-mass ratios. They found a simple dependence of the final disc size r_{disc} on these parameters:

$$r_{disc} = \begin{cases} 0.28 \cdot r_{peri} \cdot m_{12}^{-0.32}, & \text{if } r_{disc} < r_{previous} \\ r_{previous}, & \text{if } r_{disc} \geq r_{previous}, \end{cases} \quad (1.5)$$

where $m_{12} = m_2/m_1$ is the mass ratio between the disc-hosting star (m_1) and the perturber (m_2), r_{peri} the periastron distance in AU, and $r_{previous}$ is the disc size previous to the fly-by in AU. This equation is valid for all types of mass ratios typically found in clusters, but covers only coplanar, prograde, parabolic fly-bys. The disc was assumed to be flat, and to consist of mass-less tracer particles, that means that no viscosity or self-gravity was included. For a detailed description of the simulation set-up, the approximations made, and their influence on the results, see Breslau et al. (2014) and Vincke et al. (2015).

On the basis of this work, Bhandare et al. (2016) extended the parameter study to include *randomly orientated* fly-bys, meaning that the perturber orbit and the disc are not necessarily in the same plane. In extreme cases, the fly-by could also be retrograde. According to their results, the disc size after a fly-by – averaged over all inclinations ranging from 0-180 degrees – only depends on r_{peri} and m_{12}:[3]

$$r_{disc} = 1.6 \cdot r_{peri}^{0.72} \cdot m_{12}^{-0.2}. \quad (1.6)$$

This fit-formula focusses on penetrating ($r_{peri} \leq r_{previous}$) or very close fly-bys. The largest periastron distances included are 5 times the initial disc size r_{init}. For more details and the non-averaged data, see Bhandare et al. (2016).

1.2.2 Extrasolar planets

Under specific conditions, planets or planetary systems can form from protoplanetary discs on timescales of less than one to several tens of millions of years (cf. e.g. Alibert et al., 2005; Pfalzner et al., 2015a). The first confirmed extrasolar planet – or short *exoplanet* – around a pulsar was found by observations in 1992 (Wolszczan & Frail, 1992), the first one around a main sequence star three years later (Mayor & Queloz, 1995). Since then, observations have found a little more than 3 700 exoplanets[4], see Figure 1.9.

[3] An open access data base of their results for the whole parameter space covered (periastron distance, mass ratio, inclination, and angle of periastron) as well as a tool to easily plot disc/particle properties after fly-bys can be found at `http://www3.mpifr-bonn.mpg.de/encounter-properties/`.

[4] Value taken from `https://exoplanets.nasa.gov/newworldsatlas/` on 22 May, 2018.

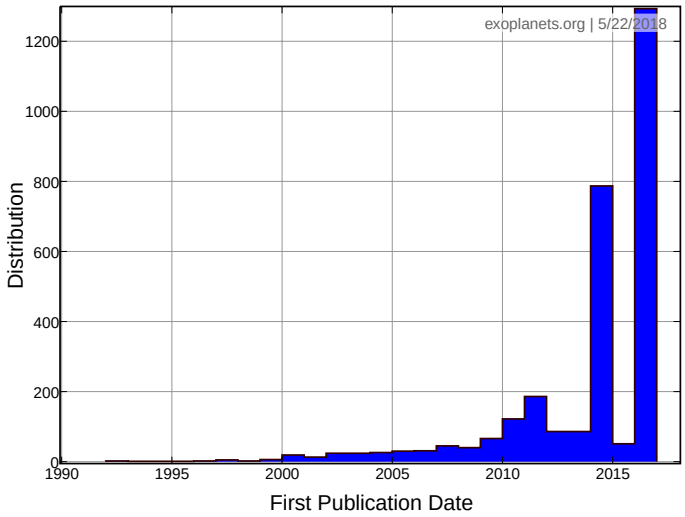

FIGURE 1.9: Number of exoplanets found since 1990. The plot was produced on `http://exoplanet.eu/` (Han et al., 2014) on 22 May, 2018.

A stellar fly-by can not only shape a protoplanetary disc, but also force an already formed planet on a different orbit. In extreme cases, planets can even become unbound. If more than one planet is present in the system after the fly-by, long-term instabilities can be triggered, leading to planet-planet scattering (Davies et al., 2014). The timescale of isolated star-disc fly-bys which influence the disc is, depending on the mass ratio and periastron distance, of the order of $10^3 - 10^4$ yr.

Detection and statistics

There is a variety of detection mechanisms for exoplanets, for example *direct imaging*, *transit photometry*, *astrometry*, *radial velocity (RV) measurements*, several *time-variation measurements*, and *gravitational microlensing*. Each of these has biases according to which type of planets it can detect. As a result, the planets and planetary systems detected might be biased towards close-in, massive, large planets, because most have been detected via transit photometry, followed by RV measurements and direct imaging.

So far, most exoplanets and exoplanetary systems have been detected around field stars. Determining the age of such planets/planetary systems and their host stars is very difficult. Without a clear restriction on a system's age, conclusions about its evolutionary phase, planet formation processes, and timescales are somewhat speculative. The advantage of stellar clusters and associations is that their ages – and therefore the stellar ages – can be determined well. However, it was speculated for a long time whether planetary systems can exist at all in the very hostile environment of dense, long-lived clusters (e.g. Paulson et al., 2004).

Table 1.1: Observed properties of planets in open clusters.

Cluster properties		Planet properties				References
Cluster	t_{cl} [Myr]	Host star	m_{pl} [$M_{\oplus}$]	a_{pl} [AU]	e_{pl}	
NGC 4349	200	No. 127	19.8[a)]	2.38	0.19	(1)
Praesepe/M44	578 ± 12	Pr 0201	0.540[a)]	0.057	0	(2), (3), (4)
		Pr 0211	1.8a), b)	0.03[b)]	0.011[b)]	(4), (5)
			7.79[a)]	5.5	0.71	(5)
		K2-95	—	0.069[d)]	0.16	(6)
		K2-100	—	0.029[d)]	0.24	(6)
		K2-101	—	0.11[d)]	0.10	(6)
		K2-102	—	0.083[d)]	0.10	(6)
		K2-103	—	0.13[d)]	0.18	(6)
		K2-104	—	0.025[d)]	0.18	(6)
Hyades	625 ± 50	ϵ Tau	7.6	1.93	0.151	(7), (8)
		HD 285507	0.917[a)]	0.06[d)]	0.086	(9)
		LP 358-348	0.0047	0.075[d)]	< 0.72	(10)
			0.0365	0.132[d)]	< 0.47	(10)
			0.0145	0.162[d)]	< 0.75	(10)
		K2-25	< 3	—	0.27	(11)
NGC 2423	750	No. 3	10.6[a)]	2.10	0.21	(1)
NGC 6811	$1\,000 \pm 170$	Kepler 66	≤ 0.06	0.1352	—	(12), (13)
		Kepler 67	≤ 0.06	0.1171	—	(13)
M 67	$3\,500 - 4\,000$	YBP1194	0.34[a)]	0.07	0.24	(14), (15), (16)
		YBP1514	0.40[a)]	0.06[d)]	0.39	(16)
		SAND364	1.54[a)]	0.53[d)]	0.35	(16)
		YBP401	0.46[a)]	0.05[d)]	0.15	(17), (18)

Notes: Column 1 indicates the cluster name and Col. 2 its age t_{cl}; Col. 3 gives the name of the planet-hosting star, m_{pl} the planet mass, a_{pl} its semi-major axis, e_{pl} its eccentricity, and Col. 7 the references.
References: (1) Lovis & Mayor (2007), (2) Delorme et al. (2011), (3) Kraus & Hillenbrand (2007), (4) Quinn et al. (2012), (5) Malavolta et al. (2016), (6) Mann et al. (2016b), (7) Perryman et al. (1998), (8) Sato et al. (2007), (9) Quinn et al. (2014), (10) Livingston et al. (2018), (11) Mann et al. (2016a), (12) Janes et al. (2013), (13) Meibom et al. (2013), (14) Sarajedini et al. (2009), (15) Richer et al. (1998), (16) Brucalassi et al. (2014), (17) Pietrinferni et al. (2004), (18) Brucalassi et al. (2016).
Comments: a) given as $m_{pl} * \sin(i)$, where i is the inclination between the orbital plane and the line of view; b) combined planet properties from (4) and (5); c) note the large error in fitted period: $P = 4\,850^{+4560}_{-1750}$ days; d) calculated from given orbital periods. Taken from Vincke & Pfalzner (2018).

The number of detected planets in clusters is still low, but to date, 23 exoplanets have been found in open clusters, among them even a planetary system in Praesepe (M44), see Table 1.1. Two planets orbit the star PR 0211, the inner one on a nearly circular orbit ($e = 0.01$) very close to the star with a semi-major axis of $a_{pl} = 0.03$ AU, the outer planet, however, resides at $a_{pl} = 5.5$ AU on a very eccentric orbit ($e = 0.7$). Such a system could have been shaped by a stellar fly-by with a probability of about 10% for a system being cut down to the size of PR 0211 (Pfalzner et al., 2018). In addition to the disc size, a fly-by can change the orbits of already formed planets at the outer rim of the system. They can be excited to eccentric orbits, while planets close to the star remain (almost) unperturbed (see Bhandare et al., 2016; Pfalzner et al., 2018).

It is expected that planetary systems in open clusters are much smaller than in associations. Simulations suggest that, the denser an association or a cluster is, and the more substructure it has, the less probable it is that a planetary system survives (Zheng et al., 2015). However, the interaction rate in associations with $100 - 1\,000$ stars was found to be low, such that most systems in such environments remain unperturbed (Adams et al., 2006).

The question is: does the environment leave an imprint on protoplanetary discs or already formed planetary systems though stellar fly-bys?

1.3 The Solar System

Investigating fly-bys in associations/clusters is not only interesting in terms of exoplanetary-system formation, but also when it comes to the formation of our own solar system. It is very probable that our Sun was – like 90% of all stars – born in an association or a cluster. Therefore, it could have undergone a stellar fly-by by one or several siblings of the Sun, i.e. stars which were born in the same environment.

1.3.1 Indications for early membership in an association or a stellar cluster

There are several indications that the Sun might have indeed been part of an association or a stellar cluster, the strongest indicators are the following:

Outer edge

The surface density of the solar system drops steeply – by a factor of more than 1 000 (Morbidelli et al., 2003) – outside Neptune's orbit at ≈ 30 AU. This so-called *outer edge cut-off* implies that the solar protoplanetary disc must have extended to at least this value to enable planet formation. A stellar fly-by could be the culprit for the cut-off, stripping

most material outside 30 AU away, leaving a clear edge behind (Ida et al., 2000; Kobayashi & Ida, 2001; Melita et al., 2002; Pfalzner et al., 2015a).

Highly eccentric Trans-Neptunian objects

In the Kuiper belt region, many objects on highly eccentric, inclined orbits can be found. For most of them, the deviation from the planetary plane can be explained by interactions with the planets. However, there exists a group of so-called *Trans-Neptunian objects (TNOs)* – with a very large pericentre and high eccentricity – whose orbits cannot be explained by interactions with the planets alone (see e.g. Gladman et al., 2002). Examples for such extreme TNOs are Sedna (Brown et al., 2004), 2012 VP_{113} (Trujillo & Sheppard, 2014), 2014 UZ_{224} (Gerdes et al., 2017), 2004 VN_{112} Becker et al. (2007), and 2010 GB_{174} (Chen et al., 2013).

Culprits responsible for the TNOs' unusual orbital parameters could be stellar fly-bys (see e.g. Brown et al., 2004; Kenyon & Bromley, 2004; Morbidelli & Levison, 2004; Rickman et al., 2004; Brasser et al., 2006; Dukes & Krumholz, 2012; Soares & Gomes, 2013; Brasser & Schwamb, 2015) or perturbations caused by an additional planet (Brown et al., 2004; Gomes et al., 2006; Soares & Gomes, 2013). This proposed *ninth planet* in the outer solar system could be responsible for the large pericentres and high eccentricities of some TNOs (Batygin & Brown, 2016a). However, it is still under debate whether one planet alone can reproduce the observed simultaneous clustering in argument of pericentre, longitude of the ascending node, and longitude of perihelion of the TNOs (Shankman et al., 2017).

Abundances of short-lived radionuclides

The abundances of precursors of *short-lived radionuclides (SLRs)*, most prominently of ^{60}Fe ($t_{1/2} = 1.5$ Myr) and ^{26}Al ($t_{1/2} = 1.7$ Myr), found in *calcium-aluminium rich inclusions (CAIs)* in chondritic meteorites (MacPherson et al., 1995) are thought to have been produced by supernova explosions. As such massive stars predominantly exist in rather massive stellar groups, it is probable that the protoplanetary solar system was part of a massive association or a stellar cluster (see e.g. Nicholson & Parker, 2017). A single supernova very close (≤ 0.3 pc, Adams, 2000) to the Sun could have enriched the protoplanetary solar disc directly during its explosion (Chevalier, 2000; Busso et al., 2003; Ouellette et al., 2007). A progenitor of such a supernova has to have a stellar mass of ≈ 25 $M_\odot$ (Adams, 2000), and is thus most probable to form in a massive cluster. However, the details of the enrichment process(es) are still under debate.

Some studies argue that ^{60}Fe does not necessarily has to have been injected by a supernova, and that typical molecular clouds already contain enough ^{60}Fe – and possibly ^{26}Al – to explain today's abundances in the solar system (Gounelle & Meibom, 2008; Gounelle

TABLE 1.2: Constraints on birth environment of the solar system.

Variable	Value	Limiting factor	References
N	$> 4\,000$	chemical composition	Lee et al. (2008)
N	$<$ several 10^4	radiation field	Adams (2010)
ρ_C	$> 10^3$ $M_\odot$ pc^{-3}	Sedna orbit	Brasser et al. (2006)
ρ_C	$< 10^5$ $M_\odot$ pc^{-3}	Sedna orbit	Schwamb et al. (2010)

NOTES: N is the number of stars in the system and ρ_C the cluster density. Taken from Pfalzner (2013).

et al., 2009). The abundance of ^{60}Fe and ^{26}Al in the early solar system could also be a hint of hierarchical star formation within an association/a cluster, with the Sun being a second- or third-generation star, and the disc being imprinted by the first and second generation stars (Gounelle & Meynet, 2012; Gritschneder et al., 2012; Gounelle, 2015).

Which of the scenarios – direct pollution or triggered star formation – is most probable is still a topic of debate, see e.g. Parker & Dale (2016). A detailed discussion of the different enrichment scenarios can be found in Sect. 4.3. The effect of chemical enrichment depends strongly on the birth environment and can thus influence the evolution of planets/planetary systems through nuclear heating (Lichtenberg et al., 2016).

1.3.2 Birth environment of the solar system

Today, the solar system is not part of an association or a cluster anymore. Either its original birth association simply dispersed over time (see Section 1.1.2 and Portegies Zwart (2009); Martínez-Barbosa et al. (2016)), or it became unbound due to gas expulsion or stellar fly-bys.

During its time in the association/cluster, the Sun probably interacted with its siblings. The current shape of the solar system strongly constrains the strength of a stellar fly-bys during this period. The solar system consists of eight confirmed planets which orbit the Sun on almost coplanar (inclination $i \leq 3.5°$) and circular (eccentricity $0 \leq e \leq 0.09$) orbits[5]. Outside the planets' orbits lies the Kuiper belt, which, in contrast, is dynamically excited (e.g. Luu & Jewitt, 2002). A stellar fly-by could have been strong enough to cause this excitement, but has to have been weak enough to leave the inner solar system unperturbed. The strength of the fly-by can be an indication for the properties of the Sun's birth environment, as close fly-bys in dense clusters are expected to be more common than in less dense associations.

[5]One exception is Mercury with an orbital eccentricity of ≈ 0.2.

For an embedded, ONC-like association, Adams (2010) approximated the rate Γ_b at which a solar system encounters another star at a distance b as

$$\Gamma_b = \Gamma_0 \left(\frac{b}{b_0} \right)^{\eta}, \tag{1.7}$$

where Γ_0 is the fiducial interaction rate, i.e. the number of encounters closer than b_0 per Myr, $\eta = 1 - 2$ the fitted power-law index, and b_0 a reference distance scale (Proszkow & Adams, 2009). They find an encounter rate of $\Gamma_0 = 0.01 - 0.1$ encounters per star and Myr, assuming $b_0 \approx 1\,000$ AU and taking an embedded solar-neighbourhood association as a model (stellar density $n_0 \approx 100$ stars/ pc^{-3} and velocity dispersion $v_0 \approx 1$km s^{-1}). Adopting the assumption that the size of a protoplanetary disc is 1/3 of the periastron distance of the fly-by (see Section 1.2.1), Adams obtains an encounter rate for a 30 AU-sized solar system of $\Gamma_{90} \approx 10^{-4} - 10^{-2}$ Myr^{-1}.

It is important to note that these values are only valid for an equal-mass fly-by, meaning that the perturbing star has the same mass as the Sun. However, in a typical cluster, a large spread of stellar masses is covered and the mass of the perturber is vital to determine the final disc size (see e.g. Breslau et al., 2014, and Sections 1.2.1 and 4.3).

Adams (2010) constrained the size of the solar birth environment taking into account the probability of (1) the system to produce a supernova, which can enrich the disc with SLRs, (2) a close fly-by with an impact parameter of $b \leq 400$ AU, and (3) the far-ultraviolet radiation not to destroy the disc ($G_0 \leq 10^4$). He concluded that the solar system has most likely been born in a moderate-sized bound cluster with $10^3 - 10^4$ stars. Pfalzner (2013) performed a study similar to the one by Adams (2010), but for a variety of cluster environments and found that their central densities are so high ($\geq 10^5$ M$_\odot$/pc^3) that most solar-system like systems would be destroyed. An association was proposed to be a much more likely birthplace of our solar system. A compilation of constraints on the birth environment from different studies can be found in Table 1.2.

However, both studies above started out with gas-free associations/clusters in virial equilibrium and thus did not cover the dynamical evolution of the systems. Furthermore, they assumed the disc to be 1/3 of the periastron distance after a fly-by, which again holds only for the special case of an equal-mass fly-by on a coplanar orbit, meaning that the disc and the perturber orbit reside in the same plane. In the work presented here, these simplifications were remedied.

In summary, the properties of the potential birth association or cluster of our solar system are still not very well constrained, as different parameters and different studies point in one or the other direction. Three basic questions remain:

1. How probable is it for a *solar-system analogue*, that is a disc with $30-50$ AU around a solar-like star, to survive long enough to form planets in associations and clusters?
2. How many other solar-system analogues can one expect in the different types of environment?
3. Was the solar system born in an association or a stellar cluster?

1.4 Simulations

Ideally, one would produce one set of simulations, where the stars and their surrounding discs are covered, and viscous forces and self-gravity in the discs are included. However, this is computationally very costly and to date was done only for low-mass associations, as for example done by Rosotti et al. (2014) for 100 equal-mass stars and a simulation time of ≈ 0.5 Myr.

For young, massive associations like the ONC, with thousands or tens of thousands of stars, covering a mass range of 0.08 to 100 or more solar masses, this is too time consuming. Especially covering a time span of 10 Myr, as would be necessary here, is currently completely out of the question.
Instead, in order to answer the above questions, a two-step approach is followed here:

1. associations and clusters of different densities and at different evolutionary stages are simulated and the fly-by history is recorded,
2. the influence of fly-bys on the sizes of protoplanetary discs is determined.

The two-step approach renders it possible to (1) simulate young, *massive* associations and clusters, (2) let them evolve over several tens of Myr – the most important period for disc-property change – and include different evolutionary stages, (3) track properties of each stellar fly-by, and (4) determine the influence of those fly-bys on protoplanetary discs. In the following, a brief summary of the simulations and their parameters is given. For more detailed descriptions, see Vincke et al. (2015); Vincke & Pfalzner (2016), and Vincke & Pfalzner (2018).

1.4.1 Association and cluster simulations

Both associations and clusters were modelled with the code NBody6++ GPU, originally developed and extended by Aarseth (1973), Spurzem (1999), and Aarseth (2003). The version of the code used here is based on that by Olczak et al. (2008), Olczak et al. (2010) and Steinhausen & Pfalzner (2014).

The NBody6++ GPU code was expanded by Olczak et al. (2012), interpolating the periastron distance r_{peri} at time t_{peri} from the regular output at timesteps t by NBody6++. A detailed description can be found in Olczak et al. (2012), appendix A.2. With this extension, the orbital parameters of each fly-by in the association/cluster modelled were saved: the periastron distance r_{peri}, the masses of the primary (m_1) and the perturber (m_2), as well as the mass ratio $m_{12} = m_2/m_1$, the eccentricity e, the time of periastron passage t_{peri}, and the primary's distance to the cluster centre (r) at periastron passage. These are the relevant parameters to analyse the influence of fly-bys on protoplanetary discs in a second step.

It is assumed that star formation is completed and that the simulations start at a point, where the associations or clusters are still embedded in gas left over from the star-formation process.[6] The stellar masses are sampled from an IMF (Kroupa, 2002), and the stellar density profile follows a modified King model as described in Olczak et al. (2010). The gas mass depends on the stellar mass and the SFE according to: $M_{gas} = M_{stars}\,(1 - SFE)\,/SFE$, and is distributed in a Plummer density profile (Plummer, 1911). As a result, the gas-mass profile is flatter in the core than the stellar-mass profile, mimicking the higher SFE in cluster centre (Gutermuth et al., 2011; Parmentier & Pfalzner, 2013). At the onset of the simulations, the systems are in virial equilibrium ($Q = 0.5$) and the initial velocity dispersion is sampled from a Maxwellian distribution.

Here, three different sets of simulations have been performed covering

- the embedded phase of associations only
- the embedded and expansion phase of associations
- the embedded and expansion phase of clusters.

Most previous simulations that investigated the effect of fly-bys on discs covered either the embedded phase, where the gas is often not explicitly considered, or the expansion phase only. Similarly, the first set of simulations – the *embedded associations* – only covered this embedded phase (Vincke et al., 2015). In the case of *evolving associations/clusters*, the embedded phase lasted between $0 - 2$ Myr. Observations found that associations are nearly gas-free at ages of about $1 - 3$ Myr, whereas for clusters no embedded candidate has been found yet. Nevertheless, young massive clusters like Arches are already gas-free at an age of ≈ 2 Myr, so a model with a very short embedded phase (model C0 with $t \ll 1$ Myr) seems a sensible approximation.

[6] This is important especially when talking about cluster ages, because *real* association/cluster ages are a few Myr older than the ones depicted in this work.

TABLE 1.3: General simulation parameters.

stellar masses	$0.08 - 150$ M$_\odot$, IMF[a]
stellar density profile	modified King profile[b]
gas mass	directly added to stellar mass, $M_{gas} = M_{stars}\,(1 - SFE)\,/SFE$
gas density profile	Plummer profile[c]
initial mass segregation	no
primordial binaries	no
gas expulsion	instantaneous
velocity dispersion	Maxwellian distribution
virial ratio	$Q = 0.5$

NOTES: (a) IMF according to Kroupa (2002), (b) King density profile King (1962), modified by Olczak et al. (2010) to fit the ONC, (c) Plummer (1911).

When modelling the expansion phase, the gas was assumed to be expelled instantaneously, leaving the associations/clusters in a supervirial state. Theoretically, the gas-expulsion timescale is proposed to be of the order of several dynamical timescales

$$t_{dyn} = \left(\frac{GM}{r_{vir}^3}\right)^{-1/2}, \tag{1.8}$$

where G is the gravitational constant, M the total association/cluster mass, and r_{vir} the virial radius, which can be approximated to be the half-mass radius (Portegies Zwart et al., 2010). This yields $t_{dyn}^{as}(1000) = 0.67$ Myr for an association with 1 000 stars (model E0) and $t_{dyn}^{cl}(32000) = 0.01$ Myr for embedded clusters (models C0 and C1). For massive associations and clusters, the approximation of instantaneous gas expulsion is legitimate. The least massive associations however expel their gas more slowly, giving the system enough time to adjust to the mass loss. In these cases, the encounter rate is underestimated in our results, as in reality, the density stays higher for a longer time, and less stars become unbound due to gas expulsion and cluster expansion.

Initially, we assume all stars in the simulations to be single to reduce the complexity of the problem of the effect of fly-bys. Furthermore, the stars were all positioned randomly within the association/cluster, independently of their mass. This means that no primordial mass segregation was included, however, within a few Myr dynamical mass segregation can be observed in the simulations. Whether associations, like for example the ONC, already form mass segregated, or observed mass segregation is the result of dynamical evolution, is still under debate (cf. Bonnell & Davies, 1998; Huff & Stahler, 2006; McMillan et al., 2007; Allison et al., 2009; Olczak et al., 2011). For a summary of the general simulation parameters, see Table 1.3.

TABLE 1.4: Summary of association/cluster simulation parameters in all publications.

	Associations r_{hm} = 1.3 pc, SFE=0.3, t_{sim} = 5 Myr and 10 Myr							Clusters r_{hm} = 0.2 pc, SFE=0.7, t_{sim} = 3 Myr			
	Embedded			Evolving							
N_{stars}	Name	$\rho_c^{init}(r_{hm})$ [$M_\odot$ pc^{-3}]	N_{sim}	Name	$\rho_c^{init}(r_{hm})$ [$M_\odot$ pc^{-3}]	t_{emb} [Myr]	N_{sim}	Name	$\rho_c^{init}(r_{hm})$ [$M_\odot$ pc^{-3}]	t_{emb} [Myr]	N_{sim}
1 000	D0	32.5	392	E0	32.2	2.0	308				
2 000	D1	64.8	260	E1	64.7	2.0	168				
4 000	D2	128.3	264	E2	128.6	2.0	94				
8 000	D3	259.1	78	E3	256.8	2.0	47				
16 000	D4	512.9	21	E4	512.9	2.0	16				
32 000	D5	1023.9	14	E52	1024.3	2.0	9				
32 000				E51	1023.8	1.0	7	C1	10922.8	1.0	1
32 000								C0	11451.1	0.0	1

NOTES: Parameters of all simulation sets performed for the publications in Section 2: Vincke et al. (2015): embedded associations, Vincke & Pfalzner (2016): embedded and evolving associations, Vincke & Pfalzner (2018): evolving associations and clusters. N_{stars} gives the number of stars in simulations, name their designation in the publications, $\rho_c^{init}(r_{hm})$ their *initial stellar* mass density within their half-mass radius in $M_\odot$ pc^{-3}, N_{sim} the number of simulations performed for each set, and t_{emb} the time during which the evolving clusters are embedded within their gas in Myr. The half-mass radius r_{hm}, the star-formation efficiency SFE, and the total simulation time t_{sim} are given below the respective type of stellar group. Note that the embedded associations were modelled for t_{sim} = 5 Myr, whereas for the evolving associations t_{sim} was 10 Myr. For more details see text and respective publications.

Associations and clusters cover a wide range of stellar densities (see e.g. compilation in Pfalzner, 2009, and Figure 1.2), for this reason, several sets of association simulations were performed. The starting point was the ONC, as it is the closest massive association. The simulation that corresponds to the ONC contains 4 000 stars. Denser and less dense associations were simulated by varying the particle number, while leaving all other parameters fixed, resulting in *density-scaled versions* of the ONC (models with designations D0-D5 and E0-E52 in Table 1.4). For each complete parameter set, a *simulation campaign* was performed, i.e. several simulations were carried out with the same parameters, but sampled with random seeds. This was done to minimize statistical fluctuations, the number of simulations is given by N_{sim} in Table 1.4. The influence of the assumed initial conditions and simplifications will be discussed in detail in Section 4.

1.4.2 Analysis of protoplanetary disc sizes

With the recorded fly-by parameters from the NBody simulations for each individual star, the disc size after each event was determined. The effect of the fly-bys is based on simulations by Breslau et al. (2014) and Bhandare et al. (2016). They modelled isolated star-disc fly-bys, where only one of the stars was surrounded by a disc (host), and determined the disc size after each interaction with another star (perturber). The discs were set up to consist of mass-less tracer particles – neglecting effects like self-gravity or viscosity – and treated on the basis of a restricted three-body problem (Breslau et al., 2017).

Long-term evolution due to viscosity, self-gravity, magnetic fields etc. might shrink or enlarge the discs again, which is not included here. For a more detailed discussion see Section 4.1.2.

Fit formulas which describe the disc size after coplanar, parabolic fly-bys (Equation 1.5, Breslau et al. (2014)), and the averaged disc size after randomly orientated encounters (Equation 1.6, Bhandare et al. (2016)) were obtained for a large parameter space typical for fly-bys in associations and stellar clusters. It is important to note that the latter formula (Eq. 1.6) for randomly orientated fly-bys is only valid for close interactions.

However, stellar fly-bys with larger periastron distances are most common in associations and clusters. Despite their large periastron distances, they are still able to influence protoplanetary discs (see also Scally & Clarke, 2001; Olczak et al., 2006). Therefore, additional simulations to the ones by Bhandare et al. (2016) were performed to extend the parameter space to distant fly-bys. Averaging the disc size after a fly-by with (m_{12}, r_{peri}) over all inclinations (0°-180°), a fit which is more accurate for distant fly-bys was found (Vincke & Pfalzner, 2018):

$$r_{disc} = \begin{cases} \left(1.6 \cdot m_{12}^{-0.2} - 1.26 \cdot m_{12}^{-0.182}\right) \cdot r_{peri}, & \text{for } r_{disc} < r_{previous} \\ r_{previous}, & \text{for } r_{disc} \geq r_{previous}. \end{cases} \tag{1.9}$$

Together with the fly-by parameters recorded by NBody6++ GPU, the size of each protoplanetary disc after every fly-by during the simulation time was calculated. Only fly-bys which change the disc size by *at least* 5% ($r_{disc}/r_{previous} = 0.95$) were accounted for in the statistics in all three publications below, because this is the typical error in the fly-by simulations.

Initial disc size

The initial disc size in Vincke et al. (2015) and Vincke & Pfalzner (2016) was set to 10^5 AU and 10^4 AU, respectively, to obtain a first impression of the importance of fly-bys in associations. This should be understood as a *numerical experiment*. This yields the maximum disc sizes for each association environment, assuming that the discs were purely shaped by stellar fly-bys.

Although individual disc sizes vary widely, the median disc size in a very massive association (model E52) at the end of the simulations was found to be roughly 100 AU (Vincke & Pfalzner, 2016). Note that in Vincke & Pfalzner (2018), the initial disc size was set to 200 AU, because it was expected that the median disc size in clusters is even smaller than in associations.

1.5 Aim of this work

The purpose of this work is to study the influence of the cluster environment on protoplanetary discs and planetary systems in terms of stellar fly-bys in detail. Therefore, a simple model of embedded associations was taken as a starting point, to get an idea of the dependency of the disc sizes on the associations' properties like density and radius (Vincke et al., 2015). The Orion Nebula Cluster is taken as a model cluster, and different density-scaled versions of it are studied to cover the broad density spectrum of associations.

In a second step, the evolution of the clusters themselves was incorporated, covering the embedded phase, gas expulsion, and expansion of associations (Vincke & Pfalzner, 2016).

Subsequently, the investigations were expanded to protoplanetary discs in much denser stellar clusters, which are long-lived, more hostile environments (Vincke & Pfalzner, 2018). The aim is to compare the numerical results with the sizes of discs and planetary systems found in associations and clusters by observations.

With the results of the three studies presented in Section 2 it is possible to make pre-

dictions about the size and the frequency of protoplanetary discs and planetary systems in both associations and clusters. Furthermore, conclusions about the birth environment of our own solar system can be drawn, which are presented in Section 3. The assumptions and simplifications made in the simulations of associations and clusters, as well as in the determination of the disc size, will be discussed. In addition, the results presented here will be put into context, they are compared to previous work and to observational results (Section 4). A short summary and concluding remarks can be found in Sections 5 and 6.

2 Publications

This chapter contains the three above mentioned publications which form the basis of this thesis in order of publication date:

1. **K. Vincke**, A. Breslau & S. Pfalzner, "*Strong effect of the cluster environment on the size of protoplanetary discs?*", 2015, Astronomy & Astrophysics 577, A115.
2. **K. Vincke** & S. Pfalzner, "*Cluster dynamics largely shapes protoplanetary disk sizes*", 2016, The Astrophysical Journal 828, 48.
3. **K. Vincke** & S. Pfalzner, "*How star cluster evolution shapes protoplanetary disc sizes*", 2018, The Astrophysical Journal 868, 1.

A&A 577, A115 (2015)
DOI: 10.1051/0004-6361/201425552

Astronomy & Astrophysics

Strong effect of the cluster environment on the size of protoplanetary discs?

Kirsten Vincke, Andreas Breslau, and Susanne Pfalzner

Max Planck Institute for Radio Astronomy, Auf dem Hügel 69, 53121 Bonn, Germany
e-mail: kvincke@mpifr-bonn.mpg.de

Received 19 December 2014 / Accepted 10 April 2015

ABSTRACT

Context. Most stars are born in clusters, thus the protoplanetary discs surrounding the newly formed stars might be influenced by this environment. Isolated star-disc encounters have previously been studied, and it was shown that very close encounters are necessary to completely destroy discs. However, relatively distant encounters are still able to change the disc size considerably.
Aims. We quantify the importance of disc-size reduction that is due to stellar encounters in an entire stellar population.
Methods. We modelled young, massive clusters of different densities using the code Nbody6 to determine the statistics of stellar encounter parameters. In a second step, we used these parameters to investigate the effect of the environments on the disc size. For this purpose, we performed a numerical experiment with an artificial initial disc size of 10^5 AU.
Results. We quantify to which degree the disc size is more sensitive to the cluster environment than to the disc mass or frequency. We show that in all investigated clusters a large portion of discs is significantly reduced in size. After 5 Myr, the fraction of discs smaller than 1000 AU in ONC-like clusters with an average number density of $\overline{\rho}_{\rm cluster} \sim 60$ pc^{-3}, the fraction of discs smaller than 1000 AU is 65%, while discs smaller than 100 AU make up 15%. These fractions increase to 84% and 39% for discs in denser clusters like IC 348 ($\overline{\rho}_{\rm cluster} \sim 500$ pc^{-3}). Even in clusters with a density four times lower than in the ONC ($\overline{\rho}_{\rm cluster} \sim 15$ pc^{-3}), about 43% of all discs are reduced to sizes below 1000 AU and roughly 9% to sizes below 100 AU.
Conclusions. For any disc in the ONC that initially was larger than 1000 AU, the probability to be truncated to smaller disc sizes as a result of stellar encounters is quite high. Thus, among other effects, encounters are important in shaping discs and potentially forming planetary systems in stellar clusters.

Key words. protoplanetary disks – planets and satellites: formation – galaxies: star clusters: general

1. Introduction

Most, if not all stars are initially surrounded by a protoplanetary disc from which a planetary system might eventually form. The observed sizes (=radii) of these discs span from a few 10 AU to several 100 AU, see Table 1 (Vicente & Alves 2005; Eisner et al. 2008; McCaughrean & O'dell 1996; Andrews & Williams 2007; Andrews et al. 2009, 2010). However, the majority of disc sizes has been found to be in the range of 100−200 AU. These discs disperse rapidly as a result of internal processes such as viscous torques (e.g. Shu et al. 1987), turbulent effects (Klahr & Bodenheimer 2003), and magnetic fields (Balbus & Hawley 2002). Observations of disc fractions in clusters show that the discs dissipate through internal processes on average at an age of ≤2.5 Myr. It is currently unclear whether this is valid for young stars in general (Pfalzner et al. 2014) and how certain absolute age estimates in clusters are (Bell et al. 2013).

There are additional environmental processes in a cluster that, depending on its stellar density, might lead to disc-mass loss, reduction in physical size, or even complete destruction. These processes are photoevaporation (see e.g. Johnstone et al. 1998; Störzer & Hollenbach 1999; Scally & Clarke 2002; Matsuyama et al. 2003; Johnstone et al. 2004; Adams et al. 2006; Alexander et al. 2006; Ercolano et al. 2008; Gorti & Hollenbach 2009; Drake et al. 2009) and stellar fly-bys or gravitational stripping (see e.g. Clarke & Pringle 1993; Scally & Clarke 2002; Pfalzner 2004; Adams et al. 2006; Olczak et al. 2006, 2010; Pfalzner & Olczak 2007; Craig & Krumholz 2013; Steinhausen & Pfalzner 2014; Rosotti et al. 2014).

Table 1. Observed disc radii in different cluster environments.

Cluster	Disc radii [AU]	$N_{\rm sources}$	References
ONC	50−200[a]	10	(1)
ONC	80−217	39	(2)
ONC	27−506[a]	6	(3)
Ophiuchus	25−700	11[b]	(4)
Ophiuchus	14−198	16[b]	(5), (6)
Ophiuchus	165−190	2	(7)
Taurus	25−600	12	(4)
Taurus	<50−100	4	(8)

Notes. Observed clusters (Col. 1) and disc-radius ranges (Col. 2). The number of sources $N_{\rm sources}$ and the references are given in Cols. 3 and 4. [(a)] Values calculated from given disc diameters. [(b)] The sources in Cols. (4)–(6) overlap.

References. (1) Vicente & Alves (2005); (2) Eisner et al. (2008); (3) McCaughrean & O'dell (1996); (4) Andrews & Williams (2007); (5) Andrews et al. (2009); (6) Andrews et al. (2010); (7) Brinch & Jørgensen (2013); (8) Harsono et al. (2014).

From observations, the sizes of protoplanetary discs are usually determined by fitting the spectral energy distributions (SEDs) to disc models using a truncated power-law (Andrews & Williams 2007). If resolved images of the discs can be obtained, the disc size is identified as the radius at which the

luminosity drops below a certain value (Vicente & Alves 2005; O'dell 1998). However, it is much more difficult to observationally constrain the disc size than the disc frequency or disc mass. Therefore, the disc sizes are only determined for a very limited number of stars. As a consequence, it is still a subject of debate whether the disc size is a function of the mass of the central star (compare e.g. Hillenbrand et al. 1998; Vicente & Alves 2005; Eisner et al. 2008). The disc frequencies in clusters of similar age (~1 Myr) reveal that the cluster environment influences the protoplanetary discs. The percentage of stars surrounded by discs decreases with increasing cluster peak density, dropping from 85% in NGC 2024 and 80% in the Orion nebula cluster (ONC) down to 40% in NGC 3603 (see also Table 2). Because the cluster ages are similar, the higher cluster density leads to a higher degree of disc destruction and thus to a lower disc frequency.

Table 2. Observed cluster properties.

Cluster	ρ[pc^{-3}]	$f_{\rm disc}$	References
NGC 2024	$\approx 10^3$	85%	(1), (2)
ONC	$\approx 10^4$	80%	(3), (4)
NGC 3603	$\approx 10^5$	40%	(5), (6)

Notes. Column 1 gives the cluster name, ρ is the cluster density (Col. 2), and $f_{\rm disc}$ the disc fraction (Col. 3). The references for the densities and disc fractions are given in Col. 4.

References. (1) Lada et al. (1991); (2) Haisch et al. (2000); (3) McCaughrean & Stauffer (1994); (4) Lada et al. (2000); (5) Harayama et al. (2008); (6) Stolte et al. (2004).

A number of theoretical investigations studying the influence of individual stellar encounters on protoplanetary discs have been performed in the past. For the case of an equal-mass encounter, Clarke & Pringle (1993) were the first to study the fate of disc matter after an interaction. They found that a coplanar, prograde encounter at a relative periastron distance of $1.25 r_{\rm peri}$ material is removed from the disc down to $0.5 r_{\rm peri}$. But material is not only removed, it is also re-distributed within the disc, changing the (mass) surface density profile of the disc (Hall 1997). As the disc masses of individual stars are observationally better constrained than disc sizes, there has been a considerable amount of theoretical research on the influence of stellar encounters on the disc mass (e.g. Olczak et al. 2010; Steinhausen & Pfalzner 2014), but fewer studies of the disc size (e.g. Hall et al. 1996; Kobayashi & Ida 2001; Breslau et al. 2014). Nevertheless, the disc size is an important parameter because it defines the physical extent of the potentially forming planetary system.

The disc size after an encounter event was investigated for example by Kobayashi & Ida (2001). They found that the disc size after an equal-mass encounter is one-third of the periastron distance. Adams (2010) found a slightly different disc size of $b/3$ where b is the impact parameter, which is not necessarily equal to the periastron distance. Two other estimates for disc-size upper limits were introduced by de Juan Ovelar et al. (2012). They derived the disc size assuming that all material outside the Lagrangian point between the two stars is stripped from the disc. Furthermore, they suggested to convert the formula for disc-mass loss for parabolic, coplanar encounters reported by Olczak et al. (2006) directly into an upper limit for disc truncation, assuming a mass-density distribution within the disc of $\Sigma = r^{-1}$. The few previous studies that considered disc sizes in stellar cluster environments (Adams et al. 2006; Malmberg et al. 2011; Pfalzner 2013) generalised, for lack of a universal description of disc sizes, the results obtained for equal-mass encounter by Kobayashi & Ida (2001) to non-equal mass encounters.

Recently, Breslau et al. (2014) showed that a generalisation of this one-third criterion postulated by Kobayashi & Ida (2001) is not advisable and that the outcome is very sensitive to the mass ratio of the two stars. They performed simulations of isolated star-disc encounters for a wide range of periastron distances and mass ratios, choosing the highest contrast in surface density to determine the disc sizes after the encounters. This is similar to the criterion used by observations, and the results by Breslau et al. (2014) can easily be applied to cluster simulations. They showed that encounters with large periastron distances and/or low mass ratios do not remove material from the disc but shift it inwards, reducing the disc size but not the mass. For disc-mass loss closer encounters and/or larger mass-ratios are needed. This finding demonstrated that the upper disc-size limits of de Juan Ovelar et al. (2012), which connect disc-size change directly to disc-mass loss, are thus too high by up to a factor of two.

Recently, Rosotti et al. (2014) investigated the effect of encounters on the disc-size distribution in an entire stellar cluster. They performed combined smoothed particle hydrodynamics (SPH)/N-body simulations of a low-mass cluster (100 stars) allowing hydrodynamical disc spreading. They found that while the masses of the discs are not much affected, the disc sizes are reduced by encounters within the ~0.5 Myr of cluster evolution.

Here, we wish to analyse numerically how encounters influence the disc size in clusters using a realistic initial mass function (IMF) and the therefore broad spectrum of encounter mass-ratios found in real clusters. We model clusters of different density to quantify the resulting disc-size dependence. Most importantly, in contrast to previous work, the effects of the encounters are modelled taking into account that the final disc size is very sensitive to the mass ratio of the two interacting stars. Although external photoevaporation might be as important as stellar encounters when describing disc sizes in clusters, we do not consider it in this work.

The simulations of the clusters with different densities as well as the disc-size definition are introduced in Sect. 2. The choice of initial disc sizes and the classification of encounters used throughout this work are also discussed there. The most important results are presented in Sect. 3, the assumptions applied and their influence on these results are detailed in Sect. 4. Our findings are briefly summarised in Sect. 5.

2. Method

We performed numerical simulations to investigate the influence of star-disc encounters on the disc size within stellar clusters of different densities. This was achieved by performing Nbody6 simulations (Aarseth 1973, 2003; Spurzem 1999) similar to those of Olczak et al. (2008, 2010), and Steinhausen & Pfalzner (2014). In those simulations, the stellar encounters in the clusters were tracked and their effect on protoplanetary discs was analysed in the diagnostics using a previously performed parameter study. In contrast to the previous work, we investigate the disc size rather than the disc mass or frequency in clusters. The disc sizes were obtained using the results from Breslau et al. (2014).

2.1. Cluster simulations

The dynamics of the stellar clusters was modelled by Nbody6 simulations taking the cluster density profile of the ONC as a prototype for a massive cluster in the solar neighbourhood. The ONC is the best observed massive cluster, rendering it possible to compare results of theoretical studies to observational data. It contains about 4000 stars, is ∼1 Myr old, has a half-mass radius of roughly 1 pc (Hillenbrand & Hartmann 1998), and extends to ∼2.5 pc (Hillenbrand & Hartmann 1998; Hillenbrand & Carpenter 2000). Lada et al. (2000) found that in the Trapezium, that is, in the inner 0.3 pc of the ONC, about 80−85% of the stars are surrounded by a protoplanetary disc, 60% of which having radii smaller than 50 AU (Vicente & Alves 2005).

Scally et al. (2005) found the density distribution in the ONC to differ from the isothermal approximation $\rho_0 \propto r^{-2}$ in the inner 0.2 pc of the cluster. The surface density there is much flatter with $\Sigma \propto r^{-0.5}$. To obtain this flat profile after 1 Myr of simulation time, which is the assumed age of the ONC, Hillenbrand (1997) and Olczak et al. (2010), for instance, used the three-dimensional initial number density distribution

$$\rho_0(r) = \begin{cases} \rho_0\,(r/R_{0.2})^{-2.3}\,, r \in (0, R_{0.2}] \\ \rho_0\,(r/R_{0.2})^{-2.0}\,, r \in (R_{0.2}, R] \\ 0, r \in (R, \infty]\,, \end{cases} \quad (1)$$

with the radius $R_{0.2} = 0.2$ pc, the cluster radius $R = 2.5$ pc, and $\rho_0 = 3.1 \times 10^3$ stars pc^{-3}. After 1 Myr of cluster evolution this distribution represents today's number density distribution of the ONC. The stellar positions, masses, and velocities were randomly attributed to the stars. All stars were assumed to be initially single and without any stellar evolution throughout the simulation. This is standard procedure to reduce the computational cost. Furthermore, the clusters were modelled without gas. The assumptions made and their influence on the outcome is discussed in Sect. 4 in detail.

The stellar masses were sampled from the IMF by Kroupa (2002)

$$\xi(m) = \begin{cases} m^{-1.3}, 0.08 \leq m/\,M_\odot < 0.50 \\ m^{-2.3}, 0.50 \leq m/\,M_\odot < 1.00 \\ m^{-2.3}, 1.00 \leq m/\,M_\odot < \infty, \end{cases} \quad (2)$$

with an upper mass limit of 150 $M_\odot$ and randomly attributed to the stars in the cluster. We neglected the effect of initial mass segregation as proposed for the ONC for example by Bonnell & Davies (1998) and Olczak et al. (2011). Using an IMF is important, as the effect of unequal-mass encounters onto discs is stronger than for equal-mass encounters (Olczak et al. 2006; Moeckel & Bally 2007).

The clusters were set up to be initially in virial equilibrium: $Q = \frac{R_{\rm hm}\sigma^2}{2GM} = 0.5$, where $R_{\rm hm}$ is the half-mass radius, G the gravitational constant, M the total cluster mass, and σ the velocity dispersion. The latter was sampled adopting a Maxwellian distribution.

As we are interested in the effect of clusters of different densities on the disc-size distribution, we set up density-scaled versions of the ONC by keeping the radius fixed at 2.5 pc and varying the number of stars within the cluster. The resulting clusters with 1000, 2000, 8000, 16 000, and 32 000 stars have average number densities of roughly 1/4, 1/2, 2, 4, and 8 times the density of the ONC, respectively (see Table 3 for the exact number and mass densities).

Table 3. Cluster model set-up.

Model	$N_{\rm stars}$	$N_{\rm sim}$	$\overline{\rho}_{\rm core}{}^{a}$ [10^3 pc^{-3}]	$\overline{\rho}_{\rm cluster}{}^{b}$ [pc^{-3}]
D0	1000	392	1.3	15.3
D1	2000	260	2.7	30.6
D2	4000	264	5.3	61.1
D3	8000	78	10.5	122.2
D4	16 000	21	21.1	244.5
D5	32 000	14	42.1	489.2

Notes. Model designation (Col. 1), initial number of stars in the cluster $N_{\rm stars}$ (Col. 2), number of simulations in the campaign $N_{\rm sim}$ (Col. 3), average number density in the cluster core $\overline{\rho}_{\rm core}$ (Col. 4), and average number density in the whole cluster $\overline{\rho}_{\rm cluster}$ (Col. 5). $^{(a)}$ The cluster core radius was assumed to be the radius of the Trapezium ($R_{\rm core} = 0.3$ pc). $^{(b)}$ The cluster radius is 2.5 pc.

References. From Olczak et al. (2010), Steinhausen & Pfalzner (2014).

For each of these clusters, a whole campaign of similar simulations with different random seeds was performed to minimise the effect of initial stellar properties on the encounter history and thus the protoplanetary discs. The numbers of simulations $N_{\rm sim}$ per model are given in Table 3. This approach renders it possible to obtain good statistics of encounters and the resulting changes in the disc size for environments of different densities.

In each simulation the encounter parameters for star-star interactions were recorded. In a diagnostic step, the disc sizes after each encounter were then calculated with these parameters, as described below in Sect. 2.2.

2.2. Encounter simulations

In the diagnostic step the influence of each tracked encounter on the size of the protoplanetary discs was determined. To do this, we used the results of the parameter study by Breslau et al. (2014). Since their study was limited to prograde coplanar parabolic (eccentricity=1) encounters, which are the most destructive, the resulting disc sizes should be regarded as lower limits compared to hyperbolic and/or inclined encounters. Breslau et al. (2014) covered the parameter space for of mass ratios and periastron distances typical for star-disc encounters in cluster environments: $m_{12} = 0.3$−500 and $r_{\rm p} = 0.4$−34, where $m_{12} = m_2/m_1$ is the ratio between the perturber mass (m_2) and the mass of the disc-hosting star (m_1) and $r_{\rm p} = r_{\rm peri}/r_{\rm previous}$ is the periastron distance $r_{\rm peri}$ normalised to the disc size before the encounter $r_{\rm previous}$.

In a diagnostic step, we analysed the cluster simulations described above, using their fit formula

$$r_{\rm disc} = \begin{cases} 0.28 \cdot r_{\rm peri} \cdot m_{12}^{-0.32}, & \text{if } r_{\rm disc} < r_{\rm previous} \\ r_{\rm previous}, & \text{if } r_{\rm disc} \geq r_{\rm previous}, \end{cases} \quad (3)$$

with $r_{\rm peri}$ being the periastron distance in AU, to calculate the disc size after each encounter in these clusters. As Eq. (3) shows, the resulting disc size is independent of the initial disc size as long as it is smaller than this initial value. It is basically the strongest encounter that determines the final disc size. At the beginning of the simulations, all disc sizes in the clusters were set to a universal value $r_{\rm init}$ (for details see Sect. 3.2). Most stars in a cluster undergo multiple encounters during the first few Myr. To take those multiple interactions of one and the same star with (different) other cluster members into account, the value of $r_{\rm previous}$ for the star's ith encounter was set to the disc size

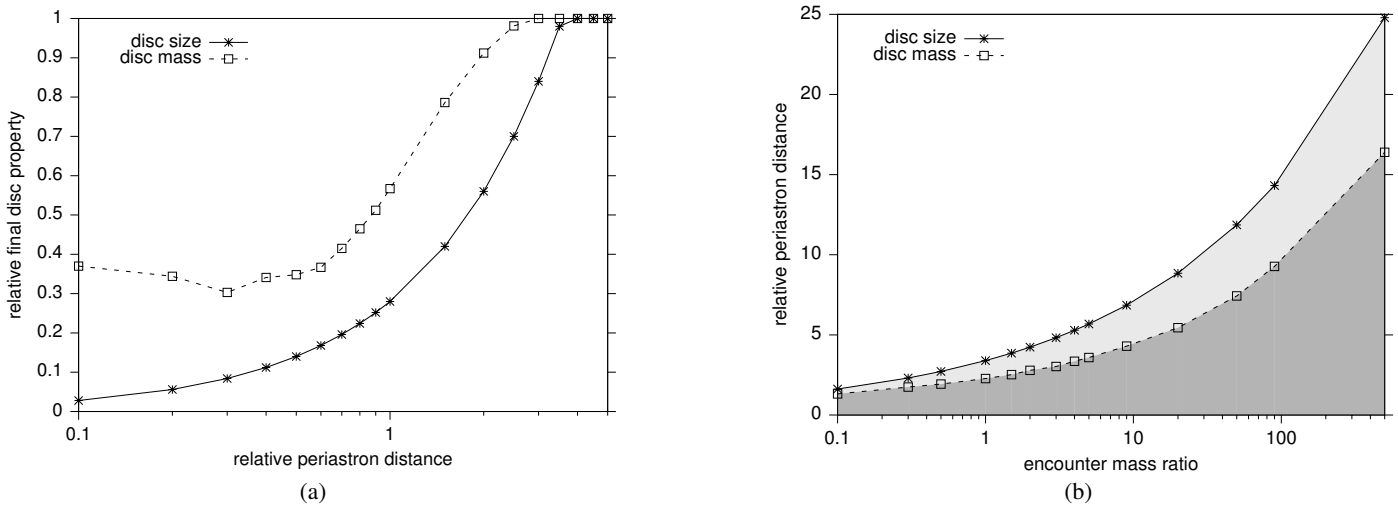

Fig. 1. a) Relative final disc size (asterisks) and disc mass (open squares) after an equal-mass encounter event ($m_{12} = 1$) as a function of the relative periastron distance $r_p = r_{peri}/r_{previous}$, with r_{peri} periastron distance [AU] and $r_{previous}$ disc size before the encounter [AU]. **b)** Parameter pairs (encounter mass ratio m_{12} and relative periastron distance r_p) leading to 5% reduction in disc-size (asterisks) and disc mass (open squares). The light and dark grey areas depict the parameter space in which the disc size and mass are reduced.

resulting from the former $(i-1)$th encounter ($r^i_{previous} = r^{i-1}_{disc}$). This is an approximation as the discs might be "hardened" by stellar fly-bys or have enough time to spread again between two encounters due to viscosity (see Sect. 4). The disc-size change due to multiple encounters needs to be investigated in more detail, taking all these effects into account.

Additionally, we assumed that every star in the clusters was initially surrounded by a thin disc of a given size. Although this results in disc-disc encounters, the stellar interactions were treated as star-disc encounters using Eq. (3). The resulting disc sizes are not expected to differ much from the sizes after disc-disc encounters. For a detailed discussion of the approximations above, see Sect. 4 and Breslau et al. (2014).

Before we present the results, we here clarify some definitions. The code Nbody6 that we used to simulate the clusters was extended to track the stellar encounters and store their properties. For every time step the star with the strongest gravitational influence on a primary star was identified and its orbit calculated, for additional restrictions and details see Olczak et al. (2012). Most such "encounters" are very distant and do not influence the sizes of discs at all. On the other hand, in extreme cases, stellar encounters cannot only alter the disc size, but destroy them completely. Here, the notion "disc-size-reducing encounter" is used for any encounter that (a) reduces the disc size by at least 5% relative to its previous disc size and (b) does not destroy the disc ($r_{disc} > 10$ AU). Consequences of this disc-size reduction limit are discussed in Sect. 4. By contrast, the first encounter that reduces the disc size by at least 5% relative to its previous size and that leads to a final disc size $r_{disc} < 10$ AU is denoted as "disc-destroying encounter". Subsequent, potentially even stronger encounters are not considered in the analysis because the disc is already destroyed. For these very small discs, effects such as viscous accretion and internal photoevaporation may become important, but they were not considered in this work because of the computational effort. Therefore, all discs smaller than 10 AU are denoted "destroyed". The term "strongest encounter" in this work describes the encounter with the strongest influence on the disc, which is not necessarily the closest encounter, because the encounter mass ratio is also factored in.

3. Results

Previous studies of protoplanetary discs mostly investigated the effect of star-disc encounters on the disc mass (e.g. Olczak et al. 2010; Steinhausen & Pfalzner 2014). Before studying this effect on the disc size in an entire star cluster, we first study the influence of a fly-by on a single star-disc system. Recently, Rosotti et al. (2014) noted in their simulations of stellar clusters that more discs are affected by disc truncation than disc-mass loss[1]. Here we wish to quantify this higher sensitivity of the disc size by systematically comparing it to disc-mass loss calculations. We used the results of Breslau et al. (2014) and Steinhausen et al. (2012) to obtain the disc sizes and masses after stellar encounters. In contrast to the disc size, the disc mass-loss strongly depends on the distribution of material in the disc. Here, we used a disc-mass distribution that follows a power-law: $\Sigma \propto r^{-1}$.

3.1. Sensitivity of disc properties

In Fig. 1a, the size (asterisks) and mass (open squares) of a disc after an encounter with an equal-mass perturber ($m_{12} = 1$) are shown as a function of the relative periastron distance $r_p = r_{peri}/r_{previous}$, where r_{peri} is the periastron distance and $r_{previous}$ the disc size before the encounter. The effect of an encounter on the size is much stronger than on the disc mass. For example, a close grazing encounter, equivalent to $r_p = 1$, reduces the disc size to nearly a quarter of its previous size (28%), but it still retains more than half of its mass (57%).

This higher sensitivity of the disc size compared to the disc mass also holds true for encounter partners that differ in mass ($m_{12} \neq 1$). The shaded areas in Fig. 1b depict the parameter space in which the encounters reduce the disc size (asterisks) and disc mass (open squares) by at least 5%. At any given mass ratio a reduction of the disc size by 5% is always achieved already with a much more distant encounter than is necessary for the same reduction in mass. And more importantly, a distant fly-by can affect the disc radius without any change of the disc

[1] They used a disc-mass density distribution according to $\Sigma \propto r^{2/3}$.

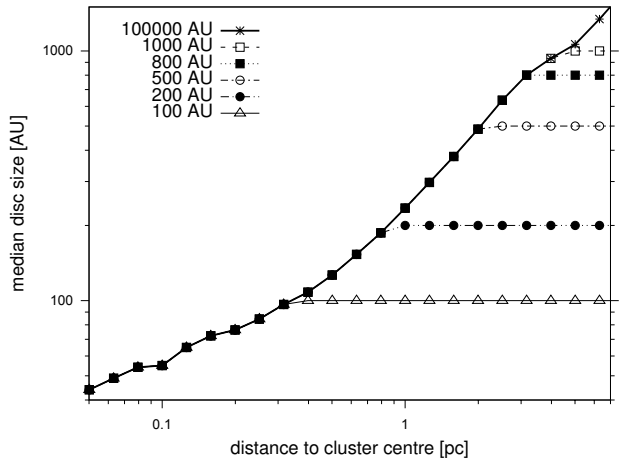

Fig. 2. Median disc size as a function of the distance to the cluster centre for model D2 with different initial disc sizes $r_{\rm init}$: 100 AU (open triangles), 200 AU (filled circles), 500 AU (open circle), 800 AU (filled squares), 1000 AU (open squares), and 100 000 AU (asterisks).

mass[2]. In other words, our data show that, for example, an encounter leading to 5% disc-mass loss can reduce the disc size down to 60% of its previous value. This knowledge can now be used to quantify the sensitivity of the disc size compared to the disc mass in a whole cluster population.

3.2. Initial disc size

Most observed discs in clusters have sizes of 100–200 AU. However, a few protoplanetary discs with radii of a few 100 AU were found in the ONC as well. This indicates that a broad spectrum of sizes exists. It is unclear whether these observed disc sizes are representative for their initial state or whether they changed during the 1–2 Myr since their formation, nor do we know which role the environment played in this context. As a consequence, there is no information available about a natal or initial disc-size distribution within the ONC, for instance.

For this reason, we first investigated how the choice of an initial disc size affects the final disc-size distributions in a cluster. We started our investigation with the model cluster D2, which is representative for the ONC. All stars in this cluster were initially surrounded by discs of the same size $r_{\rm init}$. This initial disc size was then varied from 100 AU to 100 000 AU. Although most encounters occur in the first Myr of cluster evolution (Pfalzner et al. 2006), the simulation time was chosen to be 5 Myr to ensure that all relevant encounters are accounted for.

To obtain an overview of the disc-size distribution in the cluster, the median disc sizes in different radial bins of the cluster were determined. Note that these median disc sizes were determined for each distance-bin separately, not in a cumulative way. Figure 2 shows these median disc sizes for different initial disc sizes – 100 AU (open triangles), 200 AU (filled circles), 500 AU (open circle), 800 AU (filled squares), 1000 AU (open squares), and 100 000 AU (asterisks).

Near the cluster centre the median disc sizes are significantly smaller than in the cluster outskirts. For example, for an initial disc size of 500 AU, the median disc size at the rim of the cluster core (<0.3 pc) is <100 AU, but farther out at 2 pc it is more than five times as large (~500 AU). This trend might be expected because the density is much higher in the inner parts of the clusters. Thus, more encounters occur there and more discs are reduced in size. Furthermore, the encounters in the inner cluster regions are on average closer, that is, they have lower periastrons (see e.g. Scally & Clarke 2001), which is due to the higher density. Therefore, the discs are smaller than in the less dense cluster outskirts.

Overall, if the discs in the ONC were initially larger than 100 AU they are significantly reduced in size by stellar encounters, especially in the cluster core (<0.3 pc). Any initial disc size $r_{\rm init}$ > 100 AU leads to the same median disc size distribution in the cluster core. In addition, an initial disc size >1000 AU was assumed; the final median disc size distribution in the cluster is the same up to a distance of ~4 pc, which in the case of the ONC would be the entire cluster ($R_{\rm cluster}$ = 2.5 pc). This finding was then used to set up discs in the different cluster types to study their influence on the disc-size distribution.

3.3. Numerical experiment

Building on this finding that the median final disc size in a cluster is largely independent of the initial disc size, we performed a numerical experiment to be able to separate processed from unprocessed discs. The initial disc sizes in each cluster were set to $r_{\rm init}$ = 100 000 AU (asterisks in Fig. 2). Although this is not a realistic scenario, it allowed us to determine the relevance of encounters in the cluster environments.

This numerical experiment is applied to clusters of different average densities, ranging from 15 pc^{-3} (model D0) to ~500 pc^{-3} (model D5). For the densities of the other models, see Table 3. The cluster model D2 was denoted ONC model because after 1 Myr of cluster evolution it was representative for today's ONC, see Sect. 2.1. Discs that were destroyed ($r_{\rm disc}$ < 10 AU) were excluded from the data set and treated separately. If not indicated otherwise, the outcome of the cluster simulations after 5 Myr of evolution is shown.

3.3.1. Disc-size distributions

As a first step, we quantified the amount of discs that are influenced by encounters in the different cluster environments. Figure 3 shows the fraction of stars that undergo at least one disc-size reducing encounter (solid line, filled circles) as a function of the average cluster number density. The fraction of stars with disc-size-reducing encounters increases, as expected, with cluster density. In the least dense clusters, some stars do not undergo any encounter at all or only very weak ones, that is, low mass ratios and high periastrons. Here the fraction of stars with disc-size-reducing encounters is ~65%. By contrast, in the densest cluster, stellar encounters are very frequent and stronger, that is, high mass ratios and/or lower periastrons. In this cluster type, nearly all stars (~90%) undergo at least one disc-size reducing encounter.

The initial size of the discs was set to 100 000 AU, thus, after the first disc-size-reducing encounter it might still be as large as 95 000 AU. But most encounters reduce the discs to much lower values and most discs undergo several disc-size-reducing encounters in the 5 Myr of cluster development. Consequently, two questions arise: i) what is the final disc-size distribution? and ii) how many discs are destroyed? The dashed and dashed-dotted lines with filled circles in Fig. 3 depict the fractions of discs with a final size smaller than 1000 AU and 100 AU (see also Table 4).

[2] The disc-mass change is also less sensitive than the angular momentum change, see Olczak et al. (2006), Pfalzner & Olczak (2007), Steinhausen et al. (2012).

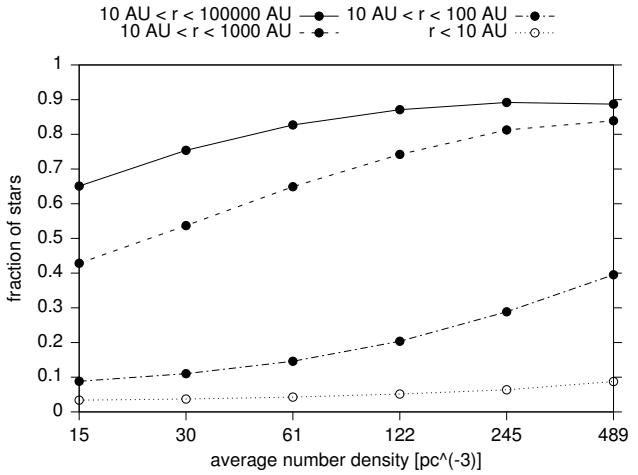

Fig. 3. Fraction of stars with destroyed discs (open circles) and whole discs (filled circles) as a function of the average cluster density. Depicted are discs smaller than 100 000 AU (solid line), smaller than 1000 AU (dashed line), and smaller than 100 AU (dashed-dotted line) after 5 Myr.

The fraction of stars with discs smaller than 1000 AU nearly doubles from low-density clusters (43%) to high-density clusters (84%). Nevertheless, even in environments with densities of 15 pc^{-3}, stellar encounters significantly reduce the sizes of discs. The slope of the curve flattens towards the high-density cluster end, see Fig. 3. This flattening can be explained by studying the fraction of destroyed discs[3] (dotted line, open circles). It amounts to ∼9% in model D5, which means that in this case, nearly all discs (97%) are either influenced by a disc-size-reducing encounter or are destroyed. This is near saturation, which is the reason for the flattening of the slope. Furthermore, the fraction of disc-destroying encounters triples from ∼3% in model D0 to ∼9% in model D5 (see Table 4), whereas the whole discs <1000 AU only double. This additionally limits the fraction of discs smaller than 1000 AU.

The fraction of stars with final disc sizes <100 AU also increases with cluster density (dashed-dotted line). In the high-density cluster model it is four times higher than in the low-density model, ∼40% and ∼10%. In this case, only 19% of all discs in model D5 are either reduced to sizes <100 AU or destroyed, so there is no flattening of the slope due to near saturation. The fraction of discs <100 AU increases much more strongly with cluster density than the fraction of discs <1000 AU. For example, in the least dense cluster the ratio between discs smaller than 1000 AU and discs smaller than 100 AU is roughly 5:1, whereas for the densest cluster it increases to nearly 2:1. The reason is that the increasing cluster density leads to closer encounters that in turn reduce many more discs to smaller sizes. Summarising, the final disc size distribution and the fraction of destroyed discs strongly depends on the average cluster number density.

3.3.2. Distance to the cluster centre

We have shown that the final disc sizes strongly depend on the average number density of their cluster environment. Each of these clusters was set up with a density profile according to Eq. (1), so they are much denser in the inner regions than in the outskirts. Therefore, the disc sizes should also be a function of the position of the disc-hosting star in the cluster. In Fig. 4 we compare the median disc sizes as a function of the star's final (after 5 Myr) distance to the cluster centre in the different clusters. For comparison, the line with asterisks is the same as in Fig. 2.

As expected, the median final disc size increases with the distance to the cluster centre for all average cluster densities. Stars that are finally located at a distance of 0.3 pc from the cluster centre have a median disc size of about 200 AU in the sparsest cluster (D0, open squares), whereas in the cluster outskirts it is much larger, for instance ∼2400 AU at a distance of 3 pc. For the densest clusters model D5, the median disc sizes are much smaller as a result of the elevated rate of close encounters, as described before, but the dependence on the host star position in the cluster is the same. At 0.3 pc the median disc size is about 20 AU, whereas at 3 pc it is ∼300 AU (open triangles).

To obtain the variation of disc sizes in the clusters, the shaded area in Fig. 4 depicts the disc-size range for 50% of all stars in the ONC model that have disc sizes of about the median size (asterisks). For example, half of the stars with final distances of 0.3 pc to the cluster centre, which represents the border of the Trapezium in the ONC, have discs with sizes of 40−200 AU. The median disc size at this distance is 100 AU. At the cluster radius of the ONC (2.5 pc), half of all discs have sizes between 300−1300 AU, the median disc size is 630 AU. This means that half of the stars in the ONC model have disc sizes that vary by about a factor of two about the median, but which are still much smaller than the initial disc size of 100 000 AU. The final disc size is a function of the host star position in the cluster, or in other words, not only of the global average cluster density, but also of the local density of its environment.

Table 4. Fractions of discs influenced by encounters.

Model	$\overline{\rho}_{\rm cluster}$ [pc^{-3}]	$f_{\rm reduced}$	$f_{<1000\ \rm AU}$	$f_{<100\ \rm AU}$	$f_{\rm destroyed}$
D0	15	65.1%	42.8%	8.8%	3.4%
D1	30	75.4%	53.7%	11.0%	3.7%
D2	61	82.7%	64.9%	14.6%	4.3%
D3	122	87.1%	74.2%	20.4%	5.2%
D4	245	89.2%	81.3%	28.8%	6.4%
D5	489	88.7%	83.9%	39.2%	8.7%

Notes. Fraction of stars with disc-size-reducing encounters (Col. 3), with discs smaller than 1000 AU (Col. 4), with discs smaller than 100 AU (Col. 5), and with destroyed discs (Col. 6) in the different cluster models (Col. 1) after 5 Myr of cluster evolution. The average number densities of the cluster models are given in Col. 2 (rounded values, taken from Table 3).

3.3.3. Disc sizes for different stellar types

As mentioned in Sect. 1, it is still a subject of debate whether the disc size is a function of the stellar mass. We investigated whether encounter-induced disc-size reduction might be responsible for this potential dependency. Figure 5 shows the median disc size as a function of stellar mass and spectral type. For clarity, only the results for models D0 (open squares), D2 (asterisks), and D5 (open triangles) are shown.

The median disc size does indeed depend on the stellar mass. For M- to B-type stars in the ONC model, the median disc size increases by roughly a factor of two, from 420 AU to 880 AU. Around O-stars the discs are smaller than around all other star

[3] A detailed description of the properties of the disc-destroying encounters can be found in the appendix.

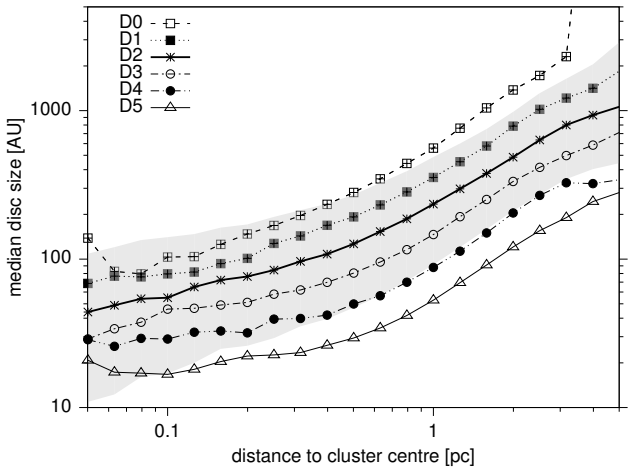

Fig. 4. Median disc size in clusters of different densities (rising from D0, open squares, to D5, open triangles) for different distances of the disc-hosting star to the cluster centre (bins). The line with asterisks indicates the ONC model, with the grey area containing 50% of all stars with disc sizes around the median disc size. For explanations, see text.

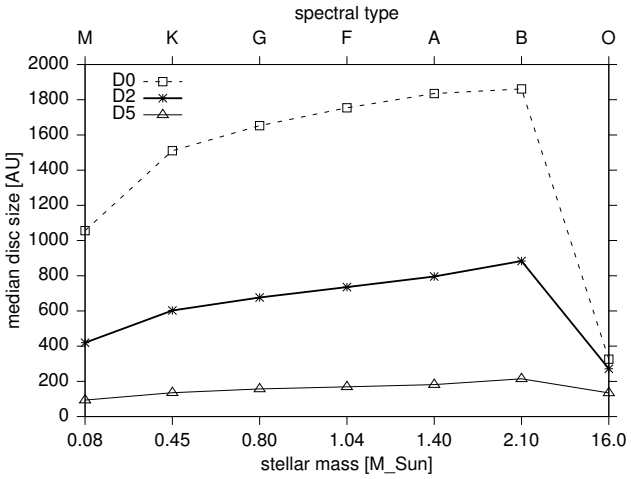

Fig. 5. Median disc size in cluster models D0 (open squares), D2 (asterisks), and D5 (open triangles) as a function of the stellar mass [$M_\odot$] and spectral type.

types with a median size of 270 AU. The same trend in median disc sizes can be found for models of lower density (e.g. model D0 in Fig. 5). The smaller sizes of discs around O-stars in models D0 and D2 can be explained by the encounter frequency, which as a function of the relative perturber mass has two peaks (see Fig. 4 of Olczak et al. 2010). One peak lies at low mass-ratios, the other one at high mass-ratios. For model D0 the high-mass stars dominate the encounter history because of gravitational focusing. Therefore, the difference between the median disc sizes of M-stars and O-stars is largest in this model.

In contrast, in model D5 the median disc size of O-stars (130 AU) is slightly larger than the one of M-stars (~90 AU). In this cluster type, the low-mass stars dominate the encounter history so that M-stars have slightly smaller discs than all other star types – including O-stars. The ONC model D2 represents a turning point: the most massive and least massive stars are equally important as encounter partners. Thus, the absolute difference between the discs around M-stars and O-stars is smaller than in model D0.

All cluster models were set up without primordial mass segregation. Nevertheless, in the 5 Myr of cluster evolution, dynamical mass segregation might occur. The final positions of the B- and O-stars showed no mass segregation in the low-density clusters and only weak mass segregation in the densest models. Therefore, the impact of gravitational focusing on the disc size – especially in the low-density clusters – is most probably stronger than the effect of dynamical mass segregation.

4. Discussion and conclusion

Our simulations include several assumptions. Their influence on the results is discussed below.

Most stellar clusters show signs of mass segregation, but whether this is the case for the ONC is still under debate, cf. Bonnell & Davies (1998), Olczak et al. (2011), Huff & Stahler (2006). It is currently unclear whether clusters are primordially mass-segregated or not. Here we did not take into account any primordial mass segregation, only dynamical mass segregation during the simulation. This was done for simplicity because we aimed to study clusters of different densities and their influence on disc sizes. Primordial mass segregation would have increased the initial cluster-core density and altered the encounter frequency. Primordial mass segregation affects this type of clusters in two ways: i) the most massive stars undergo many more encounters as a result of their location in the dense cluster centre, and therefore the disc sizes are smaller around O-stars than in the case without mass-segregation; ii) the stronger gravitational focusing increases the number of encounters. This leads to a somewhat lower disc frequency and smaller disc sizes, mainly around the O-stars.

All stars in the clusters were assumed to be initially single, neglecting primordial binaries. If these were included, more discs would be truncated to a smaller size or even destroyed by the binary stars, especially for very close binaries. Köhler et al. (2006) found that the binary frequency in the ONC is higher for stars with masses >2 $M_\odot$ than for low-mass stars. Generally, the binary frequency increases with stellar mass, see Duchêne & Kraus (2013). In our simulations, primordial binaries would therefore lead to even smaller discs for B- and O-stars than anticipated in Fig. 5.

The cluster models investigated are representative for young, massive clusters that are still embedded in their natal gas. In the solar neighbourhood the star formation efficiency is relatively low (30%) and the gas expulsion drives the expansion of the cluster, while at the same time a large portion of its stars becomes unbound (Pfalzner & Kaczmarek 2013). Observations of stellar clusters indicate that after 1–3 Myr the gas is expelled from the cluster and thus the star-formation process ends. We did not consider the effect of gas expulsion. In a follow-up paper, this case of cluster dynamics will be studied in detail.

We chose an artificially large initial disc of 100 000 AU around every star to determine the relevance of encounters in a cluster environment. Such discs are not physical, but have to be seen as part of the performed numerical experiment. The resulting median disc sizes can thus not represent any real distribution as found in the ONC, for example, but rather give a first estimate of the influence of encounters on discs after 5 Myr of evolution, especially when considering that other effects are neglected (see below). The surprisingly good match to the observed data shows that the process of disc-size reduction that is due to stellar encounters is indeed important and should not be neglected. The largest discs in the ONC could have formed even larger and already have been pruned to their current size by dynamical interactions.

All encounters in the clusters were assumed to be prograde, coplanar, and parabolic (eccentricity =1). These are the most destructive encounters (Clarke & Pringle 1993; Pfalzner et al. 2005b). Especially in very dense clusters, a large portion of encounters can have eccentricities > 1. Such eccentric orbits are less efficient in removing disc mass (Olczak et al. 2010). In addition, inclined encounters are common in cluster environments. Coplanar encounters lead to smaller disc sizes than their inclined counterparts. Therefore, the cases of parabolic coplanar encounters should be regarded as lower limits (Breslau, in prep.).

There are other effects that might influence the disc size. First, we used the formula of Breslau et al. (2014) to describe star-disc encounters. It might have been more appropriate to investigate disc-disc encounters. However, it was shown by Pfalzner et al. (2005a) that in disc-disc encounters between low-mass discs (0.01 $M_{\odot}$) material is exchanged, but it is mainly transferred to the inner disc regions. Since the disc size is determined using the steepest point in the outer slope of the disc density distribution, this captured disc material is not expected to alter the final size much.

Second, it has been suggested that photoevaporation might be an important mechanism to shrink or completely destroy discs (see e.g. Störzer & Hollenbach 1999; Scally & Clarke 2002; Johnstone et al. 2004; Adams et al. 2006; Alexander et al. 2006; Ercolano et al. 2008; Gorti & Hollenbach 2009; Drake et al. 2009). However, we modelled stellar clusters in the embedded phase, during which stage the presence of the natal gas is expected to reduce the effect of photoevaporation. If photoevaporation nevertheless played a role, the presented disc sizes would be even smaller for stars close to the most massive stars, especially near the cluster core.

Third, the discs were modelled consisting of mass-less tracer particles and hydrodynamical effects were excluded, for an in-depth discussion see Breslau et al. (2014). Rosotti et al. (2014) found that the hydrodynamical evolution of the discs is important for high viscosity. In this case, the discs spread quite rapidly after an encounter and compensate for the size reduction that is due to encounters. In the case of low viscosity, it was the closest encounter alone that determined the final disc size. The encounters were particularly important in the dense central cluster areas. We did not include viscous disc spreading in our simulations. If we had considered this effect, the discs that already underwent their strongest encounter (high mass ratio and/or small periastron distance) would have been most affected by changes due to disc spreading. If the disc had had time to expand again, the final disc size after a subsequent relatively strong encounter would have been larger than presented here. To study this effect in more detail, the next natural step would be to include viscous spreading in our type of simulations.

As a result of its sensitivity, the disc size is a suitable tool for quantifying the influence of the stellar environment. One indication that this might be the case comes from the observations by Vicente & Alves (2005). They found that roughly 60% of the Trapezium stars (<0.3 pc) have discs smaller than 50 AU. Our simulations indicate that for model D2 (ONC), the median disc size of all stars in the cluster core (<0.3 pc) is roughly 80 AU. This fits the observed values remarkably well, especially when considering that our simulations only take into account stellar encounters as a source of disc-size influence. They play an important role in terms of disc-sizes but should be taken together with the other effects discussed above (photoevaporation, viscous disc-spreading, etc.) to reproduce the actual disc-size distributions as found in stellar clusters today.

The protoplanetary discs may eventually form planetary systems. Their potential physical extent, as shown above, is defined to a high degree by the birth environment. The influence of a stellar cluster on already formed planetary systems has been studied theoretically in the past (e.g. Craig & Krumholz 2013; Malmberg et al. 2011). Craig & Krumholz (2013) found that in dispersing, substructured clusters planets close to their host stars (few tens of AU distance) are not perturbed by stellar flybys. Compared to the spherical clusters modelled here, the substructures lead to regions of enhanced stellar density and thus to a higher encounter frequency in certain areas of the cluster. These substructures dissolve in most cases at the latest when the whole cluster disperses. When the substructures are taken as regions of (transiently) enhanced stellar density, our results support their findings, as only a few per cent of discs are completely destroyed (<10 AU), while most discs are finally larger than a few tens of AU, see Fig. 3.

5. Summary

We investigated the influence of the cluster environment on the disc size. Combining Nbody simulations of clusters of different densities with simulations of protoplanetary discs after star-disc encounters, we found that unlike the disc mass, the disc size can already be changed by relatively distant encounters. We performed a numerical experiment, choosing a very large initial disc size around each star. The results show that encounters are capable of reducing disc sizes of most stars to values <1000 AU in all investigated clusters. The resulting sizes agree well with typical disc sizes found by observations in the ONC today, for example. It might be that the cluster environment rather than the initial size determines the final extent of a protoplanetary disc in many cases.

Appendix A: Properties of disc-destroying encounters

Figure A.1a shows the fraction of disc-destroying encounters as a function of the encounter mass ratio for three cluster models (D0, D2, D5). For the densest cluster model (D5, open triangles), the encounter mass-ratio distribution has two peaks: one at low mass ratios (m_{12} = 3) and a second smaller peak at very high mass ratios (m_{12} = 250). So the disc-destroying encounters most probably have quite low mass ratios in this environment. This is in accordance with the results of Olczak et al. (2010). They found that in clusters of higher density than the ONC the low-mass stars dominate the encounter history, leading to lower encounter mass ratios. They stated that the ONC itself is a turning point, low-mass and high-mass stars similarly contribute to the encounter history. This is reflected in the encounter mass-ratio distribution for the ONC model (asterisks), which is flat and does not show any sign of a preferred mass ratio for disc-destroying encounters. For the least dense cluster model (D0, open squares), one would expect, based on the work of Olczak et al. (2010), that high mass-ratio encounters should be largely responsible for disc destruction, as the most massive stars undergo many encounters due to gravitational focusing. But this is not the case, as Fig. A.1a shows. The distribution of disc-destroying encounters has a very broad peak at low mass ratios. This might be due to the mass sampling in this work: the masses were randomly sampled from an IMF (see Sect. 2) so it is more probable to obtain very massive stars in clusters with higher membership. In low-mass

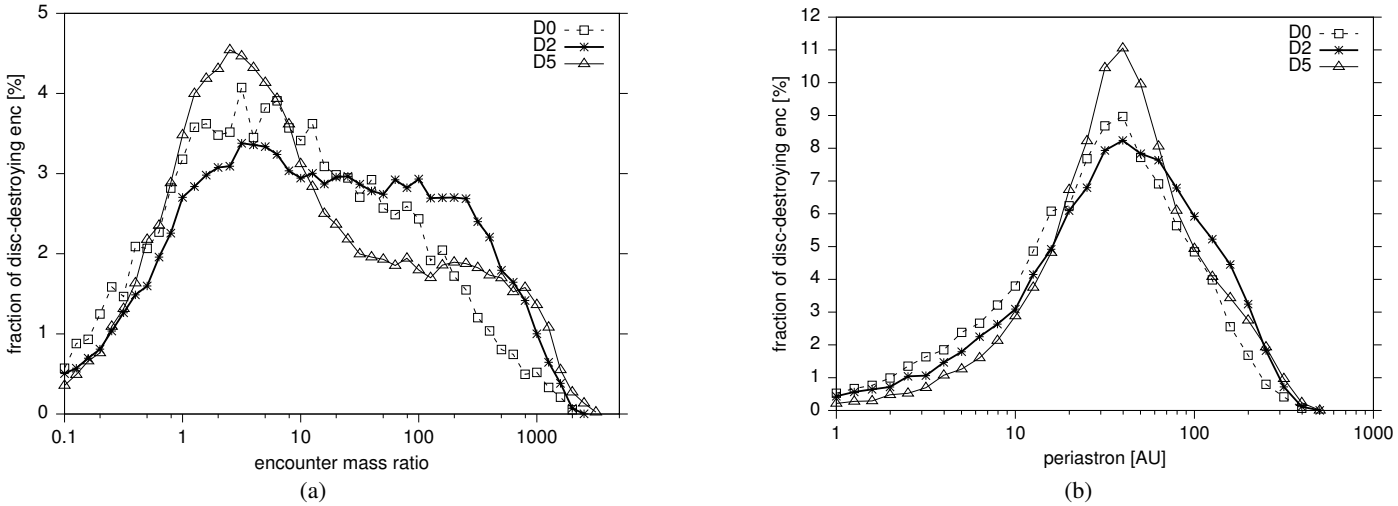

Fig. A.1. **a)** Fraction of disc-destroying encounters as function of the mass ratio and **b)** fraction of disc-destroying encounters as function of the periastron distance for cluster models D0 (open squares), D2 (asterisks), and D5 (open triangles).

clusters the most massive star is – on average – less massive than in the high-mass cluster.

Figure A.1b shows the fraction of disc-destroying encounters as a function of their periastron distance for the same cluster models as above (D0, D2, D5). For all cluster types most disc-destroying encounters typically have distances of about 30−40 AU. The distribution for model D2 is slightly broader than those of the other cluster models. The disc size is determined by both the periastron distance and the mass ratio (see Eq. (3)), thus, this is in accordance with the broad spectrum of mass ratios for the disc-destroying encounters in Fig. A.1a. If the mass ratio is low, the encounter has to be closer, meaning that the periastron distance needs to be smaller, to destroy a disc than is necessary in a high mass-ratio case.

Appendix B: Location of disc-destroying encounters

The larger part of discs is influenced by their stellar encounters (65−89%, see Table 4), but is not destroyed. As already mentioned in Sect. 3.3.1, in the sparsest cluster, about 3% of the discs are destroyed after 5 Myr; for the densest cluster this fraction increases to ∼9%. This means that the fraction of destroyed discs increases with increasing average cluster density. Analogously to the analysis in Sect. 3.3.2, we can now determine whether the disc-destroying encounters are also a function of the star's position in the cluster, or in other words, a function of the local density.

Figure B.1 shows the position of the disc-hosting stars at the time of the encounter for three different cluster models (D0, open squares, D2, asterisks, and D5, open triangles). For the least dense cluster, most disc-destroying encounters take place at a distance of 0.1−0.2 pc from the cluster centre. In the case of the ONC model cluster (D2, asterisks) the whole curve is shifted towards lower distances. As the cluster is much denser than model D0, more destructive encounters occur at such small distances from the cluster centre. For the densest cluster model (D5, open triangles), the distribution is entirely different. In this cluster type, the encounters are dominated by low-mass stars, in contrast to the low-density clusters where the most massive stars dominate the encounter history (Olczak et al. 2010). As a result,

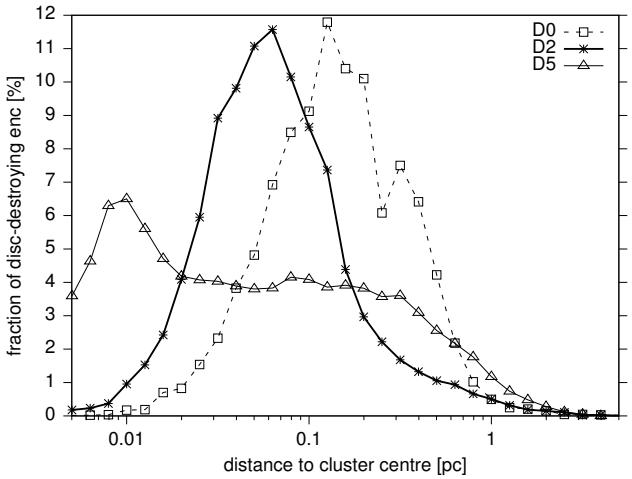

Fig. B.1. Fraction of disc-destroying encounters as function of distance to the cluster centre where they took place for cluster models D0 (open squares), D2 (asterisks), and D5 (open triangles).

the distribution of locations is much shallower and peaks only in the most inner part of the cluster (∼0.01 pc).

References

Aarseth, S. J. 1973, Vistas in Astronomy, 15, 13
Aarseth, S. J. 2003, Gravitational *N*-Body Simulations (Cambridge, UK: Cambridge University Press), 430
Adams, F. C. 2010, ARA&A, 48, 47
Adams, F. C., Proszkow, E. M., Fatuzzo, M., & Myers, P. C. 2006, ApJ, 641, 504
Alexander, R. D., Clarke, C. J., & Pringle, J. E. 2006, MNRAS, 369, 229
Andrews, S. M., & Williams, J. P. 2007, ApJ, 659, 705
Andrews, S. M., Wilner, D. J., Hughes, A. M., Qi, C., & Dullemond, C. P. 2009, ApJ, 700, 1502
Andrews, S. M., Wilner, D. J., Hughes, A. M., Qi, C., & Dullemond, C. P. 2010, ApJ, 723, 1241
Balbus, S. A., & Hawley, J. F. 2002, ApJ, 573, 749
Bell, C. P. M., Naylor, T., Mayne, N. J., Jeffries, R. D., & Littlefair, S. P. 2013, MNRAS, 434, 806
Bonnell, I. A., & Davies, M. B. 1998, MNRAS, 295, 691
Breslau, A., Steinhausen, M., Vincke, K., & Pfalzner, S. 2014, A&A, 565, A130
Brinch, C., & Jørgensen, J. K. 2013, A&A, 559, A82
Clarke, C. J., & Pringle, J. E. 1993, MNRAS, 261, 190
Craig, J., & Krumholz, M. R. 2013, ApJ, 769, 150

de Juan Ovelar, M., Kruijssen, J. M. D., Bressert, E., et al. 2012, A&A, 546, L1
Drake, J. J., Ercolano, B., Flaccomio, E., & Micela, G. 2009, ApJ, 699, L35
Duchêne, G., & Kraus, A. 2013, ARA&A, 51, 269
Eisner, J. A., Plambeck, R. L., Carpenter, J. M., et al. 2008, ApJ, 683, 304
Ercolano, B., Drake, J. J., Raymond, J. C., & Clarke, C. C. 2008, ApJ, 688, 398
Gorti, U., & Hollenbach, D. 2009, ApJ, 690, 1539
Haisch, Jr., K. E., Lada, E. A., & Lada, C. J. 2000, AJ, 120, 1396
Hall, S. M. 1997, MNRAS, 287, 148
Hall, S. M., Clarke, C. J., & Pringle, J. E. 1996, MNRAS, 278, 303
Harayama, Y., Eisenhauer, F., & Martins, F. 2008, ApJ, 675, 1319
Harsono, D., Jørgensen, J. K., van Dishoeck, E. F., et al. 2014, A&A, 562, A77
Hillenbrand, L. A. 1997, AJ, 113, 1733
Hillenbrand, L. A., & Carpenter, J. M. 2000, ApJ, 540, 236
Hillenbrand, L. A., & Hartmann, L. W. 1998, ApJ, 492, 540
Hillenbrand, L. A., Strom, S. E., Calvet, N., et al. 1998, AJ, 116, 1816
Huff, E. M., & Stahler, S. W. 2006, ApJ, 644, 355
Johnstone, D., Hollenbach, D., & Bally, J. 1998, ApJ, 499, 758
Johnstone, D., Matsuyama, I., McCarthy, I. G., & Font, A. S. 2004, in Rev. Mex. Astron. Astrofis. Conf. Ser., 22, eds. G. Garcia-Segura, G. Tenorio-Tagle, J. Franco, & H. W. Yorke, 38
Klahr, H. H., & Bodenheimer, P. 2003, ApJ, 582, 869
Kobayashi, H., & Ida, S. 2001, Icarus, 153, 416
Köhler, R., Petr-Gotzens, M. G., McCaughrean, M. J., et al. 2006, A&A, 458, 461
Kroupa, P. 2002, Science, 295, 82
Lada, E. A., Depoy, D. L., Evans, II, N. J., & Gatley, I. 1991, ApJ, 371, 171
Lada, C. J., Muench, A. A., Haisch, Jr., K. E., et al. 2000, AJ, 120, 3162
Malmberg, D., Davies, M. B., & Heggie, D. C. 2011, MNRAS, 411, 859
Matsuyama, I., Johnstone, D., & Hartmann, L. 2003, ApJ, 582, 893
McCaughrean, M. J., & O'dell, C. R. 1996, AJ, 111, 1977
McCaughrean, M. J., & Stauffer, J. R. 1994, AJ, 108, 1382
Moeckel, N., & Bally, J. 2007, ApJ, 656, 275
O'dell, C. R. 1998, AJ, 115, 263
Olczak, C., Pfalzner, S., & Spurzem, R. 2006, ApJ, 642, 1140
Olczak, C., Pfalzner, S., & Eckart, A. 2008, A&A, 488, 191
Olczak, C., Pfalzner, S., & Eckart, A. 2010, A&A, 509, A63
Olczak, C., Spurzem, R., & Henning, T. 2011, A&A, 532, A119
Olczak, C., Kaczmarek, T., Harfst, S., Pfalzner, S., & Portegies Zwart, S. 2012, ApJ, 756, 123
Pfalzner, S. 2004, ApJ, 602, 356
Pfalzner, S. 2013, A&A, 549, A82
Pfalzner, S., & Kaczmarek, T. 2013, A&A, 559, A38
Pfalzner, S., & Olczak, C. 2007, A&A, 462, 193
Pfalzner, S., Umbreit, S., & Henning, T. 2005a, ApJ, 629, 526
Pfalzner, S., Vogel, P., Scharwächter, J., & Olczak, C. 2005b, A&A, 437, 967
Pfalzner, S., Olczak, C., & Eckart, A. 2006, A&A, 454, 811
Pfalzner, S., Steinhausen, M., & Menten, K. 2014, ApJ, 793, L34
Rosotti, G. P., Dale, J. E., de Juan Ovelar, M., et al. 2014, MNRAS, 441, 2094
Scally, A., & Clarke, C. 2001, MNRAS, 325, 449
Scally, A., & Clarke, C. 2002, MNRAS, 334, 156
Scally, A., Clarke, C., & McCaughrean, M. J. 2005, MNRAS, 358, 742
Shu, F. H., Adams, F. C., & Lizano, S. 1987, ARA&A, 25, 23
Spurzem, R. 1999, J. Comput. Appl. Math., 109, 407
Steinhausen, M., & Pfalzner, S. 2014, A&A, 565, A32
Steinhausen, M., Olczak, C., & Pfalzner, S. 2012, A&A, 538, A10
Stolte, A., Brandner, W., Brandl, B., Zinnecker, H., & Grebel, E. K. 2004, AJ, 128, 765
Störzer, H., & Hollenbach, D. 1999, ApJ, 515, 669
Vicente, S. M., & Alves, J. 2005, A&A, 441, 195

The Astrophysical Journal, 828:48 (10pp), 2016 September 1 doi:10.3847/0004-637X/828/1/48

CLUSTER DYNAMICS LARGELY SHAPES PROTOPLANETARY DISK SIZES

Kirsten Vincke and Susanne Pfalzner
Max Planck Institute for Radio Astronomy, Auf dem Hügel 69, D-53121 Bonn, Germany; kvincke@mpifr-bonn.mpg.de
Received 2015 November 23; revised 2016 June 20; accepted 2016 June 21; published 2016 August 29

ABSTRACT

To what degree the cluster environment influences the sizes of protoplanetary disks surrounding young stars is still an open question. This is particularly true for the short-lived clusters typical for the solar neighborhood, in which the stellar density and therefore the influence of the cluster environment change considerably over the first 10 Myr. In previous studies, the effect of the gas on the cluster dynamics has often been neglected; this is remedied here. Using the code NBody6++, we study the stellar dynamics in different developmental phases—embedded, expulsion, and expansion—including the gas, and quantify the effect of fly-bys on the disk size. We concentrate on massive clusters ($M_{\rm cl} \geqslant 10^3$–$6 * 10^4\ M_{\rm Sun}$), which are representative for clusters like the Orion Nebula Cluster (ONC) or NGC 6611. We find that not only the stellar density but also the duration of the embedded phase matters. The densest clusters react fastest to the gas expulsion and drop quickly in density, here 98% of relevant encounters happen before gas expulsion. By contrast, disks in sparser clusters are initially less affected, but because these clusters expand more slowly, 13% of disks are truncated after gas expulsion. For ONC-like clusters, we find that disks larger than 500 au are usually affected by the environment, which corresponds to the observation that 200 au-sized disks are common. For NGC 6611-like clusters, disk sizes are cut-down on average to roughly 100 au. A testable hypothesis would be that the disks in the center of NGC 6611 should be on average ≈20 au and therefore considerably smaller than those in the ONC.

Key words: galaxies: star clusters: general – planetary systems – protoplanetary disks

1. INTRODUCTION

Most stars are born in stellar clusters, which in turn form from dense cores in giant molecular clouds (GMCs). At least for massive clusters ($M_{\rm cl} > 10^3\ M_{\odot}$), it is known that they are highly dynamical structures and follow well-defined evolutionary tracks, depending on their initial mass and size (Pfalzner & Kaczmarek 2013b). At very young ages, they are still embedded in their natal gas; the duration of this embedded phase is thought to last between 1 and 3 Myr for clusters in the solar neighborhood (Leisawitz et al. 1989; Lada & Lada 2003; Portegies Zwart et al. 2010). Comparing the gas and stellar content in nearby star forming regions, observations find that the fraction of gas in a GMC that is turned into stars (referred to as star formation efficiency—SFE) lies in the range of 10%–35% (Lada & Lada 2003). Similarly, simulations that model the expansion history of massive clusters in the solar neighborhood find that the SFE of these clusters must have been of the order of 30% (Pfalzner & Kaczmarek 2013b). In comparison, the SFE for an entire molecular cloud is much lower, only of the order of just a few percent at most (see, e.g., Murray 2011; García et al. 2014).

At the end of the star formation process, the remaining gas is expelled through various mechanisms such as, for example, the explosion of a supernova (Zwicky 1953; Pelupessy & Portegies Zwart 2012), bipolar stellar outflows (Matzner & McKee 2000), or stellar winds of the most massive stars (Zwicky 1953; Dale et al. 2012; Pelupessy & Portegies Zwart 2012; Dale et al. 2015). It is expected that supernovae will ultimately remove any remaining gas from the cluster, but probably other processes like wind are more important, as clusters are already found to be gas poor at 1–3 Myr, whereas even supernova with 25 $M_{\rm Sun}$ need already 7–8 Myr until they explode. The gas expulsion itself is thought to happen on timescales smaller than, or of the order of, the dynamical times of the cluster (Geyer & Burkert 2001; Melioli & de Gouveia dal Pino 2006; Portegies Zwart et al. 2010). Gas expulsion is supposed to happen earlier in massive than in low-mass clusters due to the larger number of high-mass stars.

The gas expulsion leaves the clusters in a supervirial state and they react by expanding with a simultaneous loss of a considerable portion of their members. The cluster dynamics after gas expulsion has been investigated thoroughly in the past (e.g., Lada et al. 1984; Goodwin 1997; Adams 2000; Geyer & Burkert 2001; Kroupa et al. 2001; Boily & Kroupa 2003a, 2003b; Fellhauer & Kroupa 2005; Goodwin & Bastian 2006; Baumgardt & Kroupa 2007; Lüghausen et al. 2012; Pfalzner et al. 2014, 2015b).

Within the clusters, their members interact with each other, influencing already formed protoplanetary disks. Processes like external photoevaporation (Johnstone et al. 1998, 2004; Störzer & Hollenbach 1999; Scally & Clarke 2002; Matsuyama et al. 2003; Adams et al. 2006; Alexander et al. 2006; Ercolano et al. 2008; Drake et al. 2009; Gorti & Hollenbach 2009), viscous torques (Shu et al. 1987), turbulent effects (Klahr & Bodenheimer 2003), and magnetic fields (Balbus & Hawley 2002) are capable of reducing the disks in size, mass, and/or angular momentum.

However, here we concentrate on the effect of the gravitational forces acting during close stellar fly-bys, which shape the disks, resulting in the loss of angular momentum (e.g., Pfalzner & Olczak 2007) and/or mass (e.g., Clarke & Pringle 1993; Hall 1997; Scally & Clarke 2001; de Juan Ovelar et al. 2012).

Ideally, one would simulate the entire cluster with each of the stars surrounded by a disk using the smoothed particle hydrodynamics (SPH) methods. In this case, effects like viscous spreading of the disks and multiple fly-bys would all be treated in a self-consistent way. Still, even with modern supercomputers, this is extremely challenging. Rosotti et al. (2014) performed a direct theoretical investigation of disk sizes

in clusters by combining *N*-body simulations of a low-mass cluster (100 stars) with SPH simulations of protoplanetary disks and determined the disk sizes. Even for such a low-mass cluster, they could only model the first 0.5 Myr of the development and had to make the artificial assumption of the stars to be of equal mass due to computational constraints. Thus, for the time being, direct modeling of massive clusters, and even more so a parameter study of them, is completely out of the question.

Therefore, the standard procedure is a two step approach. - First, *N*-body simulations of the cluster dynamics are performed where the fly-by history of each star is recorded and, second, results from parameter studies are used to post-process the data and determine the effect on the disks (e.g., Scally & Clarke 2001; Olczak et al. 2006; Pfalzner et al. 2006; Olczak et al. 2010; Steinhausen & Pfalzner 2014). These studies concentrated on the disk frequency, average disk mass, and angular momentum in the embedded phase of the cluster. However, none of these studies considered the gas content as such or the effect that the gas expulsion process has on the cluster dynamics. Here we want to concentrate instead on the disk size, because (a) it is the most sensitive indicator for the cluster influence (Rosotti et al. 2014; Vincke et al. 2015), (b) with the advent of ALMA, a direct comparison with observations is possible, and (c) it gives limits on the sizes of the potentially forming planetary systems that can be compared to exoplanetary systems.

There have been a few studies that investigated the influence of fly-bys on the disk size. However, they were usually based on the results from parameter studies of fly-bys between equal-mass stars (Clarke & Pringle 1993; Kobayashi & Ida 2001; Adams 2010). A real cluster contains a wide spectrum of masses and therefore equal-mass fly-bys are the exception rather than the rule (Pfalzner & Olczak 2007). Others proposed to convert the disk-mass criterion of Olczak et al. (2006) directly into a disk size (de Juan Ovelar et al. 2012). Nevertheless, Breslau et al. (2014) showed that this approach is error prone and devised a relation for the disk size after an fly-by that is valid over a large range of mass ratios between the star and the perturber.

Vincke et al. (2015), in the following referred to as VBP15, used this more appropriate description of the effect of fly-bys on the disk size to perform a study on embedded clusters of different mass and stellar density. They found that fly-bys in the embedded phase are capable of reducing disks to sizes well below 1000 au and that the median disk size strongly depends on the stellar density. However, as in all previous studies, they did not take into account the presence of the gas in the embedded phase and the effect of gas expulsion on the cluster dynamics.

In contrast to previous studies, we include here the effect of the gas on the cluster dynamics and model all the evolutionary stages of the clusters self-consistently—the embedded phase, the gas expulsion, and the expansion phase. We quantify the differences between the fly-by history in the embedded phase and the expansion phase. More importantly, we will demonstrate how the differences in cluster dynamics and timescales influence the fly-by dynamics and the final disk-size distribution in dense and sparse clusters.

2. METHOD

2.1. Cluster Simulations

The cluster simulations are performed using the code Nbody6++ (Aarseth 1973; Spurzem 1999; Aarseth 2003). We model clusters of different mass, which is realized by performing simulations of clusters with different numbers of stars: 1000 (E0), 2000 (E1), 4000 (E2), 8000 (E3), 16,000 (E4), and 32,000 (E52, E51). However, the initial size of the clusters is kept fixed at a half-mass radius of $r_{\rm hm} = 1.3$ pc, which allows us to study clusters of different density. Clusters depicted, e.g., in Lada & Lada (2003) usually have somewhat smaller radii (<1 pc) as they still form stars. There are strong indications that clusters' sizes increase with age during the star formation process and are typically about 1–2 pc by the time star formation is finished (Kroupa 2005; Pfalzner & Kaczmarek 2013a; Pfalzner et al. 2014).

Currently, it is not clear to what extent massive clusters are subject to substructure. Any potentially existing substructure is quickly erased in the star formation phase (Bonnell et al. 2003; Parker et al. 2014), at the latest the gas expulsion will eliminate any left-over substructure in the presented extended clusters. For simplicity, we assume here an initial stellar number density distribution according to a relaxed, smooth King distribution (Olczak et al. 2010) with a flat core, which is representative for the Orion Nebula Cluster (ONC), which is at the onset of gas expulsion and one of the best studied massive clusters in the solar neighborhood. A detailed description of the density distribution, including an illustration of the initial density distribution as a function of the cluster radius (their Figure 1), can be found in Olczak et al. (2010). Any potentially existing substructure would make close encounters more common, so that the results presented here can be regarded as lower limits for the importance of the cluster environment on the protoplanetary disks. In contrast to VBP15 and most previous work, here we take into account the potential of the gas component as well. The total mass of the system $M_{\rm cl}$ is $M_{\rm cl} = M_{\rm stars} + M_{\rm gas}$ with $M_{\rm stars}$ being the stellar component of the cluster; therefore, the gas mass is given by

$$M_{\rm gas} = \frac{M_{\rm stars}\,(1 - {\rm SFE})}{\rm SFE}. \quad (1)$$

where SFE is the star formation efficiency, which is assumed to be 30%. Various studies have shown that such SFEs are characteristic for massive clusters like NGC 2244, NGC 6611 etc. in the solar neighborhood (for example, Lada & Lada 2003). The stars are initially still embedded in the remaining gas. Note that the gas density profile was chosen to be of the Plummer form (Steinhausen 2013) with a half-mass radius similar to that of the stellar profile (1.3 pc), because King gas profiles lead to numerical difficulties.

Apart from Rosotti et al. (2014), all previous studies of this kind did not include the gas component, including it here basically results in a different velocity dispersion compared to the gas-free case. It is assumed that the cluster is initially in virial equilibrium. The stellar velocities and the individual stellar masses are sampled randomly, the former from a Maxwellian distribution, the latter from the IMF by Kroupa (2002) with a lower stellar mass limit of 0.08 $M_\odot$ and an upper mass limit of 150 $M_\odot$. The embedded phase of clusters is thought to last between 1 and 3 Myr (Leisawitz et al. 1989; Lada & Lada 2003; Portegies Zwart et al. 2010). Accordingly,

Table 1
Cluster Model Setup and Dynamical Timescales

Model	N_{stars}	N_{sim}	t_{emb} (Myr)	r_{hm} (pc)	M_{stars} ($M_\odot$)	M_{cl} ($M_\odot$)	t_{dyn} (Myr)
E0	1000	308	2.0	1.3	590.8	1969.2	0.67
E1	2000	168	2.0	1.3	1192.2	3973.9	0.47
E2	4000	94	2.0	1.3	2358.1	7860.3	0.33
E3	8000	47	2.0	1.3	4731.2	15770.6	0.24
E4	16000	16	2.0	1.3	9464.8	31549.3	0.17
E52	32000	9	2.0	1.3	18852.6	62842.0	0.12
E51	32000	7	1.0	1.3	18839.2	62797.3	0.12

Note. Column 1 indicates the model designation, followed by the initial number of stars in the cluster N_{stars}, the number of simulations in campaign N_{sim}, the duration of the embedded phase t_{emb}, the initial half-mass radius r_{hm} of the cluster, the stellar mass of the cluster M_{stars}, the total cluster mass (including the gas mass) M_{cl}, and the resulting dynamical timescale t_{dyn}. For calculation of M_{cl} and t_{dyn}, see the text.

we simulated clusters with an embedded phase lasting $t_{emb} = 2$ Myr, but also performed an additional set of simulations for the densest cluster with $t_{emb} = 1$ Myr (model E51). This allows us to also study how the length of the embedded phase influences the final distribution of protoplanetary disk sizes. For a more detailed summary of the set-up parameters, see Table 1.

In contrast to previous work, we take into account that the gas expulsion process typically happens after 1–3 Myr. The gas expulsion itself happens on short timescales, typically smaller than, or of the order of, several dynamical times t_{dyn} of the cluster (Geyer & Burkert 2001; Melioli & de Gouveia dal Pino 2006; Portegies Zwart et al. 2010), which is given by

$$t_{dyn} = \left(\frac{GM_{cl}}{r_{hm}^3}\right)^{-1/2}. \quad (2)$$

The dynamical timescales for the cluster models E0-E52 are very short, between 0.8 and 0.14 Myr, see column 7 of Table 1. Therefore, and for better comparability of our cluster models, we assume the gas expulsion process in all clusters to be instantaneous. This immediate removal of the gas mass after $t = t_{emb}$ leaves the cluster in a supervirial state, so that the cluster expands in order to regain virial equilibrium. We will discuss the consequences of such an instantaneous gas expulsion on the results compared to a longer expulsion timescale in Section 4. We follow the cluster expansion until 10 Myr have passed since the cluster was fully formed.

In each simulation, the fly-by history for each individual star was tracked and the fly-by properties recorded. For each cluster model, a campaign of simulations with different random seeds was performed in order to improve statistics and minimize the effect of the initial individual setup of a cluster on the results. The number of simulations for each setup is given in column 3 of Table 1.

2.2. Disk Size Development

Ideally, one would start out the simulation with an observed primordial disk size. However, observationally it is challenging to measure disk sizes directly especially in embedded clusters. In contrast to the disk fraction, disk size measurements are usually performed in (nearly) exposed clusters, which have expelled most of their gas. For the best observed stellar cluster in the solar neighborhood, the ONC, disk radii in the range from ~27 au up to ~500 au were found by several surveys (McCaughrean & O'dell 1996; Vicente & Alves 2005; Eisner et al. 2008; Bally et al. 2015). However, the ONC is already 1 Myr old. Whether these measurements are representative for the primordial disk-size distribution or whether photoevaporation or fly-by processes have already altered the sizes remains unclear. In other clusters, disk sizes up to several thousand astronomical units have been reported. Therefore, there is no information about a typical initial disk size or a disk-size distribution in embedded stellar clusters.

For this reason, and for simplicity, all disks in a cluster are set up with the same initial size r_{init}, ignoring any possible dependency of the disk size on the host mass (see Hillenbrand et al. 1998; Vicente & Alves 2005; Eisner et al. 2008; Vorobyov 2011; Vincke et al. 2015). We performed a numerical experiment, setting the initial disk size to a very large value of $r_{init} = 10{,}000$ au. The interpretation of this large initial disk size will be discussed in Sections 3 and 4.

In our simulations, we determine the size of the protoplanetary disks around the cluster members after each stellar fly-by using the equation

$$r_{disc} = \begin{cases} 0.28 \cdot r_{peri} \cdot m_{12}^{-0.32}, & \text{if } r_{disc} < r_{previous} \\ r_{previous}, & \text{if } r_{disc} \geqslant r_{previous}, \end{cases} \quad (3)$$

given by Breslau et al. (2014), where $m_{12} = m_2/m_1$ is the mass ratio between the disk-hosting star (m_1) and the perturber (m_2), r_{peri} is the periastron distance in astronomical units, and $r_{previous}$ is the disk size previous to the fly-by in astronomical units. This equation is valid for coplanar, prograde, parabolic fly-bys. This type of fly-by is more destructive than inclined, retrograde, or hyperbolic fly-bys (Clarke & Pringle 1993; Heller 1995; Hall 1997; Pfalzner et al. 2005c; A. Bhandare & S. Pfalzner 2016, in preparation). However, the effect of inclined, retrograde and hyperbolic fly-bys is much less investigated. First results by Bhandare & Pfalzner indicate that non-coplanar encounters have, nevertheless, a considerable effect on the disk size. Thus, the here presented result has to be regarded as the lower limit of disk size, but will not be considerably smaller than it would be in the inclined case.

Viscous forces, which might lead to disk spreading (Rosotti et al. 2014), and self-gravity between the disk particles are neglected in this model because the disks are set up containing only massless tracer particles. Every star in the cluster was surrounded by such a massless disk; therefore, each fly-by event is actually a disk–disk fly-by. Capturing of material from the disk of the passing star is disregarded in our approach as well. The formula above only holds for star–disk fly-bys, where only the primary hosts a disk. Nevertheless, Pfalzner et al. (2005a) found that a generalization of disk–disk fly-bys to star–disk fly-bys is valid as long as the disks have a low mass and not much mass is transferred between the two. For a more detailed description of the disk-size determination, its approximations, and the resulting influence on the results, see, Breslau et al. (2014). At the end of the diagnostic step the resulting fly-by and disk-size statistics are averaged over all simulations within one simulation campaign.

Before presenting the results, we want to elucidate some definitions used in the following section. We use the term "fly-by" in our study for gravitational interactions between two stars

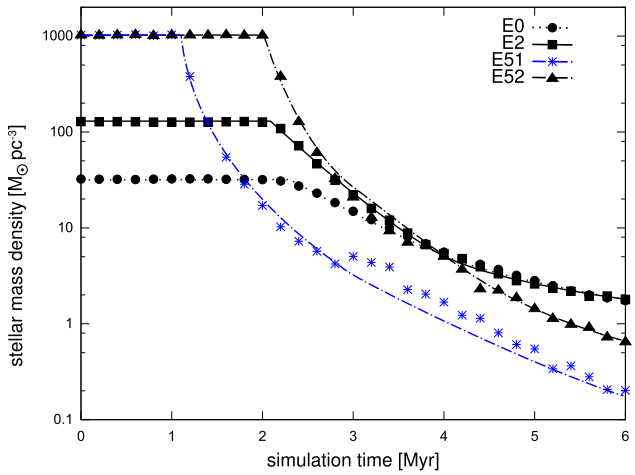

Figure 1. Stellar mass density within 1.3 pc (initial half-mass radius) as a function of time for clusters of different densities: E0 (dots), E2 (squares), E51 (asterisks, blue), and E52 (triangles). The duration of the embedded phase is $t_{\rm emb} = 1$ Myr for E51 and $t_{\rm emb} = 2$ Myr for all other models.

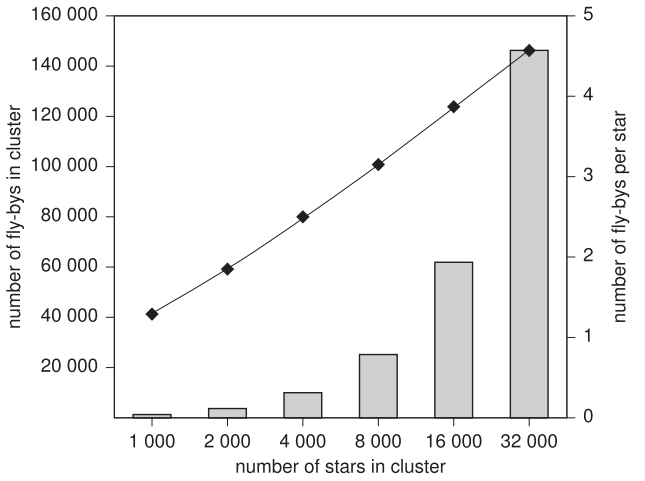

Figure 2. Number of fly-bys per cluster (gray boxes, left y-axis) and per star (black diamonds, right y-axis) for the different cluster models. The black line only serves to guide the eye.

that (a) reduce the disk size by at least 5% ($r_{\rm disk}/r_{\rm previous} \leqslant 0.95$). The term "strongest fly-by" or "disk-size defining fly-by" describes the fly-by with the strongest influence on the disk in the whole simulation—or for certain periods of cluster evolution. Note that, as Equation (3) takes into account the mass ratio of the perturber and the host star, the strongest fly-by is not necessarily the closest one.

3. RESULTS

The cluster evolution, namely the same mass and radius development—confirm previous work. However, here we have a closer look at the density evolution because this determines the fly-by history investigated here. Our simulations show that, as long as the clusters remain embedded in their natal gas ($t_{\rm emb} = 2$ Myr, for model E51 $t_{\rm emb} = 1$ Myr), the stellar mass density basically stays constant (see Figure 1). When the gas is expelled instantaneously at $t = t_{\rm emb}$, the clusters respond to the now supervirial state by expanding, leading to a significant drop in the stellar density.

The more massive clusters regain their virial equilibrium much faster than the less massive clusters (Parmentier & Baumgardt 2012; Pfalzner & Kaczmarek 2013a) due to their shorter dynamical timescales, see Table 1. As a result, their stellar density declines faster than in the lower mass clusters—the density in the most massive cluster (triangles and asterisks) drops to 10% of its initial value already $t = 0.3$ Myr after gas expulsion, whereas low-mass clusters need up to $t = 2$ Myr after gas expulsion for such a decline.

Note that around $t = 3$–4 Myr, the cluster models E0, E2, and E52 are indistinguishable in terms of their stellar mass density within 1.3 pc, while having a very different density history.

Naturally, the total number of fly-bys increases with cluster density, which in our case is equivalent to the cluster mass. In the least dense cluster roughly 1300 fly-bys that change the disk size take place during the 10 Myr simulated here whereas in the densest cluster model the number of fly-bys is approximately 150,000 (see Figure 2). However, this increase is by far not as much as one would expect from a roughly 32 times higher density of models E51 and E52 in the embedded phase (see Figure 1). The reason is that we only consider fly-bys that lead to a smaller disk size than previous to the fly-by, see Section 2. For the dense clusters the disk sizes are reduced very quickly to very small sizes so that even closer disk-size changing fly-bys are rare at later times. Similarly, the number of fly-bys per star increases with cluster density. In model E0, each star undergoes, on average, a little more than one disk-size changing fly-by as defined above, whereas in model E52 its between four and five. Although the difference in density (within the half-mass radius) between these two models is almost a factor of 100, the average number of fly-bys increases almost linearly by a factor of four due to the criteria mentioned above.

This is also reflected in the temporal development of the number of disk-size changing fly-bys. Figure 3 (a) depicts the fly-by history in the different cluster models. It shows the cumulative fraction of fly-bys as a function of time, where the vertical lines mark the time of gas expulsion (1 Myr for model E51, dotted blue, 2 Myr all other models, solid black). The steeper slopes for the most massive clusters indicate that the disks are processed faster. For example, more than 50% of all disk-size reducing fly-bys in model E52 occur within the first 0.2 Myr, whereas in model E0 it takes four times as long (~0.8 Myr) for the same portion of fly-bys to happen.

As to be expected, the majority of fly-bys happens in the dense embedded phase. However, there are differences between the different cluster types, see Figure 3 (b). Whereas in the most massive clusters disk-size changes happen nearly exclusively (~98%) in the embedded phase (black)—and most even within the first few 100,000 years—in the least dense clusters, only 87% of all disk-size changes occur in this phase. The reason for this is that, in the latter case, the density decreases more slowly so that a higher fraction of about one-seventh of disk-size reducing fly-bys happens in the expansion phase (gray).

Obviously, the length of the embedded phase plays an important role. In model E51, the gas is expelled after 1 Myr, whereas for model E52 the gas expulsion happens after 2 Myr. The earlier drop in cluster mass density in model E51 results in the total number of fly-bys in model E52 being roughly 15% larger than in model E51 (151,000 compared to 131,000).

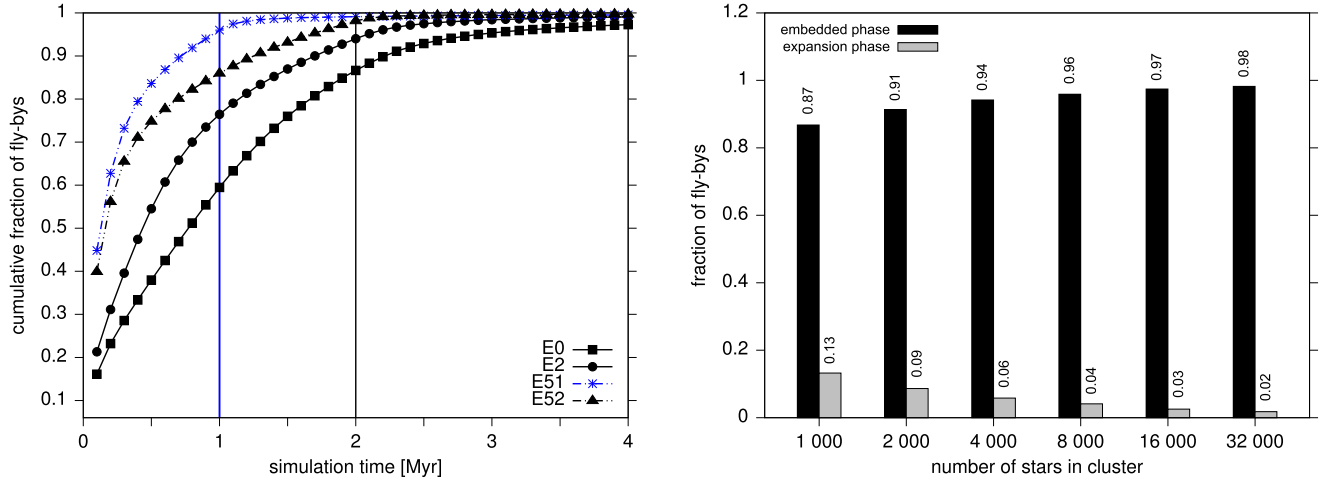

Figure 3. (Left) Cumulative fraction of fly-bys as a function of time for the cluster models E0 (squares), E2 (dots), E51 (asterisks, blue), and E52 (triangles). The vertical lines depict the points in time of gas expulsion for model E51 (1 Myr, dotted blue) and for all other models (2 Myr, solid black). (Right) Fraction of fly-bys as a function of the number of stars in the cluster for the embedded phase (black) and the expansion phase (gray).

Again, the reason why the number of fly-bys does not double for a twice as long embedded phase is that most of the disks have been reduced to a small disk size during the first million years and therefore the cross-section for a disk-size changing fly-by has been reduced. This means that the early embedded phases largely determine the disk sizes.

The distinct clusters have very different influences on their protoplanetary disks, reflected, for example, in the overall median disk size (Figure 4). This median disk size is about 13 times smaller in model E52 (32,000 stars) than in model E0 (1000 stars) because not only does the number of fly-bys increase significantly with cluster density, but the fly-bys are on average also closer or the mass ratio is higher. For the densest clusters, most fly-bys happen at the beginning of the embedded phase, thus, the median disk sizes are nearly the same at the end of the embedded phase (∼108 au, open squares) and at the end of the simulations (∼104 au, dots). However, for model E0, the median disk size is significantly larger (∼1670 au) at the end of the embedded phase (2 Myr) than at the end of the simulations (∼1350 au) as roughly one-seventh of the close fly-bys occur in the expansion phase.

It is important to note that we do not expect real disks to be generally as large as nearly 1700 au. The median disk size here only reflects the degree of the environment's influence on the disks. For example, as long as the disks are initially >100 au, they are reduced in size in the densest cluster model. By contrast, in the ONC model only disks that are initially larger than ∼500 au are affected. A real initial disk size distribution would be necessary to further constrain this, for a more detailed discussion, see Section 4.

What does the spatial disk size distribution at the end of embedded phase look like? Figure 5 (a) shows the median disk size as a function of the distance to the cluster center of the stars for different cluster models at $t = 2$ Myr (open black symbols). In the inner part of the ONC-like cluster (E2), for example, within a sphere of the initial half-mass radius (1.3 pc) the median disk sizes are considerably smaller than for the clusters outskirts. The difference is even larger when one compares the extremes—the median disk size rises from 50 au at 0.1 pc to 2000 au at 4 pc. This is due to the higher density in the cluster core and the resulting higher fly-by frequency.

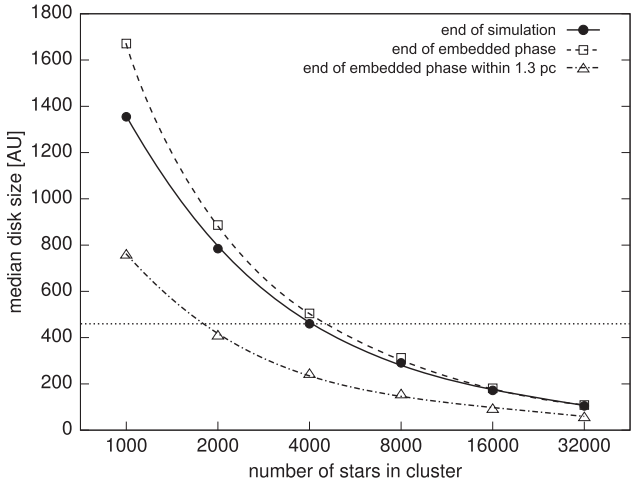

Figure 4. Overall median disk size for all stars for different cluster models at the end of the simulation (10 Myr, dots), at the end of the embedded phase (2 Myr, squares), and at the end of the embedded phase within a sphere of 1.3 pc (initial half-mass radius, triangles).

These trends have already been seen in simulations where the gas content was neglected (VBP15), however, there are quantitative differences. Figure 5(b) compares the median disk size as a function of the distance to the cluster center after 2 Myr of simulation time for the ONC cluster model (E2) obtained in VBP15 (open squares) and in this work (circles). Including the gas mass explicitly leads to a higher velocity dispersion in the embedded phase and thus stronger encounters. Therefore, the median disk sizes presented in this work are much smaller than in VBP15. For example, at the rim of the cluster core (0.3 pc), the median disk size in the work here is more than a factor of four smaller than in VBP15 (∼108 au compared to ∼470 au). At a distance of 1 pc, the situation is even more extreme, as in our work, the median disk size is roughly 400 au, whereas in VBP15 more than half of the disks are not influenced at all and still retain their initial size.

If we consider the first 10 Myr of cluster evolution, which includes the embedded, gas expulsion, and expansion phases

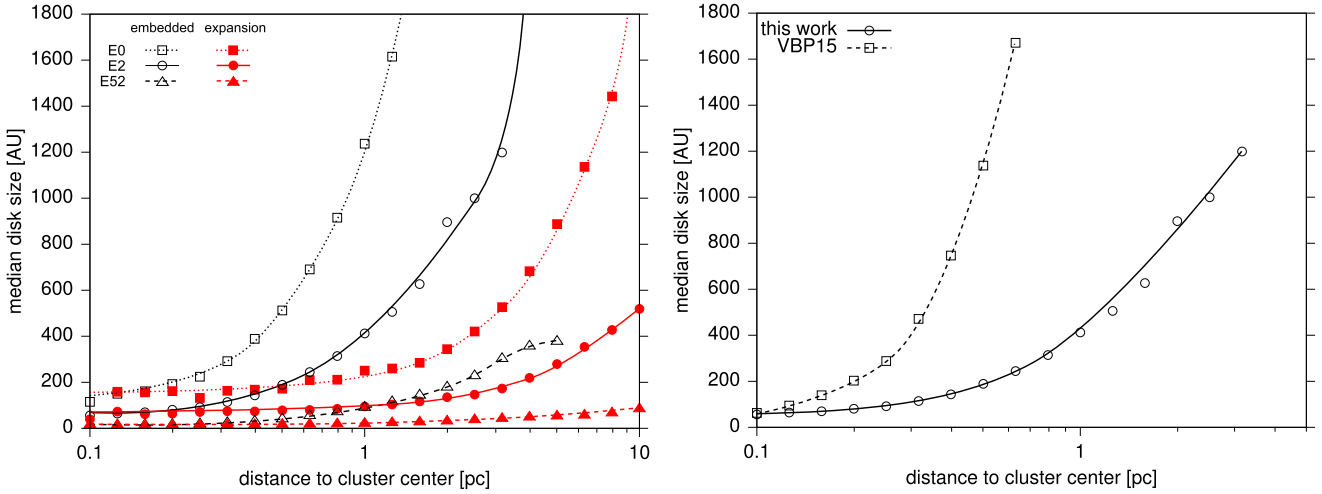

Figure 5. Median disk size as a function of the distance to the cluster center (left panel) for different cluster models (E0 squares, E2 circles, and E52 triangles) at the end of the embedded phase (2 Myr, black symbols) and at the end of the simulation covering the embedded, the gas expulsion, and the expansion phases (10 Myr (red symbols); (right panel) for the ONC model (E2) in this work, i.e., with gas mass (circles, same as in (a)), and in VBP15, i.e., without gas mass (squares). The lines in both panels only serve to guide the eye.

(black symbols in Figure 5), in general, the denser the cluster is, the smaller the median disk size remains. Nonetheless, after 10 Myr, the median disk size is nearly constant (at least for models E2 and E52) within 3 pc from the cluster center. This is not so much due to mixing, but basically mostly caused by the expansion of the cluster—the value of the median disk size in the cluster outskirts is now similar to that in the center at the end of the gas expulsion (2 Myr). While during the embedded phase most stars do not move significantly in radial directions and the dependence of the median disk size on the distance to the cluster center is preserved, after gas expulsion only about 10% of stars remain bound to the cluster and the rest leaves the cluster very quickly (Fall et al. 2009; Dukes & Krumholz 2012). The still bound stars largely move to positions more distant from the cluster center than they were originally. That is the reason why the median disk size throughout the cluster in the expansion phase is similar to the median disk size in the inner cluster region shortly before gas expulsion. This means that when older clusters are observed they work like a microscope showing us the central area of enlarged versions of younger clusters.

If observations of older clusters work like a microscope, what would an observed disk-size distribution in a cluster at different ages look like? To answer this question, we investigate the ONC-model cluster (E2) at different ages with an artificial fixed field of view (FOV) ($r_{\rm FOV} = 1$ pc) to mimic observations. Note that the FOVs for observations are usually squares, whereas here we present spheres with radii of $r_{\rm FOV}$, centered on the cluster origin. Figure 6 shows the resulting disk-size statistics for an ONC-like cluster at 1 Myr (white), 2 Myr (gray), and 10 Myr (black). The total number of small disks increases much stronger than the number of disks with sizes of several hundreds of astronomical units. The reason for this is that, in the embedded phase, disks that are already influenced but still a few hundreds of astronomical units large still reduced in size by follow-up encounters. In comparison, the shape of the disk-size distribution barely changes between the end of the embedded phase and the end of the simulations.

Observations usually study only the central areas of a cluster, because there the stellar density of cluster members is so high

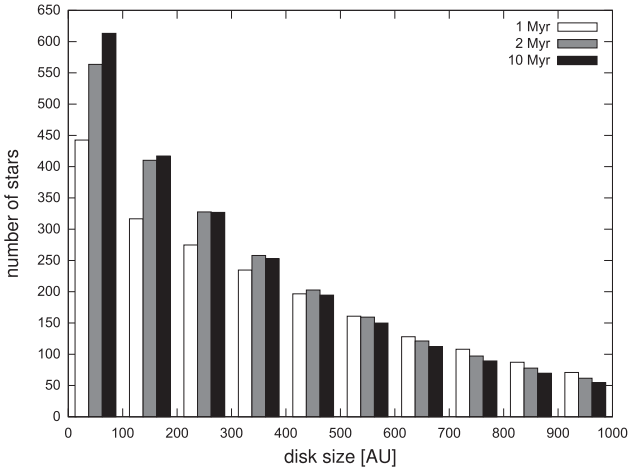

Figure 6. Disk-size distribution in the ONC-like cluster model (E2) for a fixed virtual FOV (1 pc) and different time steps: 1 Myr (white), 2 Myr (gray), and 10 Myr (black).

that member identification is relatively easy—basically, the rate of false-positives is very low. However, this concentration on the cluster center is problematic, especially for clusters after gas expulsion, which span large areas. Taking our results as a guideline, the observed median disk size in an ONC-like cluster 10 Myr after cluster formation, for example, would be ~50 au in the cluster core (0.2 pc), whereas the overall median disk size is more than nine times as large (~460 au, the dotted horizontal line in Figure 4).

Choosing initially artificially large disks of 10,000 au has the advantage that the obtained results can be applied to any smaller, real disk size. Thus, Figure 7, tells us, for example, that if all stars had an initial disk size of $r_{\rm init} \geqslant 500$ au, about half of the stars had their disks severely truncated by fly-bys to disk sizes below 500 au. An initial disk size of more than 500 au is a realistic scenario as surveys found disks in the ONC with radii of 30–500 au (McCaughrean & O'dell 1996; Vicente & Alves 2005; Eisner et al. 2008; Bally et al. 2015). Note, that at an age of approximately 1 Myr, even those might already

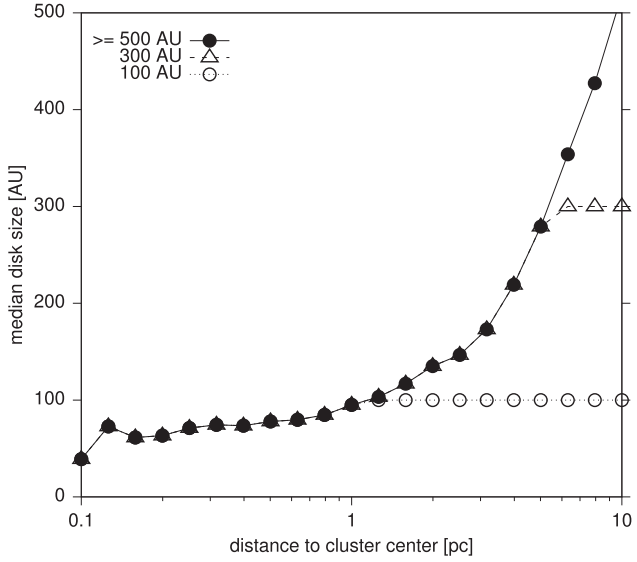

Figure 7. Median disk size at the end of the simulation (10 Myr) as a function of the distance to the cluster center for cluster model E2 for different initial disk sizes: 100 au (circles), 300 au (triangles), and ⩾500 au (dots).

have been reduced in size through photoevaporation and/or fly-bys. In the case of more massive clusters, like NGC 6611 (E52 model), there are more and closer interactions, so that independent of the initial disk size (as long as $r_{\rm init} > 100$ au) the resulting median disk is ⩽110 au, see Figure 4.

In summary, observed disk sizes or disk-size distributions in massive clusters are a strong function of the cluster age, its evolutionary stage, its initial conditions, and the FOV of the instrument. One has to act with caution when comparing and interpreting such results.

4. DISCUSSION

The above described simulations required some approximations, which we discuss in the following.

In this study, we neglect potentially existing initial substructuring of the clusters. In clusters with low velocity dispersions, the substructure will be erased quickly (see, e.g., Goodwin & Whitworth 2004; Allison et al. 2010; Parker et al. 2014). Most probably, the substructure will be erased at the end of star formation (Bonnell et al. 2003), which is when our simulations start.

The cluster models were set up without primordial mass segregation. Many clusters show signs of mass segregation, but it is unclear whether this property is primordial or if dynamical evolution caused the observed mass segregation. If we included primordial mass segregation, the most massive stars would reside in the cluster core where the density is highest. Therefore, they would undergo more fly-bys, leading in turn to smaller disks around these stars. Furthermore, stronger gravitational focussing would lead to an increase in the overall fly-by frequency in the cluster center and thus smaller disks.

All stars in the clusters were set up to be initially single excluding primordial binaries. Observations show that the multiplicity, that is, the fraction of binaries, triples, or systems of higher order, increases with stellar mass (Köhler et al. 2006; Duchêne & Kraus 2013, and references therein). The most massive stars would most probably be part of a binary then, losing their own disk quite quickly or not even forming one depending on the separation. Additionally, the gravitational focussing in the cluster due to multiple systems would be stronger than for a single, massive star, leading to an increase in the fly-by frequency and overall smaller disks.

One major difference to previous works is that we studied different evolutionary stages starting with the embedded phase, continuing with the gas expulsion, and the following expansion phase. Due to the uncertainty in the age determination of clusters, the duration of the embedded phase is not well constrained by observations. Here we modeled the duration of the embedded phase as 2 Myr. However, for the most massive clusters, this is probably too long, as at that age massive clusters are already largely devoid of gas. As most of the disk-size reducing fly-bys occur during the early stages of the embedded phase, with only 12% of fly-bys happening in the second half of the embedded phase for the most massive clusters, our results should not be very sensitive to the assumed duration of the embedded phase.

The assumption of instantaneous gas expulsion is most likely justified for the most massive clusters in our investigation (e.g., Geyer & Burkert 2001; Melioli & de Gouveia dal Pino 2006; Portegies Zwart et al. 2010). Nevertheless, for the lowest mass clusters, this is less certain. In this case, a "slow" gas expulsion lasting several million years would give the cluster more time to adjust to the gas-mass loss and fewer stars would become unbound. Furthermore, the stellar density would remain higher for a longer time span, allowing the stars to undergo more fly-bys and resulting in smaller disks than in the presented results. The influence of only the embedded phase was studied in VBP15. Comparing this to our current work, we find that the duration of the embedded phase, e.g., for the lowest density cluster[1] is strong. At the end of the embedded phase in VBP15 —lasting unrealistically 5 Myr—the mean disk size is roughly 300 au inside 0.6 pc, compared to ∼670 au) for the here adopted 2 Myr long embedded phase. If the gas was expelled slowly, a more realistic median disk size would lie between these two extremes. Further studies with an implicitly modeled gas expulsion of a few million years are necessary to constrain this rough estimate.

Here all fly-bys were assumed to be prograde, coplanar, and parabolic. Those fly-bys have a stronger effect on the disks than their retrograde, inclined counterparts (Clarke & Pringle 1993; Heller 1995; Hall 1997; Pfalzner et al. 2005c; A. Bhandare & S. Pfalzner 2016, in preparation). However, Pfalzner et al. (2005c) found that for fly-bys with inclinations of $<45°$ the final disk properties do not differ much from the prograde coplanar case. This was confirmed by A. Bhandare & S. Pfalzner (2016, in preparation), who found that even retrograde fly-bys can have a strong effect on the disk size. Disks after inclined fly-bys would be larger than the ones presented here, but at most by a factor of 1.5–1.8.

We only considered parabolic encounters; however, the typical eccentricity of a fly-by depends on the cluster density: the higher the density, the more eccentric are the fly-bys, see Figure 8. As pointed out by Pfalzner (2004), such hyperbolic fly-bys have less influence on disks than parabolic fly-bys, making the disk sizes presented here again lower limits. A detailed parameter study of hyperbolic fly-bys and their influence on the disk size would be necessary to extend our study.

[1] model D0 in VBP15, equivalent to model E0 here.

In this work, we did not include photoevaporation, which is also capable of reducing disks in size or destroying them completely (Störzer & Hollenbach 1999; Scally & Clarke 2002; Johnstone et al. 2004; Adams et al. 2006; Alexander et al. 2006; Ercolano et al. 2008; Drake et al. 2009; Gorti & Hollenbach 2009). In the embedded phase, the stars are still surrounded by the clusters natal gas, which makes the external photoevaporation ineffective. When the gas is expelled, the disks are prone to the radiation from nearby massive stars. Nevertheless, the stars move outward and may become unbound after the gas expulsion, and the stellar density decreases significantly, making it less probable for stars to be very close to their most massive companions. Only for the small fraction of stars that have a close fly-by the radiation would further reduce the disk in size making the final disks sizes smaller than presented here.

Here we study the effect on low-mass disks. In this case, viscosity and self-gravity of the disk can be neglected during the encounter as such. However, viscosity would lead to disk spreading in the long-term. Rosotti et al. (2014) performed combined Nbody/SPH simulations of low-mass clusters including viscous disks and found viscous spreading (a) counteracting the size reduction due to stellar fly-bys and (b) making the disks prone to follow-up more distant fly-bys. Recently, Xiang-Gruess (2016) compared the results of Nbody and SPH simulations of disks after stellar fly-bys, showing that viscosity can result in warped disk structures, whereas those features are not visible in massless (purely Nbody) disks. A disk-size determination in those cases would be more complicated than in the flat, massless disks used here.

We did not consider any dependence of the disk size on the host's mass (see, e.g., Hillenbrand et al. 1998; Vicente & Alves 2005; Eisner et al. 2008; Vorobyov 2011). If the initial disk size did depend on the stellar mass, the more massive stars should have started out with larger disks than the less massive stars. Vorobyov (2011) performed simulations of disks around Class 0 and Class I stars. They set a density threshold of $\Sigma < 0.1\,\mathrm{g\,cm^{-2}}$ for material belonging to the disks and found disk sizes between roughly 100 au for low-mass stars up to a little more than 1000 au for solar-like stars. If confirmed, it would mean that disks around massive stars are more prone to size changes by the environment than low-mass stars. Furthermore, this would mean that in all clusters, except model E0, more than half of the disks around solar-like stars would be influenced strongly by stellar fly-bys, see Figure 4.

Recent simulations have tried to determine the fraction of planets that become affected by the cluster environment and either move on an eccentric orbit or become unbound (Hao et al. 2013; Li & Adams 2015). However, these simulations concentrate on the initially much denser clusters that become long-lived open clusters. This type of cluster will be studied in a follow-up paper.

5. SUMMARY AND CONCLUSION

In this paper, we studied how the cluster environment changes the sizes of disks surrounding young stars. In contrast to previous work, we took the cluster development during the first 10 Myr explicitly into account. Starting with initial conditions typical for young clusters at the end of their formation phase in the solar neighborhood, we modeled the cluster dynamics from embedded throughout the expansion phase and determined the effect on the effect of gravitational interactions between the stars on the disk sizes. These types of simulations were performed for clusters of different masses and densities.

Our findings are the following.

1. It is essential to include the gas dynamics in this kind of simulation because the larger velocity dispersion leads to more encounters and significantly smaller disk sizes than in a gas-free treatment.
2. The majority of disk-size changing fly-bys always take place in the embedded phase. However, the slower expansion phase in lower mass clusters means that here still 12% of disk-size changing fly-bys happen, in comparison to just 2% for high-mass clusters.
3. For ONC-like clusters basically only disks larger than 500 au are affected by fly-bys, whereas in NGC 6611-like clusters, cutting disks below 100 au happens for 50% of stars.
4. However, in all investigated cases the disk sizes in the dense cluster centers are much more affected than the average suggests. For example, in the NGC 6611-like case the median disk size is 54 au.
5. The duration of the embedded phase influences the final median disk size, but not as strong as one would expect, because early fly-bys reduce the disk size already, leading to smaller cross-sections for later fly-bys. In the densest cluster, the median disk size after 1 Myr is already 155 au at the end of the embedded phase 108 au, which is very close to the final median disk size of 104 au.

Often disk sizes and frequencies (e.g., Haisch et al. 2001; Mamajek 2009, and references therein) of clusters of different present density are compared to obtain information about to what degree the environment influences these properties. However, clusters are highly dynamical and their current density is not necessarily representative for the past development. We showed that between 3 and 4 Myr even the most extreme cluster models of E0 and E52 have very similar cluster mass densities within a sphere of 1.3 pc[2], see Figure 1. The faster evolution of massive clusters leads to this situation where the density in massive clusters and low-mass clusters of the same age can be similar, but the clusters themselves are in very different evolutionary stages. This means that at this specific point in time and in this sphere of 1.3 pc, fly-bys are equally likely in all of these initially very different clusters. However, if we compare the median disk sizes in these "equal-density" clusters at this point in time ($t = 4$ Myr), they differ considerably. In the least dense cluster, the median disk size is roughly 480 Myr whereas it is 270 au for the densest cluster model. The reason is that the most massive clusters were once much denser than the lower mass clusters and therefore their disk sizes are reduced to a larger degree.

The different expansion of the clusters—slow for low-density and fast for high-density systems—leads to very distinct fly-by histories and, consequently, different median disk sizes and disk-size distributions. If one looks only at the embedded phase there seems to be a direct relation between stellar density and the disk size: the higher the density, the smaller the median size. Thus it seems that this is easily testable against observations. However, taking into account the

[2] Note that the given simulation time is not synonymous with cluster age because the star formation phase is not covered by our simulations.

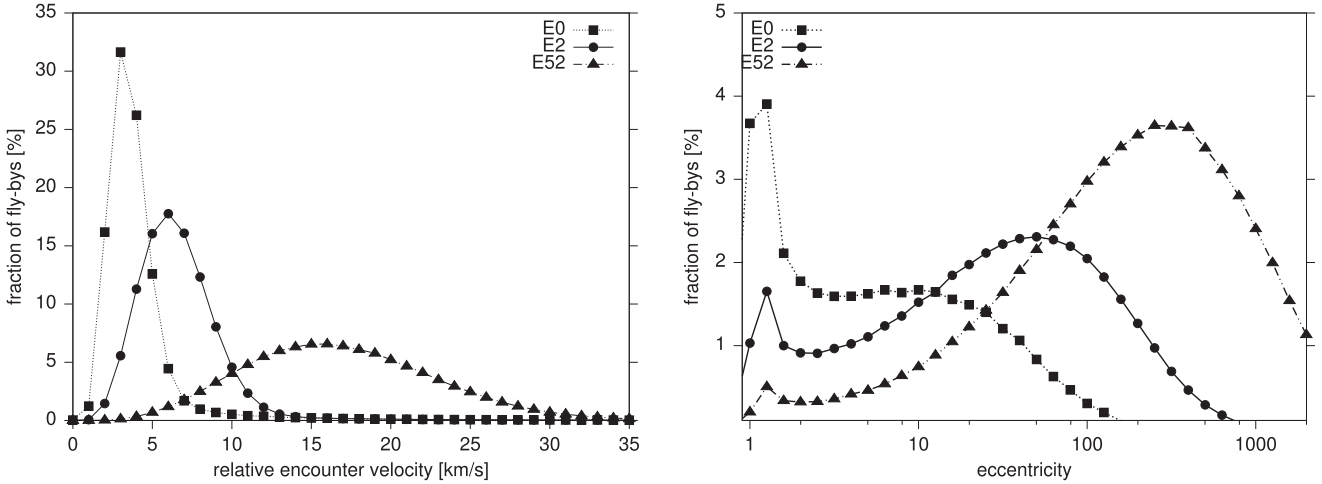

Figure 8. (Left) Relative encounter velocity distribution—that is the perturber's velocity relative the the host's velocity at the point of periastron passage—of all fly-bys and (right) eccentricity distribution of fly-bys leading to a disk size < 500 au as fractions of the total number of fly-bys for three cluster models: E0 (squares), E2 (dots), and E52 (triangles).

different evolutionary phases and their different timescales for dense and less dense clusters show that a comparison is much more complex.

All of these effects of cluster properties and observational constraints make it quite challenging to compare disk-size distributions in different clusters with each other. It does not make sense comparing the properties in clusters of different densities as long as one does not take into account their evolutionary stage and their history.

APPENDIX
FLY-BY VELOCITY AND ECCENTRICITY

The characteristics of stellar encounters change significantly with cluster density. For example, the relative velocity between two encountering stars increases for denser clusters. Figure 8(a) depicts the average relative encounter velocity—that is the velocity of the perturber relative to the host star at the time of periastron passage—for three cluster models E0 (squares), E2 (dots), and E52 (triangles). This encounter velocity can be directly correlated to the eccentricity of the perturber's orbit via

$$v_{\rm enc} = \sqrt{(1+e)\cdot\frac{G\,(m_1+m_2)}{r_{\rm peri}}}, \qquad (4)$$

where G is the gravitational constant, m_1 is the mass of the host star, m_2 is the mass of the perturber, and $r_{\rm peri}$ is the periastron distance, all in SI units. The eccentricity distribution for cluster models E0, E2, and E52 are shown in Figure 8(b) for fly-bys leading to disks smaller than 500 au.

In this study, we assumed all fly-bys to be parabolic. This approximation only holds for the least dense cluster model, as the encounter velocities and therefore the eccentricities clearly increase with cluster density (see also Olczak et al. 2010). For the denser cluster models (especially E52), a detailed study of the influence of hyperbolic fly-bys on disk sizes would be favorable. Previous studies suggest that their influence on the disks (in these cases, the disk mass and angular momentum) is much smaller than the one of parabolic encounters (for detailed discussions, see, e.g., Pfalzner et al. 2005c; Olczak et al. 2010, 2012). Therefore, the disk sizes presented here might be lower limits.

At very high densities, that is, especially in cluster model E52, fly-bys are no longer two-body encounters but many-body interactions. This leads to the extreme eccentricities of $e > 100$. Especially for this type of fly-by, we expect the disk-size change to be smaller than for the here assumed prograde, coplanar, parabolic case.

REFERENCES

Aarseth, S. J. 1973, VA, 15, 13
Aarseth, S. J. 2003, Gravitational N-Body Simulations (Cambridge: Cambridge Univ. Press)
Adams, F. C. 2000, ApJ, 542, 964
Adams, F. C. 2010, ARA&A, 48, 47
Adams, F. C., Proszkow, E. M., Fatuzzo, M., & Myers, P. C. 2006, ApJ, 641, 504
Alexander, R. D., Clarke, C. J., & Pringle, J. E. 2006, MNRAS, 369, 229
Allison, R. J., Goodwin, S. P., Parker, R. J., Portegies Zwart, S. F., & de Grijs 2010, MNRAS, 407, 1098
Balbus, S. A., & Hawley, J. F. 2002, ApJ, 573, 749
Bally, J., Mann, R. K., Eisner, J., et al. 2015, ApJ, 808, 69
Baumgardt, H., & Kroupa, P. 2007, MNRAS, 380, 1589
Boily, C. M., & Kroupa, P. 2003a, MNRAS, 338, 665
Boily, C. M., & Kroupa, P. 2003b, MNRAS, 338, 673
Bonnell, I. A., Bate, M. R., & Vine, S. G. 2003, MNRAS, 343, 413
Bonnell, I. A., & Davies, M. B. 1998, MNRAS, 295, 691
Breslau, A., Steinhausen, M., Vincke, K., & Pfalzner, S. 2014, A&A, 565, A130
Clarke, C. J., & Pringle, J. E. 1993, MNRAS, 261, 190
Dale, J. E., Ercolano, B., & Bonnell, I. A. 2012, MNRAS, 424, 377
Dale, J. E., Ercolano, B., & Bonnell, I. A. 2015, MNRAS, 451, 987
de Juan Ovelar, M., Kruijssen, J. M. D., Bressert, E., et al. 2012, A&A, 546, L1
Drake, J. J., Ercolano, B., Flaccomio, E., & Micela, G. 2009, ApJL, 699, L35
Duchêne, G., & Kraus, A. 2013, ARA&A, 51, 269
Dukes, D., & Krumholz, M. R. 2012, ApJ, 754, 56
Eisner, J. A., Plambeck, R. L., Carpenter, J. M., et al. 2008, ApJ, 683, 304
Ercolano, B., Drake, J. J., Raymond, J. C., & Clarke, C. C. 2008, ApJ, 688, 398
Fall, S. M., Chandar, R., & Whitmore, B. C. 2009, ApJ, 704, 453
Fellhauer, M., & Kroupa, P. 2005, ApJ, 630, 879
García, P., Bronfman, L., Nyman, L.-A., et al. 2014, ApJS, 212, 2
Geyer, M. P., & Burkert, A. 2001, MNRAS, 323, 988
Goodwin, S. P. 1997, MNRAS, 284, 785
Goodwin, S. P., & Bastian, N. 2006, MNRAS, 373, 752
Goodwin, S. P., & Whitworth, A. P. 2004, A&A, 413, 929
Gorti, U., & Hollenbach, D. 2009, ApJ, 690, 1539

Haisch, K. E., Jr., Lada, E. A., & Lada, C. J. 2001, ApJL, 553, L153
Hall, S. M. 1997, MNRAS, 287, 148
Hao, W., Kouwenhoven, M. B. N., & Spurzem, R. 2013, MNRAS, 433, 867
Heller, C. H. 1995, ApJ, 455, 252
Hillenbrand, L. A., Strom, S. E., Calvet, N., et al. 1998, AJ, 116, 1816
Huff, E. M., & Stahler, S. W. 2006, ApJ, 644, 355
Johnstone, D., Hollenbach, D., & Bally, J. 1998, ApJ, 499, 758
Johnstone, D., Matsuyama, I., McCarthy, I. G., & Font, A. S. 2004, RMxAA, 22, 38
Klahr, H. H., & Bodenheimer, P. 2003, ApJ, 582, 869
Kobayashi, H., & Ida, S. 2001, Icar, 153, 416
Köhler, R., Petr-Gotzens, M. G., McCaughrean, M. J., et al. 2006, A&A, 458, 461
Kroupa, P. 2002, Sci, 295, 82
Kroupa, P. 2005, in ESA Special Publication 576, The Three-Dimensional Universe with Gaia, ed. C. Turon, K. S. O'Flaherty, & M. A. C. Perryman, (Noordwijk: ESA), 629
Kroupa, P., Aarseth, S., & Hurley, J. 2001, MNRAS, 321, 699
Lada, C. J., & Lada, E. A. 2003, ARA&A, 41, 57
Lada, C. J., Margulis, M., & Dearborn, D. 1984, ApJ, 285, 141
Leisawitz, D., Bash, F. N., & Thaddeus, P. 1989, ApJS, 70, 731
Li, G., & Adams, F. C. 2015, MNRAS, 448, 344
Lüghausen, F., Parmentier, G., Pflamm-Altenburg, J., & Kroupa, P. 2012, MNRAS, 423, 1985
Mamajek, E. E. 2009, in AIP Conf. Ser. 1158, Exoplanets and Disks: Their Formation and Diversity, ed. T. Usuda, M. Tamura, & M. Ishii, (Melville, NY: AIP), 3
Matsuyama, I., Johnstone, D., & Hartmann, L. 2003, ApJ, 582, 893
Matzner, C. D., & McKee, C. F. 2000, ApJ, 545, 364
McCaughrean, M. J., & O'dell, C. R. 1996, AJ, 111, 1977
Melioli, C., & de Gouveia dal Pino, E. M. 2006, A&A, 445, L23
Moeckel, N., Holland, C., Clarke, C. J., & Bonnell, I. A. 2012, MNRAS, 425, 450
Murray, N. 2011, ApJ, 729, 133
Olczak, C., Kaczmarek, T., Harfst, S., Pfalzner, S., & Portegies Zwart, S. 2012, ApJ, 756, 123
Olczak, C., Pfalzner, S., & Eckart, A. 2010, A&A, 509, A63
Olczak, C., Pfalzner, S., & Spurzem, R. 2006, ApJ, 642, 1140
Olczak, C., Spurzem, R., & Henning, T. 2011, A&A, 532, A119
Parker, R. J., Wright, N. J., Goodwin, S. P., & Meyer, M. R. 2014, MNRAS, 438, 620
Parmentier, G., & Baumgardt, H. 2012, MNRAS, 427, 1940
Pelupessy, F. I., & Portegies Zwart, S. 2012, MNRAS, 420, 1503
Pfalzner, S. 2004, ApJ, 602, 356
Pfalzner, S., & Kaczmarek, T. 2013a, A&A, 555, A135
Pfalzner, S., & Kaczmarek, T. 2013b, A&A, 559, A38
Pfalzner, S., & Olczak, C. 2007, A&A, 462, 193
Pfalzner, S., Olczak, C., & Eckart, A. 2006, A&A, 454, 811
Pfalzner, S., Parmentier, G., Steinhausen, M., Vincke, K., & Menten, K. 2014, ApJ, 794, 147
Pfalzner, S., Steinhausen, M., & Menten, K. 2014, ApJL, 793, L34
Pfalzner, S., Umbreit, S., & Henning, T. 2005a, ApJ, 629, 526
Pfalzner, S., Vincke, K., & Xiang, M. 2015b, A&A, 576, A28
Pfalzner, S., Vogel, P., Scharwächter, J., & Olczak, C. 2005c, A&A, 437, 967
Portegies Zwart, S. F. 2016, MNRAS, 457, 313
Portegies Zwart, S. F., McMillan, S. L. W., & Gieles, M. 2010, ARA&A, 48, 431
Rosotti, G. P., Dale, J. E., de Juan Ovelar, M., et al. 2014, MNRAS, 441, 2094
Scally, A., & Clarke, C. 2001, MNRAS, 325, 449
Scally, A., & Clarke, C. 2002, MNRAS, 334, 156
Shara, M. M., Hurley, J. R., & Mardling, R. A. 2016, ApJ, 816, 59
Shu, F. H., Adams, F. C., & Lizano, S. 1987, ARA&A, 25, 23
Spurzem, R. 1999, JCoAM, 109, 407
Steinhausen, M. 2013, PhD thesis, Mathematisch-Naturwissenschaftliche Fakultät der Universität zu Köln
Steinhausen, M., & Pfalzner, S. 2014, A&A, 565, A32
Störzer, H., & Hollenbach, D. 1999, ApJ, 515, 669
Vicente, S. M., & Alves, J. 2005, A&A, 441, 195
Vincke, K., Breslau, A., & Pfalzner, S. 2015, A&A, 577, A115
Vorobyov, E. I. 2011, ApJ, 729, 146
Xiang-Gruess, M. 2016, MNRAS, 455, 3086
Zwicky, F. 1953, PASP, 65, 205

The Astrophysical Journal, 868:1 (14pp), 2018 November 20 https://doi.org/10.3847/1538-4357/aae7d1

How Do Disks and Planetary Systems in High-mass Open Clusters Differ from Those around Field Stars?

Kirsten Vincke and Susanne Pfalzner
Max Planck Institute for Radio Astronomy, Auf dem Hügel 69, D-53121 Bonn, Germany; spfalzner@mpifr.de
Received 2018 March 17; revised 2018 October 9; accepted 2018 October 9; published 2018 November 13

Abstract

Only star clusters that are sufficiently compact and massive survive largely unharmed beyond 10 Myr. However, their compactness means a high stellar density, which can lead to strong gravitational interactions between the stars. As young stars are often initially surrounded by protoplanetary disks and later on potentially by planetary systems, the question arises to what degree these strong gravitational interactions influence planet formation and the properties of planetary systems. Here, we perform simulations of the evolution of compact high-mass clusters like Trumpler 14 and Westerlund 2 from the embedded to the gas-free phase and study the influence of stellar interactions. We concentrate on the development of the mean disk size in these environments. Our simulations show that in high-mass open clusters 80%–90% of all disks/planetary systems should be smaller than 50 au just as a result of the strong stellar interactions in these environments. Already in the initial phases, three to four close flybys lead to typical disk sizes within the range of 18–27 au. Afterward, the disk sizes are altered only to a small extent. Our findings agree with the recent observation that the disk sizes in the once dense environment of the Upper Scorpio OB association, NGC 2362, and h/χPersei are at least three times smaller in size than, for example, in Taurus. We conclude that the observed planetary systems in high-mass open clusters should also be on average smaller than those found around field stars; in particular, planets on wide orbits are expected to be extremely rare in such environments.

Key words: open clusters and associations: general – planets and satellites: dynamical evolution and stability – protoplanetary disks

1. Introduction

Unlike most clusters/associations in the solar neighborhood, which often dissolve within 10 Myr (Lada & Lada 2003; Porras et al. 2003), some clusters can remain intact for hundreds of megayears and more. These clusters are characterized to be compact (1–3 pc) and relatively massive—properties they have inherited from their formation phase when they were likely even more compact (0.1–0.5 pc). Clusters like NGC 3603, Arches, Trumpler 14, and Westerlund 2 (~2 Myr) are thought to be younger counterparts.[1]

Given their small sizes and large masses ($M_c > 10^4\,M_\odot$; Figer 2008), the stellar density in such clusters is very high, for example, up to $\sim 2 \times 10^5\,M_\odot\,\mathrm{pc}^{-3}$ (Espinoza et al. 2009) in the central areas of Arches. Initially, the stars are mostly surrounded by disks from which planetary systems may form. However, the high stellar density means that protoplanetary disks in such dense environments can be influenced by external processes like external photoevaporation (Johnstone et al. 1998; Störzer & Hollenbach 1999; Scally & Clarke 2002; Matsuyama et al. 2003; Johnstone et al. 2004; Adams et al. 2006; Alexander et al. 2006; Ercolano et al. 2008; Drake et al. 2009; Gorti & Hollenbach 2009; Clarke & Owen 2015; Haworth et al. 2016b) or gravitational interactions (e.g., Clarke & Pringle 1993; Hall 1997; Scally & Clarke 2001). The latter can also alter already-formed planetary systems (see, e.g., de La Fuente Marcos & de La Fuente Marcos 1997; Laughlin & Adams 1998; Spurzem et al. 2009; Shara et al. 2016). In extreme cases these two processes can lead to disk destruction, decreasing the disk lifetime in such clusters. However, more frequently the disk is truncated, leading to a smaller disk size. Here, we concentrate on the effect of flybys on the disk size in compact clusters that develop into long-lived clusters, because this effect is present throughout all the cluster stages and it affects protoplanetary disks, as well as already-formed planetary systems. Taking Trumpler 14 and NGC 3603 as templates means that we look at the high-mass end of clusters ($M_c \geqslant 10^4\,M_\odot$), which are sometimes referred to as starburst clusters. Many open clusters have somewhat lower masses. A comparison to lower-mass compact clusters will be given in Section 4.3.

There are only a few surveys providing disk sizes in compact young massive clusters, because determining the disk sizes in these environments is challenging. One reason is that most of these high-mass compact clusters are located at relatively large distances, for example, Trumpler 14 is 2.7 kpc away. In addition, the compactness and high mass of these clusters mean that crowding is a major issue. A further problem is that, owing to their high mass, these clusters contain many massive stars that dominate the radiation. However, disk frequencies are better constrained by observations than the disk sizes. For example, in the young compact clusters Arches (2.5 ± 0.5 Myr) and the Quintuplet (4 ± 1 Myr) disk frequencies of $6\% \pm 2\%$ and $4.0\% \pm 0.7\%$, respectively, have been observed (Stolte et al. 2010, 2015). These are considerably smaller than the ones found in less dense environments such as the Orion nebula cluster, with approximately 70% (Hillenbrand et al. 1998), as shown in Figure 1. Therefore, it can be concluded that a dense environment has a strong effect on the disks. Whether the lower disk fraction in compact clusters is mainly due to the effect of flybys or external photoevaporation is an open question, as will be discussed in Section 4.3. Here, we concentrate on the effect of

[1] Currently the nomenclature is ambiguous, as these two groups are sometimes referred to as compact versus extended/loose/leaky clusters or clusters versus associations. In the following, we will use the terms compact and extended clusters.

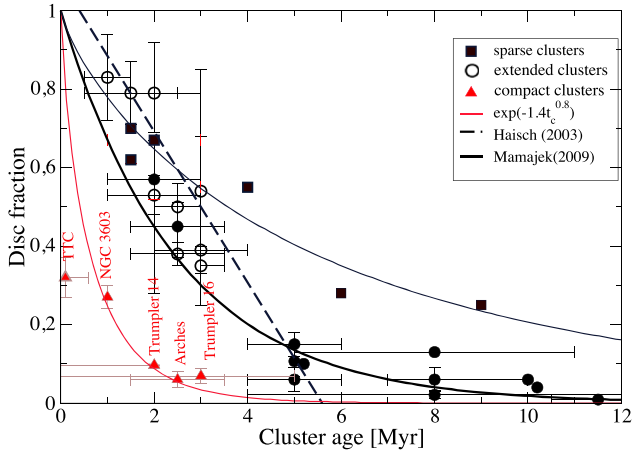

Figure 1. Disk fraction as a function of cluster age for sparse, extended, and compact clusters. Values from Pfalzner et al. (2014) and Stolte et al. (2015).

flybys on the disk size, but future investigations should also consider the effects of external photoevaporation, which have been neglected here.

As protoplanetary disks are the prerequisite for planet formation, there have been speculations whether planets could form at all in such harsh environments. Early surveys of exoplanets in long-lived open and globular clusters could only give upper limits for the portion of stars having a Jupiter-like companion (see, e.g., Paulson et al. 2004; Mochejska et al. 2006; Pepper et al. 2008; Hartman et al. 2009; van Saders & Gaudi 2011). So far about 20 planets around main-sequence stars have been found in seven different open clusters (see Table 1), among them even planetary systems containing at least two planets. In addition, some planetary candidates have been found (Brucalassi et al. 2017). Apart from the planets listed in Table 1, there is also indirect evidence for the presence of so-far-undetected planets through external metal pollution of white dwarfs, for example, in the Hyades (Farihi et al. 2013; Zuckerman et al. 2013). However, most of these clusters have a lower mass than the ones studied here. In addition, let us consider the system PSR B162026, which consists of a millisecond pulsar–white dwarf binary surrounded by a Jupiter-mass planet in a 40 yr orbit (Thorsett et al. 1993) in the globular cluster NGC 6121 (M4). Its formation has been related to dynamical interactions that occurred in the cluster (Sigurdsson et al. 2003). In summary, at least some planetary systems are able to survive in such dense stellar environments for many gigayears. Given the low number of known planets in clusters, it is still unclear whether planets are as frequent in clusters as in the field (van Saders & Gaudi 2011; Meibom et al. 2013).

As mentioned above, we concentrate here on the typical disk and planetary system (DPS) size in dense clusters as a result of flybys. More specifically, we address the question whether the sizes of the DPS in open clusters differ from those found around field stars and, if so, how to quantify these differences in size.[2]

We tackle these questions by performing numerical simulations of young compact clusters and following their evolution over the first 10 Myr of their existence. Afterward, we have analyzed the data to study the influence of the cluster environment on protoplanetary disks. There have been numerous studies investigating the effect of the gravitational interactions on protoplanetary disks and planetary systems in cluster environments. However, many of them concentrated on the flyby rate or disk frequency (Olczak et al. 2006, 2010; Pfalzner et al. 2006; Craig & Krumholz 2013; Steinhausen & Pfalzner 2014). In addition, they mostly focus on the less dense clusters typical for the solar neighborhood (Rosotti et al. 2014; Vincke et al. 2015; Portegies Zwart 2016; Vincke & Pfalzner 2016). A recent study investigates the environmental effects during the interesting star formation phase (Bate 2018); however, here again a less dense environment is considered and only the first 0.5 Myr have been modeled. Studies that investigate the effect on disk sizes or planetary system sizes including dense clusters were recently carried out by Portegies Zwart & Jilkova (2015) and Winter et al. (2018b). However, Portegies Zwart & Jilkova (2015) only gives a rough analytical estimate of an unaffected zone, and Winter et al. (2018b) look at the current density in the considered clusters but do not take into account the temporal development of the clusters.

However, dense clusters evolve along well-defined radius–age and mass–age tracks, changing their stellar density by orders of magnitude during the first 10 Myr (Pfalzner 2009; Pfalzner & Kaczmarek 2013b). In stark contrast to their less dense counterparts like the Taurus or even the Orion Nebula Cluster (ONC), in dense clusters only a few stars become unbound owing to gas expulsion at the end of the star formation process. Actually, stellar encounters are the main driving force of cluster expansion (Pfalzner & Kaczmarek 2013b), so stellar density in these clusters steadily declines with age. The effect of cluster expansion on disk sizes has so far not been modeled for dense clusters. Only the effect of a more or less fixed density environment was modeled in the above-mentioned studies. However, expansion naturally occurs during the development of such clusters, which might influence crucially the effect on DPS.

Ideally one would like to model the cluster dynamics and resolve at the same time the evolution of the disk that initially surrounds each star. There have been first attempts in such a direct method (Rosotti et al. 2014) at a fixed density. However, these simulations are limited to a low number (100) of stars that have equal mass and are in a lower-density environment. Therefore, much fewer interactions happen, and only the first ∼0.5 Myr can be modeled owing to computational limitations. By contrast, modeling the compact cluster progenitors requires us to treat at least 1000 stars with an approximately 1000 times higher stellar density, and it is essential that the stellar masses are chosen according to the initial mass function (IMF), as the effect of gravitational focusing is very important in this context (Pfalzner et al. 2006). Therefore, we perform here a two-step approach, where we first model the cluster dynamics while recording all the flybys and then post-process the data to determine the effect of the close flybys on the DPS.

In addition, the model adopted here has as its main advantage that it can be used equally for the disk and the planetary system stage, referred to here as DPS. Thus, we do not need to know how fast planet formation actually happens, which is still a major point of discussion. For disks the simulation particles are representative of the mass distribution of the dust, whereas for planetary systems they represent the parameter space where planets potentially move on circular orbits before the flyby.

An additional difference to previous studies is that most of them considered all encounters to be prograde and coplanar.

[2] DPS sizes refer here and in the following to the disk radius rather than the DPS diameter.

Table 1
Observed Properties of Planets in Open Clusters

Cluster Properties			Planet Properties				References
Name	t_{cl} (Myr)	M_{cl} ($M_{\odot}$)	Host Star	m_{pl} (M_{Jup})	a_{pl} (au)	e_{pl}	
NGC 4349	200	⋯	No. 127	19.8[a]	2.38	0.19	(1)
NGC 2632	578 ± 12	550 ± 40	Pr 0201	0.540 ± 0.039[a]	0.057	0	(2), (3), (4)
(Praesepe)			Pr 0211	1.8 ± 0.1[a,b]	0.03 ± 0.01[b]	0.011 ± 0.011[b]	(4), (5)
			Pr 0211	7.79 ± 0.33[a]	$5.5^{+3.0,c}_{-1.4}$	0.71 ± 0.11	(5)
			K2-95		0.069	0.16	(20)
			K2-100		0.029	0.24	(20)
			K2-101		0.11	0.10	(20)
			K2-102		0.083	0.10	(20)
			K2-103		0.013	0.18	(20)
			K2-104		0.025	0.18	(20)
Hyades	625 ± 50	300–400	ϵ Tau	7.6 ± 0.2	1.93 ± 0.03	0.151 ± 0.023	(6), (7)
			HD 285507	0.917 ± 0.033[a]	0.06[d]	$0.086^{+0.018}_{-0.019}$	(8)
			K2-136		Period: 7.97d	< 0.72	(17), (18), (19)
			K2-136		Period:17.31d	<0.47	(17), (18), (19)
			K2.136		Period: 25.57d	<0.75	(17), (18), (19)
NGC 2423	750	⋯	No. 3	10.6[a]	2.10	0.21	(1)
NGC 6811	1000 ± 170	∼3 000[e]	Kepler 66	⩽0.06	0.1352 ± 0.0017	⋯	(9), (10)
			Kepler 67	⩽0.06	0.1171 ± 0.0015	⋯	(10)
Rup 147	3000		K2-231	7^{+5}_{-3}			(16)
NGC 2682	3500–4000	1 080	YBP1194	0.34 ± 0.05[a]	0.07	0.24 ± 0.08	(11), (12), (13)
(M67)			YBP1514	0.40 ± 0.11[a]	0.06[d]	0.39 ± 0.17	(13)
			SAND364	1.54 ± 0.24[a]	0.53[d]	0.35 ± 0.08	(13)
			YBP401	0.46 ± 0.05[a]	0.05[d] 0.15 ± 0.08	(14), (15)	

Notes. Columns (1)–(3): cluster name, its age t_{cl}, and its mass M_{cl}. Columns (4)–(7): name of the planet-hosting star, the planet mass m_{pl}, its semimajor axis a_{pl}, and its eccentricity e_{pl}. and Column (8): references. References: (1) Lovis & Mayor 2007; (2) Delorme et al. 2011; (3) Kraus & Hillenbrand 2007; (4) Quinn et al. 2012; (5) Malavolta et al. 2016; (6) Perryman et al. 1998; (7) Sato et al. 2007; (8) Quinn et al. 2014; (9) Janes et al. 2013; (10) Meibom et al. 2013; (11) Sarajedini et al. 2009; (12) Richer et al. 1998; (13) Brucalassi et al. 2014; (14) Pietrinferni et al. 2004; (15) Brucalassi et al. 2016; (16) Curtis et al. 2018; (17) Livingston et al. 2018; (18) Livingston et al. 2018; (19) Ciardi et al. 2018; (20) Mann et al. 2016.
[a] Given as $m_{pl} * \sin(i)$, where i is the inclination between the orbital plane and the line of view.
[b] Combined planet properties from references (4) and (5); errors give differences between both data sets.
[c] Note the large error in fitted period: $P = 4\,850^{+4560}_{-1750}$ days.
[d] Calculated from given orbital periods.
[e] Crude estimate for 6000 cluster members as suggested by reference (10).

These types of flybys are the most destructive ones, and the determined losses can be interpreted as the upper limit of the effect of flybys on DPS in general (Clarke & Pringle 1993; Heller 1995; Hall 1997; Bhandare et al. 2016). Here we will investigate the more realistic situation of randomly orientated flybys. In summary, the study presented here differs from previous work as it (i) models all phases of the cluster development (embedded, expansion, and semi-equilibrium), (ii) treats dense clusters that will likely develop into long-lived open clusters, and (iii) includes flybys of arbitrary orientation.

In Section 2 we will describe the cluster simulations and the disk size determination in detail. Afterward, we present our results on the effect of the dense cluster environment on the disk size distributions in Section 3. The assumptions that we have made in our setup will be discussed in Section 4. In Section 5, we will discuss the differences that can be expected when comparing planetary systems in open clusters to those around field stars, and we give a short summary.

2. Method

As mentioned in the introduction, we use a two-step approach to determine the effect of flybys on the DPS around stars in dense clusters. First, while simulating the cluster dynamics we simultaneously record the flyby history. This is similar to what has been done in our earlier work described in Vincke & Pfalzner (2016) and Pfalzner et al. (2018a), where more details of the method can be found.

2.1. Cluster Dynamics

The cluster simulations are performed using the code Nbody6++GPU (Aarseth 1973; Spurzem 1999; Aarseth 2003; Wang et al. 2015), which is an optimized version of NBODY6++ with hybrid parallelization methods (MPI, GPU, OpenMP, and AVX/SSE) to accelerate large direct N-body simulations. In contrast to Vincke & Pfalzner (2016), we focus here on very dense—potentially long-lived—clusters representative for the case of Arches or Westerlund 2. As such, they are more massive than the special case of M44 studied in Pfalzner et al. (2018a). We start at that point in time when star formation is completed. This means that the times given are not necessarily equivalent to the cluster age, as the star formation phase is not covered in our simulations. We study two cases: one without an embedded phase (C0) and the other one where we have considered a 1 Myr long embedded phase (C1). For the other properties of the simulated clusters, see Table 2.

Table 2
Compact Cluster Model Setup and Dynamical Timescales

Model	Represents	N_{stars}	N_{sim}	SFE	r_{hm}	t_{emb}	M_{stars}	M_{cl}	t_{dyn}
					(pc)	(Myr)	($M_\odot$)	($M_\odot$)	(Myr)
C0	Westerlund 1	32 000	10	0.7	0.2	0.0	18 839	26 913	0.01
C1	Westerlund 1	32 000	10	0.7	0.2	1.0	18 824	26 891	0.01
E52	NGC 2244	32 000	9	0.3	1.3	2.0	18 852	62 842	0.1
E2	ONC	4 000	94	0.3	1.3	2.0	2 358.1	7 860.3	0.33

Note. Column (1): model name. Column (2): representative cases. Column (3): number of stars in the model, N_{stars}. Column (4): number of simulations in the simulation campaign, N_{sim}. Column (5): star formation efficiency, SFE. Column (6): initial half-mass radius of the stellar and the gas component, r_{hm}. Column (7): duration of the embedded phase, t_{emb}. Column (8): stellar mass of the cluster, M_{stars}. Column (9): total cluster mass (stars + gas), M_{cl}. Column (10): dynamical timescale, t_{dyn}. See text for calculation.

In order to study to what extent the planetary systems in compact/open clusters resemble or differ from those found around field stars and those formed in less dense clusters, we compare our results to our earlier work, where we modeled less dense clusters typical for the solar neighborhood. The parameters of this cluster (model E52) are also given in Table 2. Most importantly, E52 has the same initial mass as C0 and C1, but the half-mass radius is larger (1.3 pc) and the star formation efficiency (SFE), which is the fraction of gas in the cluster that is turned into stars, is smaller (30% compared to 70%). In this case the embedded phase, t_{emb}, was assumed to last 2 Myr.

2.1.1. Cluster Initial Conditions

The starting point of our simulations, $t_0 = 0$, corresponds to a fully formed cluster. In NBody6++ the gas is not modeled explicitly but just as a background potential. The clusters are set up with an initial half-mass radius of 0.2 pc that is typical for compact clusters at the start of the expansion phase (Pfalzner & Kaczmarek 2013b). The SFE is assumed to be 70%. There are two reasons why it is necessary to assume such a high SFE value: (i) observations hint at much higher SFEs for compact clusters (Rochau et al. 2010; Cottaar et al. 2012; Hénault-Brunet et al. 2012) than for those in the solar neighborhood, and (ii) if one interprets the size–age relation in compact clusters as a temporal sequence, because this demands also such a high SFE (Pfalzner & Kaczmarek 2013b).

Usually, the stellar density distribution is modeled either as a King or a Plummer profile (see Bastian & Goodwin 2006; Rosotti et al. 2014; Banerjee & Kroupa 2015; Wang et al. 2015). Here we choose a modified King profile for the stars and a corresponding Plummer profile for the gas that reflects the situation in observed clusters (Espinoza et al. 2009; Steinhausen 2013).[3] The total cluster mass is given by $M_{cl} = M_{stars}+M_{gas}$, with M_{stars} being the stellar component of the cluster and M_{gas} the gas mass. It follows that

$$M_{gas} = \frac{M_{stars}(1 - \mathrm{SFE})}{\mathrm{SFE}}. \quad (1)$$

The stellar masses were sampled from an IMF (Kroupa 2002) with a lower limit of 0.08 $M_\odot$ and an upper limit of 150 $M_\odot$, and the velocities were sampled from a Maxwellian distribution.

[3] Note that the simulations are not supposed to exactly reproduce the Arches cluster, but to represent compact clusters in general.

2.1.2. Flyby Frequency

In all cases we assume the clusters to be initially in virial equilibrium. The gas expulsion is modeled as being instantaneous, as $t_{gas} < t_{emb} < 1$ Myr. It is not clear how long the embedded phase of compact clusters lasts. None of the compact clusters younger than 3 Myr, such as the Arches cluster, show signs of considerable amounts of gas (see Pfalzner 2009). Thus, to date, no unambiguous embedded precursor cluster has been identified. From the absence of embedded massive compact cluster precursors and the observed gas-free clusters (t_{age} = 1–2 Myr), it can be assumed that the embedded phase is short, probably lasting <1 Myr.

Given the absence of observed timescales for the embedded phase, we modeled two cases: $t_{emb} = 1$ Myr (C1) and $t_{emb} = 0$ Myr (C0) (see also Table 2), the latter being representative for a cluster with a very short embedded phase $t_{emb} \ll 1$ Myr. The consequences of these choices will be analyzed in Section 4. Table 1 also gives the simulation parameters of two of the extended clusters modeled in Vincke & Pfalzner (2016), for comparison.

The gas expulsion process brings the cluster out of equilibrium, leading to members becoming unbound. However, as the SFE is quite high, this gas expulsion is only a secondary cause for cluster expansion for models C0 and C1. The main reason why the clusters expand by a factor of 10–20 is the ejection of stars from the densest cluster regions (Pfalzner & Kaczmarek 2013b).

During the simulations, we record for each flyby the relevant parameters (time, duration, periastron, distance of primary to cluster center, mass ratio of encounter partners). This information is then used to post-process the data to obtain the effect of such a flyby on the DPS. For each model, simulations of only the first 3 Myr were performed.

2.2. Modeling the Effect of a Flyby on the DPS Size

We assume that initially each star was surrounded by a protoplanetary disk, equivalent to a 100% initial disk frequency. Observationally it is quite difficult to determine the initial disk frequency, especially in such dense environments. The highest disk frequency observed for a compact cluster is approximately 30% for NGC 3603 (Stolte et al. 2015). However, as disk destruction could be very rapid in such environments, a 100% initial disk frequency may be still a good assumption. Even if the initial disk frequency would be considerably less, this would not be a problem for the results presented here, as we are predominantly interested in the

disk sizes. In this case, our results would still hold for the stars that had initially disks.

Similarly, it is not straightforward what value one should assume for the primordial disk size. Here we make one major assumption that currently is not testable by observations because there exist no observations of disk sizes in young massive compact clusters. This assumption is that disks around stars in compact clusters have initially the same properties concerning their size, mass, etc., as those around nearby young stars that are part of a sparse cluster or associations. One has to keep in mind that those disks might differ in their properties because they normally form in an environment of higher gas and dust density and the embedded phase in compact clusters is much shorter. Consequences might be more massive compact disks, but there are equally strong arguments for less massive, more extended disks. Without observations, that is so far just speculation. Therefore, we assume a low-mass disk as characteristic for young stars in compact clusters.

In Taurus, a very sparse association, the disk size distribution peaks at 200 au, and disks of up to 700 au are found (Andrews & Williams 2007). Observations show disk sizes of 27–500 au in the ONC (McCaughrean & O'dell 1996; Vicente & Alves 2005; Bally et al. 2015); however, the ONC is denser than Taurus, and at an age of at least 1 Myr it is questionable whether the measured disk sizes correspond to primordial ones. It is more likely that the disk size has already been altered owing to photoevaporation or stellar flybys.

Disk size values found, for example, in Taurus should correspond to those unaffected by the environment. Therefore, we assume 200 au as the initial disk size for all stars in our simulations. We will see in the following that almost all disks in the compact clusters are stripped to sizes well below 100 au, so the result is completely independent of this initial choice. With this, we can separate processed from nonprocessed disks easily.

The question is whether and to what degree the DPS sizes can increase again after they have been reduced in size by a flyby. There are various processes that could lead to DPS size growth, which in an extreme case could result in the disks becoming as large as or even larger than they were initially. This is discussed in Section 4.2.

2.2.1. DPS Size Determination after Flybys

For post-processing the flyby data we make use of the computational results from extensive numerical parameter studies, which determine DPS size as a function of the mass ratio $m_{12} = m_2/m_1$, the periastron distance $r_{\rm peri}$ (Breslau et al. 2014), and the inclination (Bhandare et al. 2016) during the flyby. A detailed description of the different treatment of coplanar and inclined flybys is given in Appendix A.

In contrast to previous studies (see, e.g., Clarke & Pringle 1993; Heller 1995; Hall 1997; Portegies Zwart & Jilkova 2015; Vincke et al. 2015), Bhandare et al. (2016) implicitly took into account randomly orientated DPS, which is a realistic situation for stellar clusters. They find that non-coplanar encounters have a still considerable effect on the DPS size. A database of the computational results can be found at http://www3.mpifr-bonn.mpg.de/encounter-properties/. Averaged over all inclinations, including the coplanar prograde and coplanar retrograde case, they find the following approximate dependence:

$$r_{\rm disk} = 1.6 \cdot r_{\rm peri}^{0.72} \cdot m_{12}^{-0.2}, \tag{2}$$

where $r_{\rm disk}$ is smaller than or equal to the DPS size before the encounter $r_{\rm previous}$ (all sizes and distances are in au).

Equation (2) holds for mass ratios in the range of 0.3–50; however, it is unfortunately not straightforwardly applicable to our study. The reason is that their fit formula focuses on very close to penetrating ($r_{\rm peri} \leqslant r_{\rm previous}$) encounters, with the largest periastron distances included being $5 \times r_{\rm init}$. In stellar clusters, even in the most compact ones, flybys with even larger periastron distances are the most common (see also Scally & Clarke 2001; Olczak et al. 2006). For this reason, we set up additional simulations analogous to the ones by Bhandare et al. (2016) with a focus on distant flybys. We obtained a slightly different fit formula for the DPS size after a flyby with (m_{12}, $r_{\rm peri}$) averaged over all inclinations, which gives a better fit for distant flybys:

$$r_{\rm disk} = \begin{cases} (1.6 \cdot m_{12}^{-0.2} - 1.26 \cdot m_{12}^{-0.182}) \cdot r_{\rm peri} & \text{for } r_{\rm disk} < r_{\rm previo} \\ r_{\rm previous}, & \text{for } r_{\rm disk} \geqslant r_{\rm previo} \end{cases} \tag{3}$$

A detailed description of the simulations, the data, and the fit are given in Appendix B. Equation (3) enables us to indirectly study randomly orientated flybys without having to simulate DPS and clusters simultaneously (as done by Rosotti et al. 2014), which would not be possible for groups of 32,000 stars over timescales of 3 Myr.

Previous simulations treated all flybys as coplanar and could only give upper limits for the effect of flybys; as such, they overestimated it. However, Figure 2 shows that there is a difference between coplanar and inclined flyby, but it is relatively small. For example, a 200 au sized disk would be truncated to 84 au by a flyby at a periastron distance of 300 au, whereas the disk size after a randomly orientated encounter would be 102 au, which is about 20% larger. This is also reflected in the overall median DPS size in each cluster type (see Appendix B). In the following, unless stated otherwise, we will present the outcome of our simulations assuming randomly orientated flybys. Here we only take into account events that lead to a DPS-size reduction of at least 5% ($r_{\rm disk}/r_{\rm previous} \leqslant 0.95$).

Comparing theoretical and observational disk sizes poses many difficulties. On the one hand, there are different definitions of disk sizes in the theoretical treatment, as well as in observations. This issue is discussed in detail in Breslau et al. (2014), and we use their definition of steepest gradient at the outside of the disk, owing to its similarity to most observational methods. On the other hand, observational disk sizes depend on the wavelength range of the observations, whether one looks at the size of the gas or dust disk, the development stage of the disk, and many other parameters (Balog et al. 2016; van der Marel et al. 2018). Given the scarcity of disk size measurements in compact clusters, we just take the given data as their face value. However, when more data will be available in the future, this will require finer specification.

We neglect effects other than flybys that could potentially lead to DPS size changes, for example, viscous spreading or mass transport between disks, meaning that we assume that the disk size remains constant throughout our simulations unless altered by a consecutive flyby (see Rosotti et al. 2014). For a

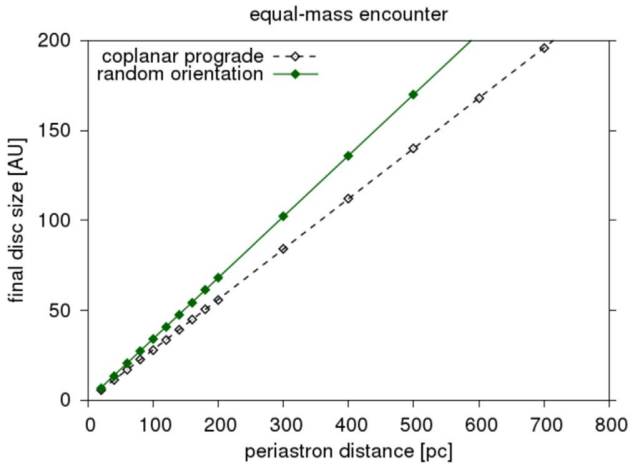

Figure 2. Final DPS size as a function of the periastron distance for coplanar, prograde flybys (black open diamonds; Breslau et al. 2014) and randomly orientated flybys given by Equation (3) between two stars of equal mass ($m_{12} = 1$).

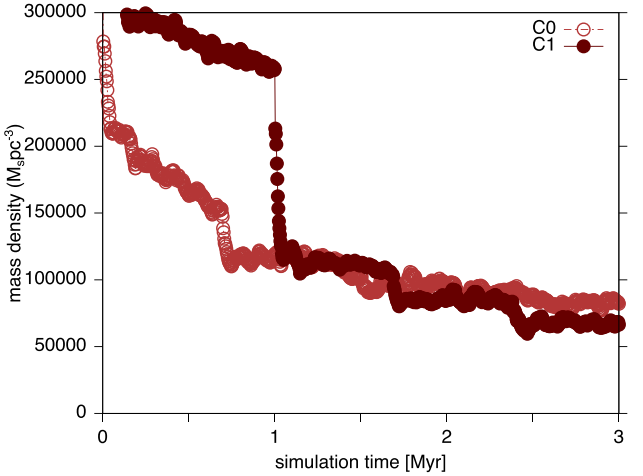

Figure 3. Mass density within the half-mass radius ($r_{\rm hm} = 0.2$ pc) as a function of time for the compact clusters (C0: light-red circles; C1: dark-red circles). The vertical line depicts the point in time of gas expulsion for model C1 (1 Myr).

detailed discussion of potential DPS size changing processes other than flybys, see Section 4.

3. Results

The dynamical evolution of the compact clusters, which might develop into long-lived open clusters, differs considerably from that of the short-lived extended clusters/association that dominate the solar neighborhood. It has been long expected that in such environments interactions are strong and very frequent and as such have a significant influence on the DPS. In the following we quantify the effect on the DPS sizes.

3.1. Cluster Evolution

First, we want to look at the cluster evolution over the first 3 Myr. As mentioned in the introduction, in contrast to associations, compact clusters have a 70% SFE, so the gas loss on its own only leads to a slight increase in the clusters size, but it is rather the ejection of stars in the dense cluster center that is responsible for the strong increase in cluster size (Pfalzner & Kaczmarek 2013b). In Figure 3 the stellar density development of the clusters within a sphere of their half-mass radius (0.2 pc) as a function of time is depicted for our compact models C0 and C1 (light-red circles and dark-red circles, respectively). Note that here the total system mass is taken into account, meaning the gas plus stellar mass. The gas expulsion at $t = 0$ for C0 and $t = 1$ Myr for C1 results therefore in a drop in mass density by 30%. In addition, the loss of stars due to close flybys leads to a steady decrease in stellar density. As the stellar density decreases, stellar ejections become less common, leading to a gradual slowing down of the expansion process.

3.2. Cluster Density

The cluster density determines the degree of influence of the environment on the protoplanetary disks surrounding its members. Naturally, the number of flybys potentially changing the disk size in the compact clusters is high, about three to four flybys per star during a period of 3 Myr. This is not much more than for an extended cluster of the same mass, which has one to two such flybys per star despite having a lower initial density of roughly 150,000 $M_\odot$ pc^{-3} within 0.2 pc.

The reason is the qualitative difference between these encounters: whereas in extended clusters the DPS size is reduced step by step, in compact clusters most disks experience very close flybys already within the first 0.1 Myr; see Figure 4. These very close flybys lead to such DPS disk sizes that the cross section for a follow-up flyby becomes small. As a consequence, the number of flybys that are actually necessary to produce such small DPS sizes is relatively small.

3.3. Median DPS Size

Next, we study the DPS size development in the different cluster environments. As expected, the high density in the compact clusters leads to small protoplanetary disks (see, e.g., Bonnell et al. 2001; Vincke et al. 2015). Most of the change occurs in the early phases of the cluster development. At 3 Myr the mean DPS size is 21 au for model C0 and 11 au in the case of model C1. For model C1 most of the DPS changes happen during the embedded phase, at the end of which the mean DPS size is already 12 au.

As mentioned above, an embedded phase of such compact clusters is probably shorter than 1 Myr, such that the real mean DPS size can be expected to be in the range of 12 au to 21 au by 3 Myr. Figure 5(a) shows that the mean disk size within the half-mass radius is even smaller, approximately 10 and 8 au for C0 and C1, respectively. The interaction dynamics can vary considerably between different realizations (Parker & Goodwin 2012); this is reflected in the relatively large error bars in Figure 5(a), which correspond to the standard deviation of the values.

The DPS sizes are relatively small, as, for example, our own solar system with a Neptune semimajor axis of ~30 au could not have formed from such a small disk. On average, the DPS sizes in compact clusters are considerably smaller than extended clusters. For our model E52 a factor of four larger values are obtained, and for the ONC (see Figure 4(a), blue), we obtain a typical value of 160 au for the mean disk size within the half-mass radius, which would be characteristic of the dense clusters in the solar neighborhood.

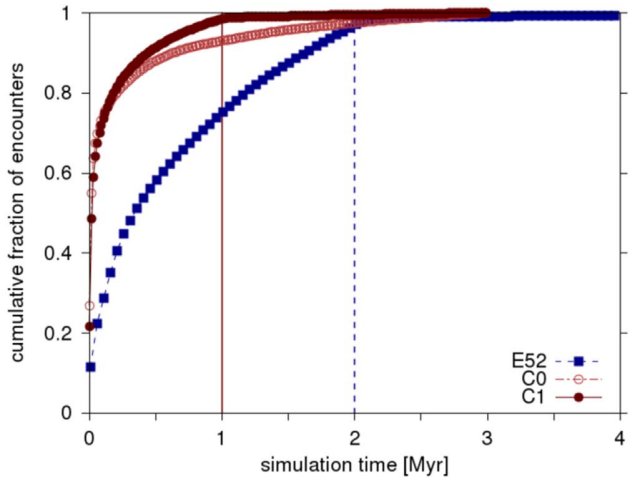

Figure 4. Cumulative fraction of randomly orientated encounters as a function of time for cluster models C0 (light-red circles), C1 (dark-red circles), and E52 (dark-blue filled squares). The vertical black lines depict the point in time of gas expulsion for model C1 (1 Myr; dashed) and model E52 (2 Myr; solid).

As the density contrast between the cluster center and its outskirts is very high, one expects that more encounters take place in the cluster core than in the outskirts. This is reflected in the median DPS size as a function of the distance to the cluster center shown in Figure 5(b). For models C0 and C1 (red) the median DPS size is smaller than 10 au close to the cluster center. For model C0 the median DPS size in the cluster core (<0.3 pc) is 8 au, and for model C1 it is 5 au at 0.3 pc. On the other hand, the DPS sizes are only larger than 10 au at distances larger than 0.5 pc for C0 and 0.8 pc for model C1. Again, the scatter in the obtained values is relatively large, but the general trend is always the same, with smaller values closer to the cluster center. As will be discussed in Section 4, it is an open question whether planets can form in such small disks at all. In comparison, for model E52 the median disk size even in the most central area is at least 20 au (Vincke & Pfalzner 2016). For model C0 even the stars at the outskirts of the cluster (>10 pc), which mostly become unbound and leave the clusters, still have a median disk size of 46 au. This means that any star that has been part of a compact cluster, even just for a short time, bears its marks by its small DPS size.

Next, we discuss the question whether stars of different mass are affected to a different degree. Figure 6 shows that the final DPS size depends only slightly on the stellar mass. From low-mass stars to B stars there is only a slight increase in final mean DPS. However, O stars are much more affected by flybys than B stars, as it is very conspicuous in model C0, where the average disk size of O stars is 8 au, compared to 34 au for the B stars. The reason for the slight increase for M to B stars, as well as the decrease for O stars, is the flyby statistics. M stars are most common and are therefore involved in most flybys, whereas the very massive ($\gg 20\,M_{\odot}$) stars act as gravitational foci, therefore undergoing many strong flybys. A similar effect for the disk frequency has been noticed before, e.g., by Pfalzner & Olczak (2007). However, for very large masses the statistics is less good, as there are relatively few very high mass stars.

We assumed that initially all stars had the same disk size independent of the stellar mass, although theoretical (see, e.g., Vorobyov 2011) and observational reasons support a slight dependence of the disk size on the stellar mass. It is often assumed that the disk size increases with stellar mass, ranging from roughly 100 au for stars with $0.08\,M_{\odot}$ up to nearly 1000 au for solar-like stars (see, e.g., Vorobyov 2011). Such an initial dependence would not alter the results presented here because all final mean DPS sizes are much smaller than 100 au.

3.4. Disk Size Distributions in Different Environments

How does the disk size distribution look like in such compact clusters? Figure 7 shows the size distributions for the two compact cluster models. Here we try to mimic observations and consider only stars within 3 pc—the typical field of view (FOV) in observation at 200–400 pc distance, for example, with the *Spitzer* telescope. Outside this radius, member determination is very difficult owing to the usually high stellar back-/foreground densities.

Surprisingly, disk sizes smaller than 10 au are the most common (35% and 47%, respectively) in such compact clusters; see Figure 7(a). If the disks are cut down to such a small size before planet formation took place, it is unlikely that there is enough material left for gas giants to form by accretion afterward, because the remaining mass in the disk is relatively small. However, if one of the formation channels is hierarchical fragmentation, gas giants might still form in such hostile environments. In some cases there might be sufficient material to form terrestrial planets by accretion, but this requires further investigation.

Large disks are quite rare: only as much as 23%, or even 14% for model C1, of disks are larger than 100 au, and they are mostly located at the outskirts of the clusters. In the extended cluster only about 37% of all stars are smaller than 100 au after 10 Myr. Even though the simulation time was much longer, the majority of disks remain large and only very few are destroyed (6%).

4. Discussion

In our cluster simulations we have made a number of assumptions and simplifications, namely, we (1) assumed instantaneous gas expulsion, (2) did not include mass segregation, and (3) did not include primordial binaries. We will discuss the potential influence of each of these in the following section.

4.1. Cluster Dynamical Evolution

4.1.1. Cluster Dynamics

We investigated the effect of the duration of the embedded phase by comparing models $t_{\rm emb} = 0$ (C0) and $t_{\rm emb} = 1$ Myr (C1). Model C0 can be used to set constraints to disk size distributions of clusters that are embedded for less than 1 Myr (C1). The duration of the embedded phase does make a difference for the resulting disks and possibly forming planetary systems: the fraction of small disks ($\leqslant$20 au) is much larger in the embedded model, and the median disk sizes differ by up to a factor of two; see Figures 7 and 5(b).

We assumed the gas expulsion itself to happen instantaneously. This is, at least for the investigated very massive and dense clusters, a justified approximation. In reality, the gas expulsion is thought to last a few dynamical timescales, which are of the order of 0.01 Myr for the compact clusters and 0.1 Myr for the extended model E52, so modeling the gas

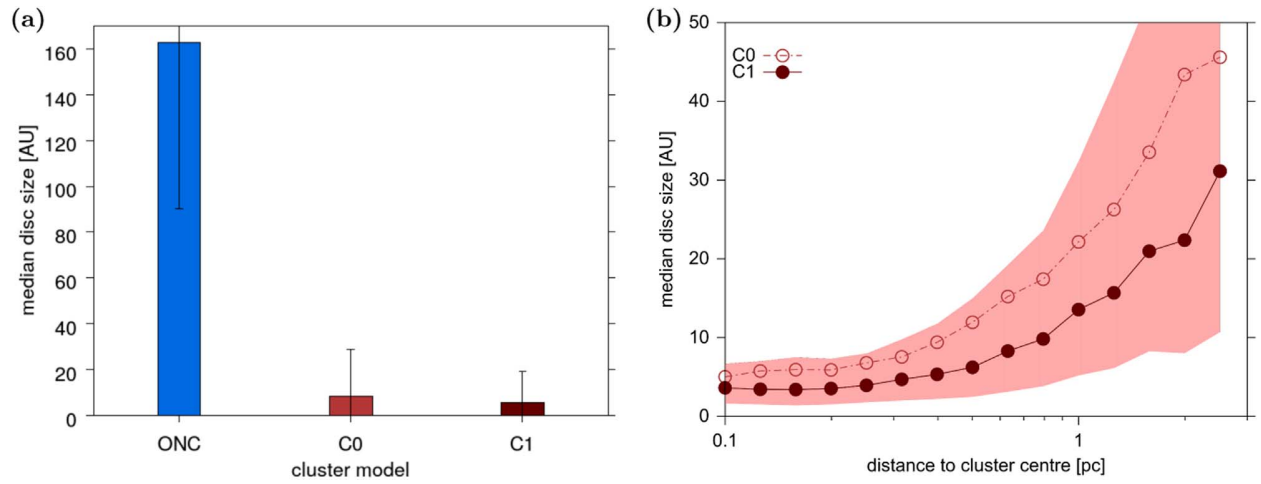

Figure 5. (a) Median DPS size at the end of the embedded phase for C0, C1, and the ONC at the end of the simulations within the half-mass radius of the cluster, with errors indicated by the bars. (b) Median DPS size as a function of the distance to the cluster center after 3 Myr. Here the standard deviation is indicated by the shaded area. Distance bins containing less than 10 stars for the whole simulation campaign were excluded.

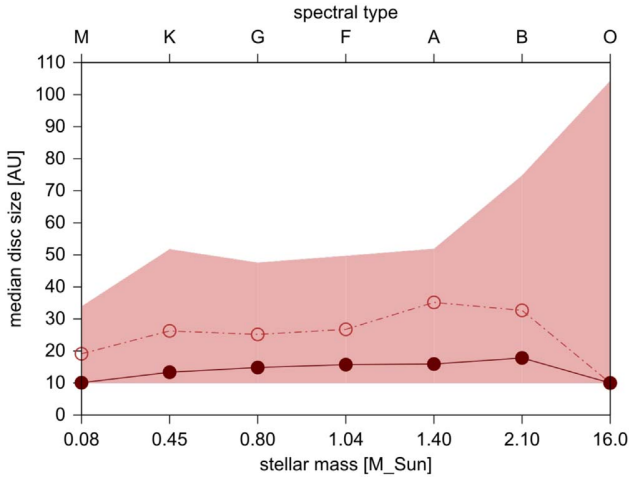

Figure 6. Median DPS size as a function of stellar mass and stellar type for the three cluster models (C0: light-red circles; C1: dark-red circles; E51: dark-blue squares). The shaded region shows the standard deviation of the values.

expulsion instantaneously is reasonable. If the gas expulsion were to last longer, the clusters would have enough time to adjust to the gas mass loss, so fewer stars would become unbound. Additionally, the mass density would stay higher for a longer time span, leading to a higher encounter frequency and thus smaller disks.

4.1.2. Mass Segregation

In our study, the masses and positions of stars in the clusters were picked out randomly from the respective distributions disregarding initial mass segregation. Although a lot of clusters seem to be mass segregated, it is still under debate whether this is an initial property or a consequence of dynamical evolution. If the number density would remain the same but with the more massive stars concentrated in the center, the encounter rate in the cluster core would increase because of the larger gravitational focusing by the massive stars. Hence, the disks around the most massive stars would be smaller or could even be destroyed.

4.1.3. Binaries

In our simulations all stars were initially single and binaries were not included in the setup. The reason why we neglected binaries is that the data for the effect on the disk of binaries are only available for single cases, but no systematic parameter studies like the ones required here do exist. However, observations show that a large portion of stars are binaries (Köhler et al. 2006; Duchêne & Kraus 2013). This means that the fraction of stars surrounded by disks presented here is an upper limit, as more disks would be destroyed when—or not even form—as part of a binary. The periodic interactions between a disk and its binary star would have to be investigated in more detail to make further predictions about its size and structure.

The inclusion of binaries would also affect the cluster evolution: Kaczmarek (2012) demonstrated that binaries lead to an accelerated cluster expansion on timescales of a few megayears, but as most flybys that lead to disk-size truncation occur during the first megayear, this should not alter the results presented here about the disk sizes. In addition, observations and simulations show that the most massive stars are most probably part of binary systems. This increases gravitational focusing, which in turn might result in even smaller disk sizes.

In our simulations some captures of stars into binaries do occur; however, these are relatively rare processes. They are resolved in the cluster simulation. However, in the effect on the disk size they are treated like that of a flyby at the resulting binary separation. Like in the above case of primordial binaries, this leads to underestimating the effect and would require further investigation in the future.

4.1.4. Parabolic Encounters

All flybys were assumed to be parabolic, that is, the eccentricities are $e = 1$. The encounter eccentricity depends on the cluster density (Olczak et al. 2010, 2012), especially in the case of very dense clusters investigated here where the real eccentricities can be fairly high owing to the dominance of three-body interactions. The topic of the dependence of the disk size on the eccentricity of the flyby has been scarcely investigated in the literature. However, studies of the disk mass loss indicate that hyperbolic flybys might be less

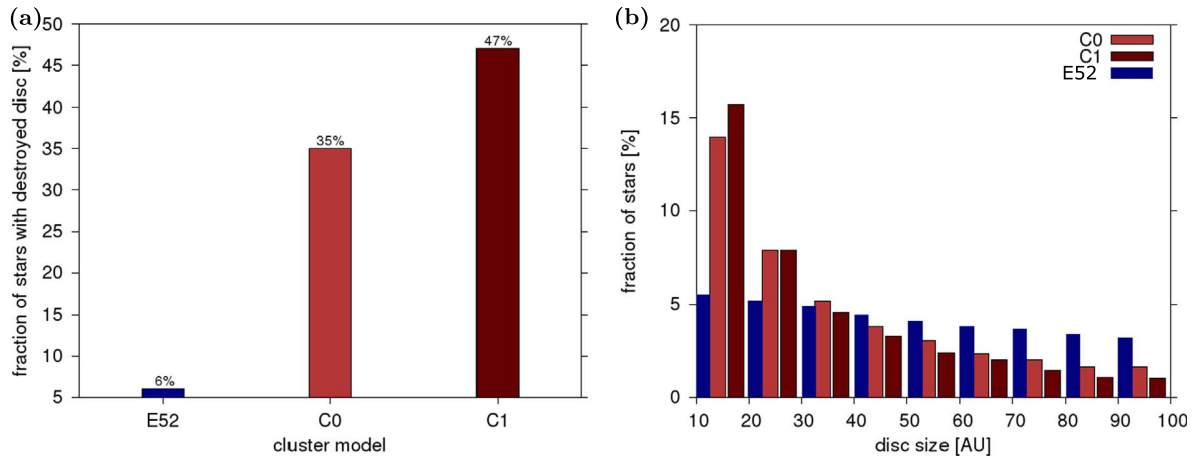

Figure 7. (a) Fraction of stars with disk sizes smaller than 10 au at the end of simulation in the whole cluster. (b) Disk size distribution within an artificial field of view of 3.0 pc at the end of the simulations (t_{sim}) for the different cluster models for disk sizes smaller than 100 au. The compact clusters are depicted in red (C0: light red; C1: dark red), the extended cluster (E52) in dark blue.

destructive (Pfalzner 2004). Recent investigation by Winter et al. (2018b) indicates that this is also true for disk sizes.

4.1.5. Stellar Evolution

We did not include stellar evolution in our simulations, as we think that the influence on the results is limited. The minimum mass for a star to become a supernova during the 3 Myr covered here is 70 $M_\odot$. Thus, some of the realizations could in principle experience a supernova explosion toward the end of the simulation. However, then most of the disk truncation processes have already taken place, so that the influence of the supernova on the cluster dynamics should be very small. To have a considerable influence on the cluster dynamics, it would be required that the supernova explosion would take place within the first megayear, but the required stellar mass would be about 400 $M_\odot$.

Even if no supernova explosion were to take place, the mass loss of the massive stars, even during their first few megayears, might be important (Vink 2015). We did not include mass loss in our simulations because, first, the number of high-mass stars is very low in comparison to the low-mass stars; thus, their effect on the average disk size is low. Second, in clusters like the ONC the massive stars play a fundamental role in the dynamics, as they act as gravitational foci. In this type of cluster mass loss of the massive stars might possibly play some role. However, for the much denser clusters, which we discuss here, the massive stars lose this role, as interactions with the lower-mass members become much more common (Olczak et al. 2010). Basically, there needs to be sufficient space around the massive stars to become a focus; if that space is filled up, the massive stars lose their special role as foci. Therefore, the resulting average disk size is dominated by the interactions between the low-mass stars. Thus, even if the massive stars would lose considerable amounts of their mass, this would not influence the result in any sizable way. Third, if we take $10^{-7}\,M_\odot\,\mathrm{yr}^{-1}$ as an example, this would correspond to a 0.3 $M_\odot$ loss. A 100 $M_\odot$ star would be reduced to a 99.7 $M_\odot$ star after 3 Myr, which makes hardly any difference on the size after a flyby. Even the 3 $M_\odot$ difference expected with a $10^{-6}\,M_\odot\,\mathrm{yr}^{-1}$ mass loss would change the disk size value by less than 2 au even in a very close encounter, which is negligible in an averaging computation over 32,000 stars. A constant mass-loss rate of $10^{-5}\,M_\odot\,\mathrm{yr}^{-1}$ would be a problem, especially for stars of 30 $M_\odot$ and smaller, as they would have dispersed completely by then. However, we doubt that high-mass stars continuously have such high mass-loss rates over the entire 3 Myr modeled here. It is much more likely that the mass-loss rate varies strongly with time, even showing bursts like those known for accretion. Nevertheless, the role of mass loss in such massive clusters should be considered in future studies.

4.2. Other Influence on DPS Size

The results from the effect of flybys described in Section 2.2.1 can be used under certain conditions to describe the effect on the disk and also on planetary systems. The difference is that for disks the simulation particles are representative of the mass distribution of the dust, whereas for planetary systems they represent the parameter space where planets potentially move on circular orbits before the flyby.

The question is whether and to what degree the DPS sizes can change after they have been reduced in size by a flyby. There are various processes that could lead to DPS size growth, which in an extreme case could result in the disks becoming as large as or even larger than they were initially. We have to distinguish between the processes that play a role in the disk phase and those that are only relevant in the phase where a planetary system has already formed.

4.2.1. Disk Phase

The main process that can change the disk size in addition to flybys is external photoevaporation (Haworth et al. 2016a). The radiation from the massive stars is strong enough to ionize the material in the disk, and gradually material is removed from the outskirts of the disk. Therefore, the disk size can be reduced by external photoevaporation. Thus, the above results can be considered as upper limits of the disk size, because external photoevaporation could lead to a further decrease in disk size. Unfortunately, the degree and especially the timescale on which external photoevaporation happens are less constrained than the gravitational effect of flybys (Gorti et al. 2016). In addition, comparison between the expected effect of external photoevaporation and observations indicates that the real effect

is smaller than that predicted by theory (Gorti et al. 2016). Therefore, the average effect of external photoevaporation in clusters is currently unknown. It is also important to note that external photoevaporation is only efficient when the cluster is no longer heavily embedded in gas. This means that one would only expect additional disk reduction by photoevaporation after the embedded phase has ended.

However, there are not only processes that could lead to further disk size reduction but also those that potentially would lead to a size increase. One of them is viscous spreading during the disk phase, which could lead to an increase in disk size before and after the flyby. The disk size growth before the flyby does not influence our results because basically all disks are affected by flybys to such a degree that they become smaller than 100 au independently of their pre-flyby size. Potentially more important is the viscous spreading that might take place after the flyby. However, considerable disk size increase can only happen if (i) the disk is relatively massive, so that the disk has a sufficiently high viscosity, and (ii) the gas stays in disks for a sufficiently long time. As we have no observational information about the disks masses in compact clusters, we have no idea whether they are more or less massive than around nearby stars. Assuming that it is the same as around nearby young stars, this corresponds to a typical disk mass $m_d \sim 0.01\,M_s$. For such low-mass disks considerable viscous spreading (>20 au) is noticeable after ≈5–10 Myr. However, in compact clusters the average lifetime of disks is very short, at most 1–2 Myr, so that disk spreading is ≪20 au. This means that the potentially resulting planetary systems are mostly ≪40 au.

4.2.2. Planetary System Phase

There are basically two processes that could lead to changes in the system size of an already-formed planetary system after the flyby: capture of one or more planets, or excitation of planets onto eccentric orbits by planet–planet scattering.

Generally capturing requires a close flyby, but in this case not only is material captured but at the same time the disk size is reduced. The material captured from another star tends to go onto highly eccentric orbits with the periastron being relatively small. The latter means that in most cases $r_{\rm peri}(\text{captured}) < r_d$. As soon as there are objects on eccentric orbits, it is no longer straightforward how to define the disk size. If we consider the periastron distance, then only captured matter does not influence the disk size. However, if one considers the outermost periastron as relevant, then an increase in DPS size could in principle happen.

How common would such a capture event be? Capturing a planet from another star requires a relatively close flyby, and many flybys that lead to DPS truncation are too distant to lead to capturing. In other words, capturing is less common than DPS disk size decrease. This again implies that planet-capturing processes are most common during the early cluster phases and are even rarer than DPS decrease in later phases. Therefore, the question is whether planets that could be potentially captured have already formed during the first ≈5 Myr, so that they could lead to a larger DPS size than expected from our results. It is still an open question what is the shortest time span required for planet formation, with estimates ranging from 1 to 10 Myr. The additional difficulty is that the context here implies captured planets that would have been originally orbiting at relatively large distances (>50 au) from their previous host star, because only this lightly bound matter can be swapped between stars during a flyby. According to the standard accretion model, planet formation proceeds more slowly in the outer disk regions. Therefore, the only alternative would be that these planets formed early on owing to gravitational instability in a relatively massive disk. In summary, there might be some cases where planet capture can lead to a larger DPS afterward, but these cases are likely quite rare, meaning that they should not significantly alter the results presented above.

The only process that could lead to considerably larger DPS in compact clusters than the ones discussed above is, in our opinion, planet–planet scattering. Here long-term interactions between the planets orbiting a star can lead to the ejection of planets or the excitation of the orbit of one or more members of the system to a larger distance from the host star. How common such a process is depends on the compactness of the original planetary system. Again, it is not known how compact planetary systems around stars and particularly around cluster stars typically are. Even if we assume that compact systems are common and excitation to more distant orbits happens often, this would probably not result in a larger observed DPS size in the near future. The reason is that mostly the least massive planet is excited onto a wider generally eccentric orbit. Unfortunately, in the foreseeable future it will not be possible to detect low-mass planets moving on wide orbits in mostly fairly distant compact clusters.

In summary, the above-presented results should be representative not only for the situation at an age of 10 Myr but also for the long-term appearance of planetary systems in such compact clusters.

4.3. Comparison with Other Models

As mentioned in the introduction, most simulations so far concentrated on DPS sizes in less dense clusters. These are more typical in the solar neighborhood, and as such more observational data exist for comparison. Winter et al. (2018a) investigate clusters spanning from low-density clusters to those similar to the ones studied here. They did not take into account the cluster development, meaning that the cluster density stays constant for the entire 3 Myr they model in their Monte Carlo approach. However, they also treat the effect of external photoevaporation. Taking both processes into account, Winter et al. (2018a) obtain a mean disk size of approximately 85 au at a cluster age of 3 Myr for their low-density model (model D). The density in this model is slightly lower than the one by Vincke & Pfalzner (2016); however, both these values for typical disk sizes in low-density clusters are significantly larger than the value of 21 au we obtain for the compact clusters considered here. This means that there is a significant difference between the typical DPS sizes in the typical solar neighborhood clusters and the ones likely to develop into long-lived open clusters.

Pfalzner et al. (2018a) modeled one specific open cluster, namely, M44. This cluster probably had a similar size to the one modeled here but an approximately 10 times lower mass to start with, and therefore an ~10 times lower stellar density. Therefore, it might be considered a prototype for many of the open clusters with lower masses. As the stellar density is lower than in the case modeled here, one can expect that the disk sizes should on average be slightly larger, or that the relative number of very small disks should be slightly smaller. Figure 6 in Pfalzner et al. (2018a) confirms this expectation. There one

can see that 13% of all disks in M44 are smaller than 10 au compared to about 35%–47% in the case studied here.

Winter et al. (2018a) considered also compact clusters similar to the ones we consider here. They find that generally external photoevaporation dominates as a disk truncation process over the effect of flybys. Does this mean that flybys are only a second-order effect for the disk size? Not really; they specifically point out that their model only applies to the situation when the cluster is no longer strongly embedded, as only then external photoevaporation can act to its full extent. We saw in Section 3 that 80% of the disk-truncating flybys happen during the first 0.2 Myr of cluster development, meaning during the deeply embedded phase, i.e., the phase when external photoevaporation does not act yet. The mean disk size at the end of the embedded phase is well below 30 au. We have to compare that to the value provided by Winter et al. (2018a), who give a mean disk size of 35–38 au for their highest-density cluster (model D). This means that the disk sizes at the end of the embedded phase are already smaller than what one would expect to happen as a result of photoevaporation in the consecutive 3 Myr. In other words, flybys dominate the disk truncation process during the embedded phase. It is not clear what happens afterward, as the results of Winter et al. (2018a) cannot simply be transferred to these smaller disks. A future study is required that includes not only the effect of flybys and external photoevaporation but also the embedded phase and the cluster expansion process.

The clusters investigated here differ from extended clusters not only through their much higher density but also by having a star formation efficiency that is at least 60%. In a recent study, Wijnen et al. (2017) compare the effect of dynamical encounters with that of a special model of face-on accretion and ram pressure stripping. They find that the latter are dominating as long as the total cluster mass in stars is $\leqslant$30% regardless of the cluster mass and radius. In other words, encounters dominate over face-on accretion and ram pressure in the compact clusters that we have investigated here. However, in the early star formation this effect could be important and should be investigated in a dedicated study.

5. Summary and Conclusion

For a long time it was unclear whether planets could form and survive in the dense stellar environment of open clusters. However, during the past few years several protoplanetary disks and about 20 planets have been found in open clusters, showing that planets can indeed withstand such harsh environments. Some open clusters are probably older counterparts of young compact clusters like Arches or Westerlund 2. Here, we have studied the influence of stellar flybys on the size of protoplanetary disks and eventually forming planetary systems by performing simulations of such young, compact clusters. We have considered two models, one with a very short phase (C0) and the other with a 1 Myr long embedded phase (C1). Starting with an initial disk size of 200 au, we find that in both cases stellar flybys are responsible for significant changes in the disk size. After 3 Myr, all disks are reduced in size by flybys, with 77% and 86% being smaller than 100 au in C0 and C1, respectively. However, what is most interesting is that disk sizes $<$10 au are the most common in such environments; 35% and 47% of all disks are smaller than 10 au in model clusters C0 and C1, respectively. This corresponds to mean disk sizes of 21 au for C0 and 11 au for C1.

Table 3
Observed Properties of Disks in Open Clusters

Name	Cluster Properties		Disk Properties		References
	t_{cl} (Myr)	M_{cl} (10^3 $M_\odot$)	No.	r_{disk} (au)	
NGC 2362	4–5	$>$0.5	4	6.2–40.9[a]	(1), (2)
h/χPersei	13 $\pm$ 1	$\gtrsim$4/3	10	1.0–38.4	(3), (4)

Note. Columns (1)–(3): cluster name, its age t_{cl}, and its mass M_{cl}. Column (4): number of observed disks. Column (5): (dust) disk radius r_{disk}. Column (6): references. References: (1) Dahm 2005; (2) Currie et al. 2009 and references therein; (3) Slesnick et al. 2002; (4) Currie et al. 2008.
[a] Lower dust radius for 200 K and upper dust radius for 120 K.

Disks that are reduced to sizes smaller than 10 au have a relatively small mass, and their structure is very complex (Breslau et al. 2014). It is not certain that the remaining material would be identified as a disk any more by observations. As their structure differs considerably from a flat Keplerian disk, it is not clear what effect that feature has on the planet formation process. It could either prevent it altogether, because at least in the outer areas the matter is unevenly distributed, or it could actually accelerate dust growth owing to an induced increase in collision frequency. This has to be considered in more detail in future work.

Here we only consider the effect of flybys on the disk size; however, in such dense and massive clusters the strong radiation from the massive stars—external photoevaporation—can lead to additional disk size reduction. However, in contrast to flybys, external photoevaporation works most efficiently at the end of the embedded phase; the relative importance of these two effects should be determined in the future.

The observational statistics of DPS sizes in compact and/or open clusters are still scarce, so comparing our results with observations has to be done with great care. The estimated sizes vary in the range of a few au up to roughly 40 au; see Table 3. We can conclude that the overall median DPS sizes found in our simulations (11 au and 21 au) agree surprisingly well with the sizes of DPS found in open clusters (1–40 au; see Tables 1 and 3.)

It should be emphasized that the clusters in Table 3 differ considerably from those in clusters in the solar neighborhood, such as the ONC. The Arches cluster at 7 kpc might be a bit far away, but in clusters like NGC 3606 the disk sizes might be possible to determine with ALMA. However, the above results restrict not only the disk sizes in such compact clusters but also the sizes of the planetary systems that can form and survive in such hostile environments. Our simulations predict also that planetary systems in such environments will usually have sizes of $<$10 au, and it will basically be impossible for systems with sizes of 100 au to form and survive in open clusters.

Observations show disk sizes of 27–500 au in the ONC and $\geqslant$3–12 au in the Arches cluster (Eisner et al. 2008; Stolte et al. 2010). A comparison with the solar system puts these sizes in perspective. Neptune orbits at an approximate distance of 30 au from the Sun. However, every fourth protoplanetary disk and/or planetary system in such open cluster progenitors has a size of less than 30 au (model C1). A size of 21 au corresponds roughly to the distance to Uranus, and 11 au is just outside Saturn's orbit.

Another question is how many of these small disks contain sufficient material to form planets or even planetary systems. As the 23 observed planets in open clusters show, obviously at least some do. Two of those planets even form a planetary system consisting of a hot Jupiter and a very eccentric Jupiter-like planet. However, we expect that these planetary systems differ considerably from those found around field stars. So systems with planets on orbits 100 au wide should be very rare or even nonexistent unless they were captured from another star (Jílková et al. 2015).

In addition, many of the systems should have sharp outer edges like our own solar system (Pfalzner et al. 2018b), and the orbits of the outer planets should be often very eccentric and inclined relative to the inner system. Actually, one planetary system found so far in an open cluster—Pr 0211 in M44—looks just like we would predict from our simulations: the outer planet moves on a highly eccentric orbit with $a_{\rm pl} \leqslant 5.5$ au (Pfalzner et al. 2018a). This is exactly the kind of planetary system that we would expect to dominate in such open cluster environments.

The authors would like to thank Asmita Bhandare for providing and extending the star–disk encounter simulations. Our additional thanks go to the anonymous reviewer, for a thorough and insightful review that has led to a substantial improvement of the manuscript.

Appendix A
Inclined versus Coplanar, Prograde Flybys

The size of a disk around a star with mass m_1 after a flyby with a star of mass m_2 at a periastron distance of $r_{\rm peri}$ has been recently investigated numerically in two large parameter studies. The first, by Breslau et al. (2014), analyzed a thin disk of massless tracer particles around a star after it was perturbed by a second star on a coplanar, prograde orbit with respect to the disk. They found a simple description of the disk size after such a flyby depending on the mass ratio of the two stars ($m_{12} = m_2/m_1$) and the periastron distance:

$$r_{\rm disk}^{\rm copl} = \begin{cases} 0.28 \cdot r_{\rm peri} \cdot m_{12}^{-032}, & \text{if } r_{\rm disk} < r_{\rm previous} \\ r_{\rm previous}, & \text{if } r_{\rm disk} \geqslant r_{\rm previous}, \end{cases} \quad (4)$$

where $r_{\rm previous}$ is the disk size previous to the flyby in au.

This parameter study was extended by Bhandare et al. (2016) by including flybys of different inclinations, that is, different angles between the disk plane and the plane of the perturber's orbit. Averaging over all inclinations for one set of (m_{12}, $r_{\rm peri}$), they obtained the following fit formula:

$$r_{\rm disk}^{\rm avg} = \begin{cases} 1.6 \cdot r_{\rm peri}^{0.72} \cdot m_{12}^{-0.2}, & \text{if } r_{\rm disk} < r_{\rm previous} \\ r_{\rm previous}, & \text{if } r_{\rm disk} \geqslant r_{\rm previous} \end{cases}. \quad (5)$$

This formula describes flybys with mass ratios of 0.3–50.0 and up to periastron distances of five times the initial disk size $r_{\rm init}$. However, the focus of the fit was disk-penetrating and close flybys (roughly up to two times $r_{\rm init}$). In stellar clusters, even in the most compact ones, flybys with larger periastron distances and/or high mass ratios are still the most frequent type of flyby. Despite the distance, these flybys can lead to disk truncation if the mass ratio is large (see also Scally & Clarke 2001; Olczak et al. 2006). To be able to describe such distant flybys more precisely, we have performed additional encounter simulations, analog to the ones by Bhandare et al. (2016): a disk of 10^6 massless tracer particles was set up around a star, and a second star passed by, removing particles from the disk and reshaping the remnant disk. The disk size after such an encounter was chosen to be the steepest point in the time-averaged density distribution. The initial disk size was set to 200 au, with mass ratios of 0.3–50, and all inclinations (0°–180°) were covered. Periastron distances between 400 au and 1000 au were covered in steps of 50 au to obtain a better resolution than before in this parameter range, which is important for our simulations; see Figure 8. In this case the points for closer flybys were excluded from the fit:

$$r_{\rm disk} = \begin{cases} (1.6 \cdot m_{12}^{-0.2} - 1.26 \cdot m_{12}^{-0.182}) \cdot r_{\rm peri}, & \text{if } r_{\rm disk} < r_{\rm previous} \\ r_{\rm previous}, & \text{if } r_{\rm disk} \geqslant r_{\rm previous} \end{cases} \quad (6)$$

Note that self-gravity and viscosity within the disk were neglected. More details about the simulation setup, the disk size determination, and the influence of the above-made assumptions are given in Breslau et al. (2014) and Bhandare et al. (2016).

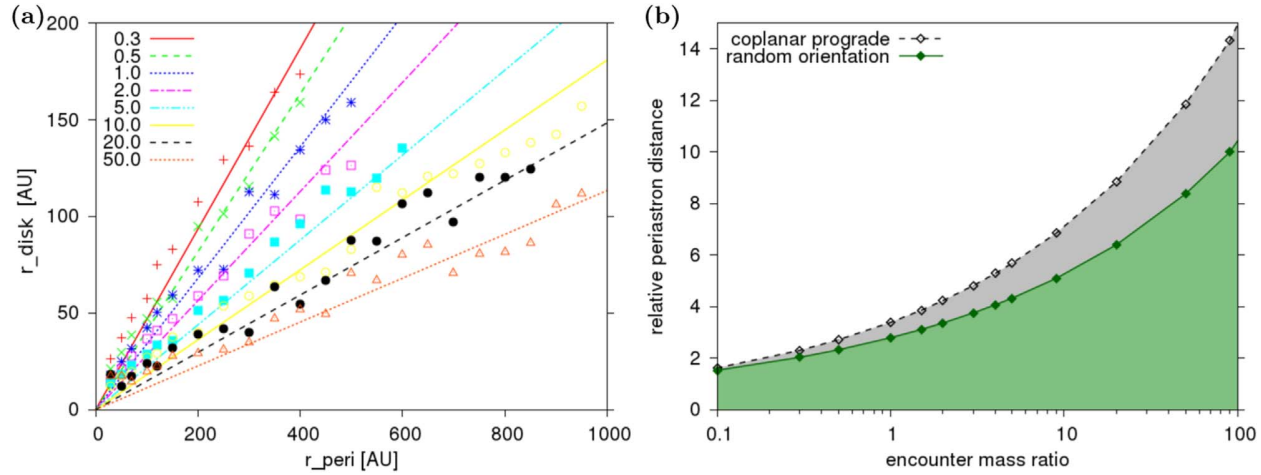

Figure 8. (a) Combined data sets of Bhandare et al. (2016) and new simulations, including the best fit to data given by Equation (6). The different colors depict different encounter mass ratios from $m_{12} = m_2/m_1 = 0.3$ (red) to $m_{12} = 50$ (orange). For details about simulations and excluded data points, see text. (b) Parameter pairs (encounter mass ratio and relative periastron distance $r_{\rm peri}^{\rm rel} = r_{\rm peri}/r_{\rm previous}$) leading to 5% reduction in disk size for coplanar, prograde encounters (black open diamonds, Equation (4); Breslau et al. 2014) and randomly orientated encounters used in this work (green filled diamonds, Equation (6)). The light-gray and green areas depict the parameter space in which the disk size is reduced for the respective flyby types.

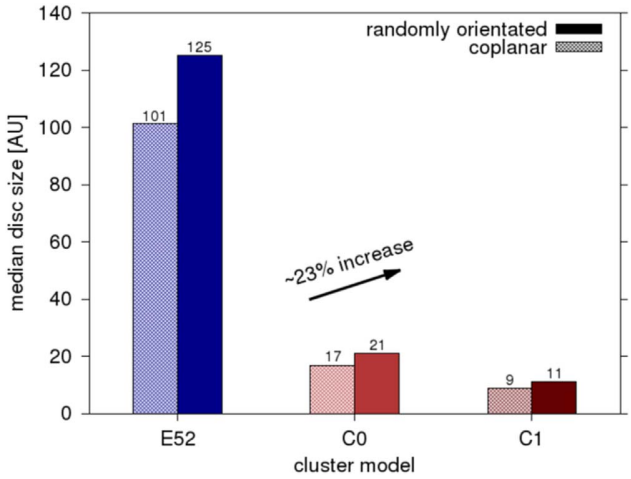

Figure 9. Median disk size after 10 Myr assuming all flybys to be coplanar and prograde (hatched) vs. including all inclinations (filled) for the different cluster models.

Appendix B
Average Disk Size after Randomly Orientated Flybys

With the fit formula above, we can now quantify the difference in disk size obtained assuming flybys to be coplanar to those where it is assumed that all inclinations are equally likely. Figure 9 depicts the median disk size after 10 Myr, (1) where all flybys were assumed to be prograde and coplanar, using the disk size description by Breslau et al. (2014) (hatched boxes), and (2) taking into account all inclinations using the average disk size as defined by Equation (6) above (filled boxes).

As expected, the median disk size of randomly orientated flybys is larger than for purely coplanar, prograde ones in all cluster models. The absolute difference is actually quite small, especially in the compact clusters. Nevertheless, in relative terms, the median disk size increases by 23% comparing coplanar to randomly orientated flybys, independently of the cluster.

ORCID iDs

Susanne Pfalzner https://orcid.org/0000-0002-5003-4714

References

Aarseth, S. J. 1973, VA, 15, 13
Aarseth, S. J. 2003, Gravitational N-Body Simulations (Cambridge: Cambridge Univ. Press)
Adams, F. C., Proszkow, E. M., Fatuzzo, M., & Myers, P. C. 2006, ApJ, 641, 504
Alexander, R. D., Clarke, C. J., & Pringle, J. E. 2006, MNRAS, 369, 229
Andrews, S. M., & Williams, J. P. 2007, ApJ, 659, 705
Bally, J., Mann, R. K., Eisner, J., et al. 2015, ApJ, 808, 69
Balog, Z., Siegler, N., Rieke, G. H., et al. 2016, ApJ, 832, 87
Banerjee, S., & Kroupa, P. 2015, arXiv:1512.03074
Bastian, N., & Goodwin, S. P. 2006, MNRAS, 369, L9
Bate, M. R. 2018, MNRAS, 475, 5618
Bhandare, A., Breslau, A., & Pfalzner, S. 2016, A&A, 594, A53
Bonnell, I. A., Smith, K. W., Davies, M. B., & Horne, K. 2001, MNRAS, 322, 859
Breslau, A., Steinhausen, M., Vincke, K., & Pfalzner, S. 2014, A&A, 565, A130
Brucalassi, A., Koppenhoefer, J., Saglia, R., et al. 2017, A&A, 603, A85
Brucalassi, A., Pasquini, L., Saglia, R., et al. 2014, A&A, 561, L9
Brucalassi, A., Pasquini, L., Saglia, R., et al. 2016, A&A, 592, L1
Ciardi, D. R., Crossfield, I. J. M., Feinstein, A. D., et al. 2018, AJ, 155, 10
Clarke, C. J., & Owen, J. E. 2015, MNRAS, 446, 2944
Clarke, C. J., & Pringle, J. E. 1993, MNRAS, 261, 190
Cottaar, M., Meyer, M. R., Andersen, M., & Espinoza, P. 2012, A&A, 539, A5
Craig, J., & Krumholz, M. R. 2013, ApJ, 769, 150
Currie, T., Kenyon, S. J., Balog, Z., et al. 2008, ApJ, 672, 558
Currie, T., Lada, C. J., Plavchan, P., et al. 2009, ApJ, 698, 1
Curtis, J. L., Vanderburg, A., Torres, G., et al. 2018, AJ, 155, 173
Dahm, S. E. 2005, AJ, 130, 1805
David, T. J., Mamajek, E. E., Vanderburg, A., et al. 2018, arXiv:1801.07320
de Juan Ovelar, M., Kruijssen, J. M. D., Bressert, E., et al. 2012, A&A, 546, L1
de La Fuente Marcos, C., & de La Fuente Marcos, R. 1997, A&A, 326, L21
Delorme, P., Collier Cameron, A., Hebb, L., et al. 2011, MNRAS, 413, 2218
Drake, J. J., Ercolano, B., Flaccomio, E., & Micela, G. 2009, ApJL, 699, L35
Duchêne, G., & Kraus, A. 2013, ARA&A, 51, 269
Eisner, J. A., Plambeck, R. L., Carpenter, J. M., et al. 2008, ApJ, 683, 304
Ercolano, B., Drake, J. J., Raymond, J. C., & Clarke, C. C. 2008, ApJ, 688, 398
Espinoza, P., Selman, F. J., & Melnick, J. 2009, A&A, 501, 563
Farihi, J., Gänsicke, B. T., & Koester, D. 2013, MNRAS, 432, 1955
Figer, D. F. 2008, in IAU Symp. 250, Massive Stars as Cosmic Engines, ed. F. Bresolin, P. A. Crowther, & J. Puls (Cambridge: Cambridge Univ. Press), 247

Gorti, U., & Hollenbach, D. 2009, ApJ, 690, 1539
Gorti, U., Liseau, R., Sandor, Z., & Clarke, C. 2016, SSRv, 205, 125
Hall, S. M. 1997, MNRAS, 287, 148
Hartman, J. D., Gaudi, B. S., Holman, M. J., et al. 2009, ApJ, 695, 336
Haworth, T. J., Boubert, D., Facchini, S., Bisbas, T. G., & Clarke, C. J. 2016a, MNRAS, 463, 3616
Haworth, T. J., Clarke, C. J., & Owen, J. E. 2016b, MNRAS, 457, 1905
Heller, C. H. 1995, ApJ, 455, 252
Hénault-Brunet, V., Evans, C. J., Sana, H., et al. 2012, A&A, 546, A73
Hillenbrand, L. A., Strom, S. E., Calvet, N., et al. 1998, AJ, 116, 1816
Janes, K., Barnes, S. A., Meibom, S., & Hoq, S. 2013, AJ, 145, 7
Jílková, L., Portegies Zwart, S., Pijloo, T., & Hammer, M. 2015, MNRAS, 453, 3157
Johnstone, D., Hollenbach, D., & Bally, J. 1998, ApJ, 499, 758
Johnstone, D., Matsuyama, I., McCarthy, I. G., & Font, A. S. 2004, RMxAC, 22, 38
Kaczmarek, T. 2012, PhD thesis, Universität zu Köln
Köhler, R., Petr-Gotzens, M. G., McCaughrean, M. J., et al. 2006, A&A, 458, 461
Kraus, A. L., & Hillenbrand, L. A. 2007, AJ, 134, 2340
Kroupa, P. 2002, Sci, 295, 82
Lada, C. J., & Lada, E. A. 2003, ARA&A, 41, 57
Laughlin, G., & Adams, F. C. 1998, ApJL, 508, L171
Livingston, J. H., Dai, F., Hirano, T., et al. 2018, AJ, 155, 115
Lovis, C., & Mayor, M. 2007, A&A, 472, 657
Malavolta, L., Nascimbeni, V., Piotto, G., et al. 2016, A&A, 588, A118
Mann, A. W., Newton, E. R., Rizzuto, A. C., et al. 2016, AJ, 152, 61
Matsuyama, I., Johnstone, D., & Hartmann, L. 2003, ApJ, 582, 893
McCaughrean, M. J., & O'dell, C. R. 1996, AJ, 111, 1977
Meibom, S., Torres, G., Fressin, F., et al. 2013, Natur, 499, 55
Mochejska, B. J., Stanek, K. Z., Sasselov, D. D., et al. 2006, AJ, 131, 1090
Olczak, C., Kaczmarek, T., Harfst, S., Pfalzner, S., & Portegies Zwart, S. 2012, ApJ, 756, 123
Olczak, C., Pfalzner, S., & Eckart, A. 2010, A&A, 509, A63
Olczak, C., Pfalzner, S., & Spurzem, R. 2006, ApJ, 642, 1140
Parker, R. J., & Goodwin, S. P. 2012, MNRAS, 424, 272
Paulson, D. B., Cochran, W. D., & Hatzes, A. P. 2004, AJ, 127, 3579
Pepper, J., Stanek, K. Z., Pogge, R. W., et al. 2008, AJ, 135, 907
Perryman, M. A. C., Brown, A. G. A., Lebreton, Y., et al. 1998, A&A, 331, 81
Pfalzner, S. 2004, ApJ, 602, 356
Pfalzner, S. 2009, A&A, 498, L37
Pfalzner, S., Bhandare, A., & Vincke, K. 2018a, A&A, 610, A33
Pfalzner, S., Bhandare, A., Vincke, K., & Lacerda, P. 2018b, ApJ, 863, 45
Pfalzner, S., & Kaczmarek, T. 2013b, A&A, 559, A38
Pfalzner, S., & Olczak, C. 2007, A&A, 462, 193
Pfalzner, S., Olczak, C., & Eckart, A. 2006, A&A, 454, 811
Pfalzner, S., Steinhausen, M., & Menten, K. 2014, ApJL, 793, L34
Pietrinferni, A., Cassisi, S., Salaris, M., & Castelli, F. 2004, ApJ, 612, 168
Porras, A., Christopher, M., Allen, L., et al. 2003, AJ, 126, 1916
Portegies Zwart, S. F. 2016, MNRAS, 457, 313
Portegies Zwart, S. F., & Jilkova, L. 2015, MNRAS, 451, 144
Quinn, S. N., White, R. J., Latham, D. W., et al. 2012, ApJL, 756, L33
Quinn, S. N., White, R. J., Latham, D. W., et al. 2014, ApJ, 787, 27
Richer, H. B., Fahlman, G. G., Rosvick, J., & Ibata, R. 1998, ApJL, 504, L91
Rochau, B., Brandner, W., Stolte, A., et al. 2010, ApJL, 716, L90
Rosotti, G. P., Dale, J. E., de Juan Ovelar, M., et al. 2014, MNRAS, 441, 2094
Sarajedini, A., Dotter, A., & Kirkpatrick, A. 2009, ApJ, 698, 1872
Sato, B., Izumiura, H., Toyota, E., et al. 2007, ApJ, 661, 527
Scally, A., & Clarke, C. 2001, MNRAS, 325, 449
Scally, A., & Clarke, C. 2002, MNRAS, 334, 156
Shara, M. M., Hurley, J. R., & Mardling, R. A. 2016, ApJ, 816, 59
Sigurdsson, S., Richer, H. B., Hansen, B. M., Stairs, I. H., & Thorsett, S. E. 2003, Sci, 301, 193
Slesnick, C. L., Hillenbrand, L. A., & Massey, P. 2002, ApJ, 576, 880
Spurzem, R. 1999, JCoAM, 109, 407
Spurzem, R., Giersz, M., Heggie, D. C., et al. 2009, ApJ, 697, 458
Steinhausen, M. 2013, PhD thesis, Mathematisch-Naturwissenschaftliche Fakultät der Universität zu Köln
Steinhausen, M., & Pfalzner, S. 2014, A&A, 565, A32
Stolte, A., Hußmann, B., Olczak, C., et al. 2015, A&A, 578, A4
Stolte, A., Morris, M. R., Ghez, A. M., et al. 2010, ApJ, 718, 810
Störzer, H., & Hollenbach, D. 1999, ApJ, 515, 669
Thorsett, S. E., Arzoumanian, Z., & Taylor, J. H. 1993, ApJL, 412, L33
van der Marel, N., Williams, J. P., Ansdell, M., et al. 2018, ApJ, 854, 177
van Saders, J. L., & Gaudi, B. S. 2011, ApJ, 729, 63
Vicente, S. M., & Alves, J. 2005, A&A, 441, 195
Vincke, K., Breslau, A., & Pfalzner, S. 2015, A&A, 577, A115
Vincke, K., & Pfalzner, S. 2016, ApJ, 828, 48
Vink, J. S. 2015, in Very Massive Stars in the Local Universe, Astrophysics and Space Science Library, Vol. 412 (Cham: Springer International), 77
Vorobyov, E. I. 2011, ApJ, 729, 146
Wang, L., Spurzem, R., Aarseth, S., et al. 2015, MNRAS, 450, 4070
Wijnen, T. P. G., Pols, O. R., Pelupessy, F. I., & Portegies Zwart, S. 2017, A&A, 604, A91
Winter, A. J., Clarke, C. J., Rosotti, G., et al. 2018a, MNRAS, 478, 2700
Winter, A. J., Clarke, C. J., Rosotti, G., & Booth, R. A. 2018b, MNRAS, 475, 2314
Zuckerman, B., Xu, S., Klein, B., & Jura, M. 2013, ApJ, 770, 140

3 The birth environment of the solar system

Is our solar system special? This question has been asked for centuries and it is more up-to-date than ever, since thousands of exoplanetary systems have been found in the last two decades. Many of those systems show features which are very different from what we know from our own solar system. Some host, for example, Jupiter-like planets on very close orbits (*Hot Jupiters*) or planets on very eccentric orbits, for example PR 0211c ($e = 0.71 \pm 0.11$) in Praesepe (Malavolta et al., 2016).

As outlined above, it is still under debate in which kind of environment – association or cluster – our solar system formed, and to what degree it was influenced by this environment, for example through stellar fly-bys, see Section 1.3. With help of the extensive parameter study that was performed in the course of this theses (Vincke et al., 2015; Vincke & Pfalzner, 2016, 2018), it is now possible to investigate the possible role of stellar fly-bys in the formation of our solar system in detail, and thus to start answering the open questions, as outlined in the introduction:

1. How probable is it for a *solar-system analogue*, that is a disc with $30 - 50$ AU surrounding a solar-like star, to survive long enough to form planets in associations and clusters?
2. How many other solar-system analogues can one expect in the different types of environment?
3. Is it more likely that the solar system was born in an association or a stellar cluster?

3.1 Method

The starting point for the investigation are the evolving association and evolving cluster models as described in Section 1.4.1. The discussion here is focussed to the models E0 (equivalent to Taurus), E2 (equivalent to the ONC), E52 (equivalent to NGC 6611), and C1 (equivalent to Arches) covering all typical densities. The simulation parameters are the ones listed in Tables 1.3 and 1.4.

First, discs around *solar-like stars* were investigated, which we assume to have masses between $0.8 - 1.2$ $M_\odot$. Those amount to a subgroup containing roughly 5% of the stellar

population in the association and cluster models studied here. The steep drop in surface density within today's solar system (Morbidelli et al., 2003), as well as Neptune's orbit at ≈ 30 AU provide limits for the size of the solar protoplanetary disc. One can assume that an initially larger disc was reduced to $30 - 50$ AU by a fly-by. Such a disc around a solar-like star is called *solar-system analogue (SSA)*. Here, all fly-bys that lead to such an SSA are tracked, they are referred to as *solar-system-forming (SSF)* fly-bys.

3.2 Properties of solar-system-forming fly-bys

The properties of SSF fly-bys in sparse associations and dense clusters differ significantly. For a long time, fly-bys in clusters were thought to be too violent to yield any SSAs (see e.g. Pfalzner, 2013). However, many solar-like systems were found at the end of the simulations,

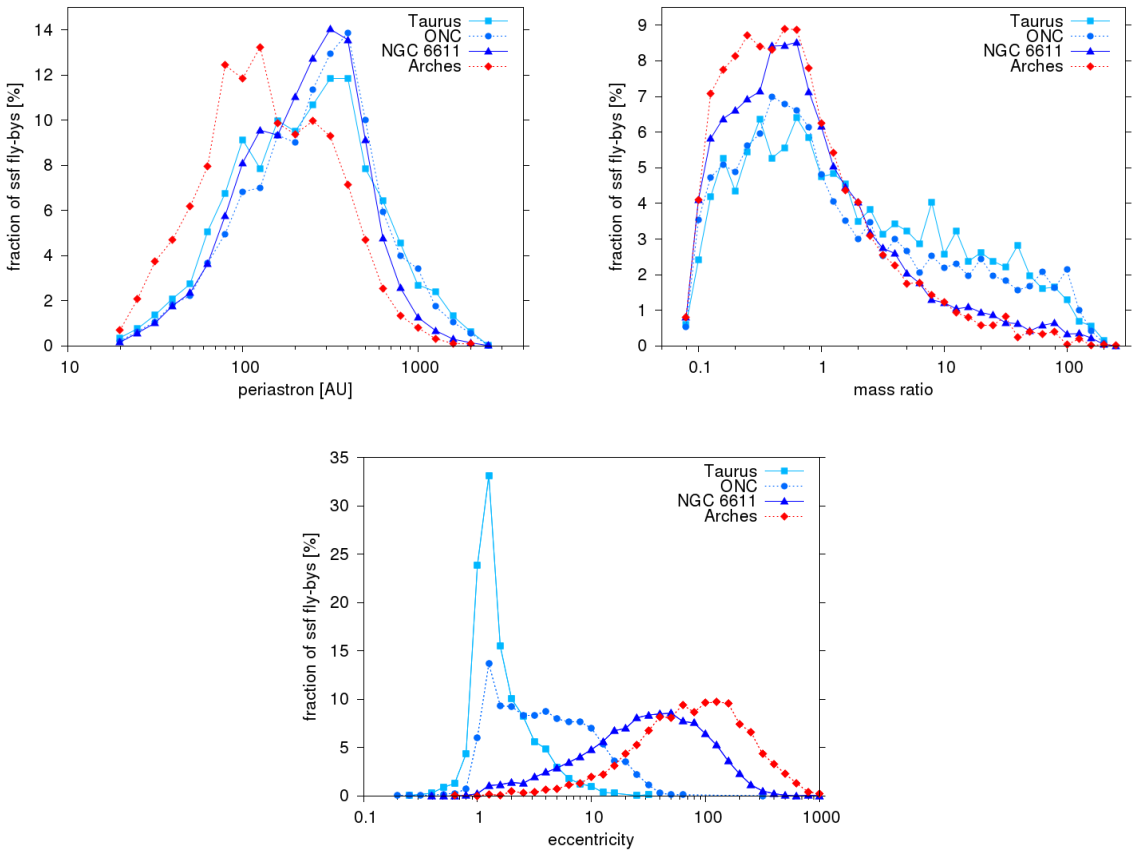

FIGURE 3.1: Properties of SSF fly-bys for simulations equivalent to Taurus (model E0, light blue squares), ONC (model E2, blue circles), NGC 6611 (model E52, dark blue triangles), and Arches (model C1, red diamonds). The top left shows the distribution of periastron distances, the top right the one of the mass ratios, the bottom the distribution of the eccentricities.

indicating that fly-bys may play a much more important role than previously believed.

Figure 3.1 depicts the periastron distances (top left), the mass ratios (top right), and the eccentricities (bottom) of SSF fly-bys in different environments.

As expected from the publications above, the SSF fly-bys in the Arches-analogue are on average much closer than in the Taurus model, because of the higher stellar density. Due to their proximity, the perturbers in Arches tend to have lower mass ratios (≤ 1 $M_\odot$) than in Taurus. Maybe the most interesting variable is the eccentricity. The eccentricity distribution shows that, for the least dense systems, it is appropriate to assume the fly-bys to be parabolic. However, in the denser systems the eccentricities become *much* larger, reflecting the higher stellar density. The "simple" interaction between two stars become three- or many-body interactions in the densest systems, therefore, the fly-bys become hyperbolic. A detailed study which extends the work of Bhandare et al. (2016) and the formula in this work to hyperbolic fly-bys and their influence on discs is necessary to make accurate predictions about the effect on the SSF fly-by statistic. However, hyperbolic fly-bys are expected to have a weaker influence on the disc (see e.g. Pfalzner, 2004). On the one hand, this means that fly-bys in very dense systems might be less destructive, therefore, the number of SSAs in these systems might be higher than found in this work, because fewer SSAs are destroyed. On the other hand, SSF fly-bys in Taurus-like systems might be even fewer and the number of SSAs smaller.

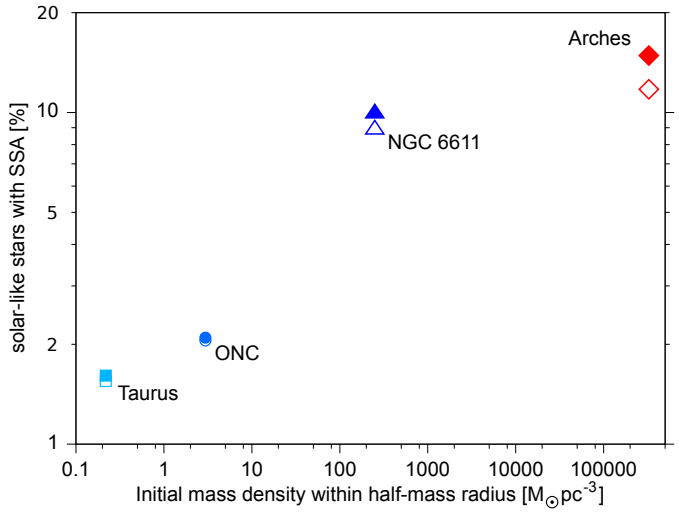

FIGURE 3.2: Number of SSAs at $t = 3$ Myr (filled symbols) and at $t = 10$ Myr (open symbols) as a function of the *initial cluster-mass density within the initial half-mass radius* for Taurus (model E0, light blue squares), ONC (model E2, blue dots), NGC 6611 (model 52, dark blue triangles), and Arches (model C1, red diamonds). Note that (1) the cluster-mass density includes stellar and gas mass and (2) the initial half-mass radius is 1.3 pc for the associations and 0.2 pc for Arches and (3) the value for $t = 10$ Myr for Arches is an extrapolation, assuming a linear decrease in the number of SSAs with time.

3.3 Solar-system analogues

How probable is it for an SSA to survive long enough to form planets in associations and clusters?

Associations and clusters differ in mass density by several orders of magnitude. The higher the mass density is, the more frequent and violent are stellar fly-bys. This means that, in principle, denser clusters lead to closer fly-bys, which result in more systems in the range of $30 - 50$ AU. However, denser clusters can lead to even smaller system sizes, meaning they "destroy" SSAs. To quantify the role of the association/cluster density, Figure 3.2 depicts the *final* number of SSAs as a function of the initial mass-density (stars+gas) within the initial half-mass radius (1.3 pc for associations, 0.2 pc for the cluster).

In the simulations, the discs "formed" with an initial size of 200 AU. As expected, the rate of close fly-bys in associations like the ONC and Taurus is low, cutting only $1 - 2\%$ of the discs to SSAs. However, when the SSAs have formed, they most probably stay unperturbed afterwards, because the number of fly-bys after 2 Myr becomes negligible, see Figure 3 in Vincke & Pfalzner (2018). This implies that planets can form undisturbed, the number of SSAs remains almost constant after 3 Myr, see Figure 3.3.

For the compact clusters like Arches, the development of SSAs is very different: at the beginning of the simulations, a large fraction of discs around solar-like stars is cut down to solar-system size ($\approx$ 50%). Although the number of SSAs seems to remain almost constant after 2 Myr (see Fig. 3.3), the fluctuation is very high. SSAs are constantly formed and "destroyed", i.e. cut down to $r_{disc} < 30$ AU, due to fly-bys. At the end of the simulation time $\approx 15\%$ of all discs around solar-like stars are SSAs – this fraction is an order of magnitude higher than in the small associations and a factor of two higher than in NGC 6611.

Summarising, the number of SSAs in the system increases as a function of the environment's density in the association/cluster models studied here, see Figure 3.2. For a cluster with a density even higher than in the Arches model, the final fraction of SSAs would be expected to decrease again. The fly-bys might then become so strong and frequent that probably more SSAs would be destroyed than formed.

How many other solar-system analogues can one expect in the different types of environment?

As pointed out by Vincke & Pfalzner (2018), the final disc-size distributions in associations are very different from the ones for clusters. Therefore, the absolute number of SSAs at the end of the simulation, as well as their relative abundance differ considerably.

Figure 3.4 depicts the disc-size distributions at the end of the simulations in Taurus (top

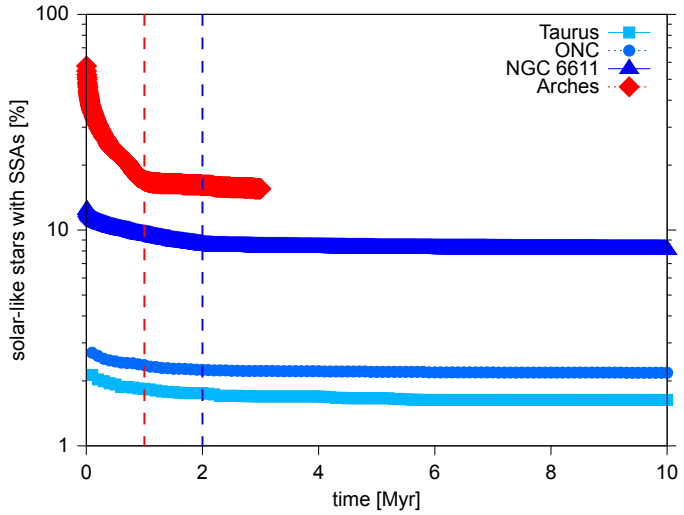

FIGURE 3.3: Number of SSAs in the different models as a function of time: Taurus (model E0, light blue square), ONC (model E2, blue dot), NGC 6611 (model 52, dark blue triangle), and Arches (model C1, red diamond). The vertical lines depict the point in time of gas expulsion for the cluster model (red) and the association models (blue).

left), the ONC (top right), NGC 6611 (bottom left), and the Arches cluster (bottom right). The red bars depict the SSAs in the systems, the percentage of SSAs is given next to them. Note that the last bin contains all discs which underwent disc-size changing fly-bys, and have final sizes between 100 AU $\leq r_{disc} <$ 200 AU.

In systems like Taurus, roughly 4% of all discs around solar-like stars are smaller than 30 AU, $\approx$ 2.4% are destroyed. About $\approx$ 1.2% of the systems resemble SSAs, while $\approx$ 5% are perturbed, but finally still larger than 50 AU, see Fig. 3.4. However, the majority ($\approx$ 90%) of all discs around solar-like stars remain unperturbed in such an environment.

In the ONC, the fraction of solar-like stars with small discs ($\leq$ 30 AU) is roughly 5%, i.e. a little larger than in a Taurus-like environment. The fraction of SSAs remains low with $\approx$ 1.8%, most discs remain larger than 50 AU ($\approx$ 10%) or unperturbed (85%).

Almost half of the discs around solar-like stars in the very massive association (NGC 6611) are perturbed. The fraction of SSAs is roughly 7%, which is more than a factor of five larger than in Taurus and almost factor of four larger than in the ONC.

In contrast, for Arches, two thirds of the discs around solar-like stars become smaller than the solar system. The majority of roughly 40% becomes smaller than 10 AU which might mean that they contain so little mass that no planets are able to form. However, about 10% of all solar-like stars are surrounded by SSAs, which is a factor of ten more than in Taurus and a factor of five more than in the ONC. As mentioned above, many discs undergo multiple fly-bys, such that SSAs are probably destroyed again, whereas larger discs are cut down to SSAs.

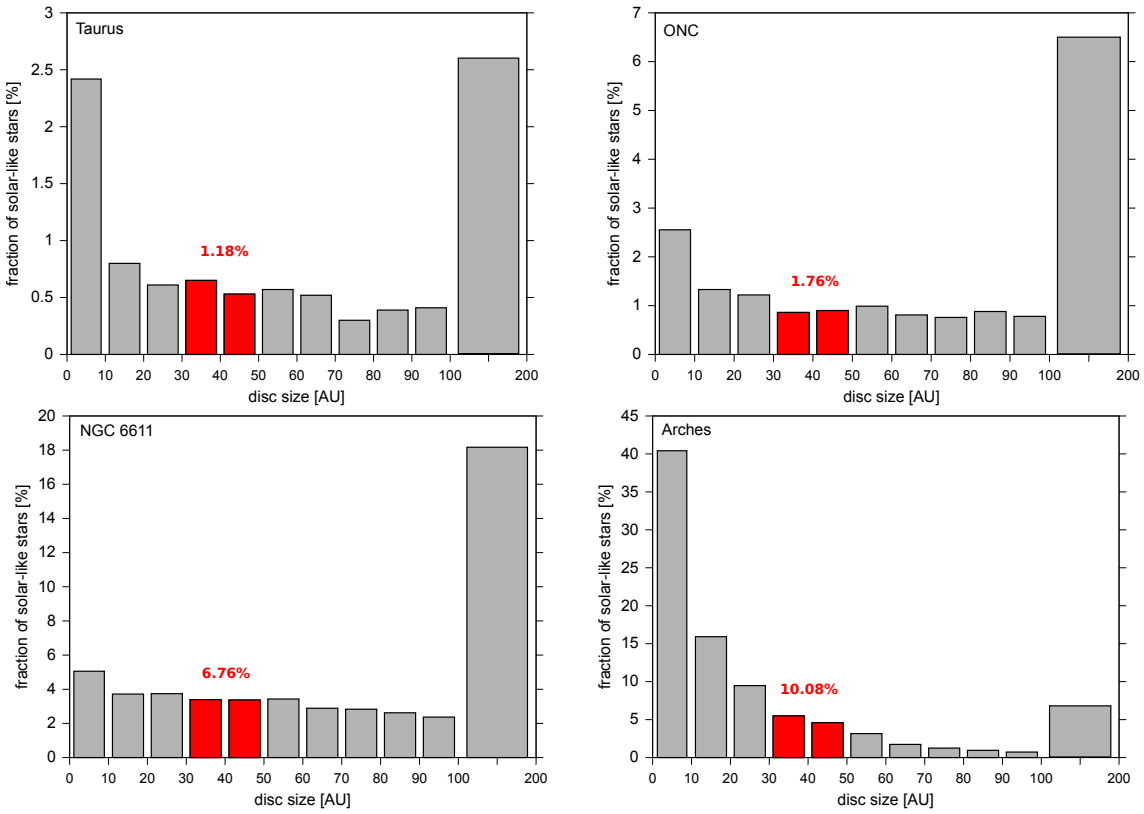

FIGURE 3.4: The disc-size statistics for solar-like stars at the end of the simulations (10 Myr for associations – Taurus, ONC, and NGC 6611 – 3 Myr for the cluster Arches). The red bars show the SSAs, the red numbers depict the fraction of solar-like stars with solar-system like discs. Note that the first bin includes discs which are assumed to be *destroyed* (see text) and the last, broader bin depicts all discs with sizes larger than 100 AU but *smaller than* 200 AU, excluding discs which were not perturbed.

Is it more likely that the solar system was born in an association or a stellar cluster?

To answer this key question exhaustively, more observations are necessary to further constrain the formation and evolution of the planets, the Kuiper Belt, and the Oort Cloud. In addition, much more extensive simulations will have to be performed, covering the lifetime of our solar system of 4.5 Gyr. However, the present work, elucidating the first 10 Myr, where most stellar fly-bys happen, already provides valuable information. The results presented here can serve as a starting point for future work. Moreover, it allowed the conclusion that our solar system was most probably born in a very massive association or a stellar cluster, as will be detailed in the following.

Associations

Solar-system analogues in "small" associations are rare, because the protoplanetary discs in associations usually remain larger than 50 AU. Quantitatively, the absolute number of SSAs in Taurus-like environments is, on average, less than one, in ONC-like associations approximately four, and it increases significantly in very massive associations like NGC 6611 to roughly 130, see also Figure 3.4. Note that solar-like stars in all environments make up for about 5% of the stellar population.

The Sun is not part of an association today, which could be a result of the birth association's disruption due to the galactic field (Portegies Zwart, 2009) or gas expulsion (Pfalzner, 2011), after which only between $10-20\%$ of all stars remain behind as a bound remnant. Therefore, form the total of 130 SSAs in an NGC 6611-like system, $104-117$ systems are ejected due to gas expulsion after 20 Myr. It is important to note, that on longer timescales of >100 Myr the bound remnants might also dissolve, increasing this number.

Clusters

The Arches-like cluster produces nearly twice as many SSAs as compared to the NGC 6611 model, namely ≈ 250 after 3 Myr. However, in contrast to NGC 6611, this number decreases slowly with time, because fly-bys continue to cut-down the disc size. As a result, there will be roughly 210 systems left after 10 Myr. If the Sun was part of a cluster, it would have to have been ejected from it. Clusters similar to our model ($SFE = 70\%$) lose up to $\approx 15\%$ of their stellar mass within the first 10 Myr after star formation, mostly due to stellar interactions. This means that about 32 out of 210 SSAs would be ejected after 10 Myr. This number might seem small, however, the clusters continue to lose stars with time due to stellar interactions, so the total number of ejected systems increases with time, e.g. ≈ 42 (20%) ejected SSAs after 20 Myr. This is a roughly a factor of two to three smaller than for NGC 6611. However, additional simulations covering longer timescales of several tens of Myr would be necessary to make further predictions about the number of SSAs destroyed and ejected by clusters.

3.4 The birth environment of the solar system

The chances of the solar system being formed in associations like Taurus or the ONC are relatively low, as stellar fly-bys are usually not strong enough to cut down discs to the right size. For *massive* associations like NGC 6611, the number of SSAs ejected are twice as large as from clusters like Arches, which makes them better formation sites for the solar

system. However, long-term simulations covering the next Gyrs of cluster development are necessary to further constrain the number of SSAs which are ejected from clusters.

Summarising, the solar system was most probably born *in a massive association like NGC 6611 or a cluster like Arches*. It is important to note, however, that we only consider the formation and destruction of SSAs by stellar fly-bys. Other effects, like for example external photoevaporation, have to be taken into account to finally answer the question where our solar system has been born. A detailed discussion of the approximations and assumptions made as well as a comparison of our results to other work can be found in Section 4.3.

4 Discussion

In this chapter, a discussion of the approximations and assumptions made in the association and cluster simulations, as well as in the disc-size determination is presented (Section 4.1). In the second part, the results described in the publications are compared to other theoretical work and to observational findings (Section 4.2). In the last section, the effects of associations and clusters on solar-system like discs are discussed, and the findings are compared to other studies about the solar-system origin (Section 4.3).

4.1 Simulations

In both types of simulations, i.e. the Nbody simulations of the associations and clusters and the disc-size simulations, a few assumptions and simplifications were made. Their influence on the presented results will be discussed in the following.

4.1.1 Cluster simulations

The cluster simulation started at the point in time, where star formation is already finished and the systems are still embedded in their natal gas. At the beginning of the simulations, the associations and clusters are all spherical entities, without substructure or primordial mass segregation, with a homogeneous SFE, and consist purely of single stars. The importance of these assumptions and their influence on the presented results are analysed in this section.

Substructure

The associations/clusters modelled in all publications here are initially spherical, with their stellar- and gas-density profiles following King profiles and Plummer profiles, respectively. Observations found that clusters do not necessarily form spherically, but that large star-forming regions show different types of sub-clustering (see e.g. Elmegreen & Lada, 1977; Kuhn et al., 2014). Earlier simulations show that approximately within the first crossing time, the "natal" substructure within a cluster is already erased by dynamical interactions (Craig & Krumholz, 2013). During this time, however, the number of close fly-bys is increased compared to spherical, relaxed clusters, making them initially more hostile

environments for protoplanetary discs or planetary systems (Craig & Krumholz, 2013). Furthermore, substructured associations/clusters are more likely to retain a bound remnant after gas expulsion (e.g. Smith et al., 2011, and Sect. 1.1.2).

If substructure was included, some of the associations modelled would retain a (more massive) bound remnant after gas expulsion. This, together with the enhanced initial density, would increase the fly-by rate due to the substructure and result in smaller discs. However, as the substructure is erased rather quickly, its effect on the discs is probably small.

Locally varying SFE

Here, as in almost all simulations of the dynamics of associations/clusters, it was assumed that the SFE within the systems is constant. However, observations seem to indicate that the star formation efficiency within an association or a cluster is not homogeneous, but that the density of *young stellar objects (YSOs)* depends on the local gas-surface density (Σ_g) within a cloud: $\Sigma_{YSO} \simeq 10^{-3}\Sigma_g^{\alpha}$, where $\alpha \approx 2$ (Gutermuth et al., 2011).

It is not clear whether the star formation in the outer, less dense region of a cloud, is delayed, or whether all stars begin to form simultaneously, but on longer timescales in the outskirts. In the latter case, the crucial timescale for star formation is the free-fall time of the system, τ_{ff}. With this, the *star formation efficiency per free-fall time* ϵ_{ff} can be defined (see e.g. Krumholz & McKee, 2005; Elmegreen, 2007; Krumholz & Tan, 2007; Parmentier & Pfalzner, 2013), which describes the quick star formation in the dense inner regions of the cluster, and the slower formation in the outskirts.

Here, the star formation itself was not modelled, therefore, the SFE was assumed to be constant throughout the association/cluster. However, the gas mass was distributed according to a Plummer profile, which is flatter than the stellar King profile in the association/cluster core. This crudely mimics the enhanced star formation in the core. A real density-dependent SFE would mean that the central dense regions are less affected by gas expulsion and expansion, or, that the effects are delayed. This could result in more of the closest fly-bys. Therefore, the results should be understood as an upper limit for the disc size.

Primordial mass segregation

Some clusters and associations show signs of mass segregation, meaning that the most massive stars are located in the centre of the stellar group. There are two types of mass segregation: (1) the primordial mass segregation, where the most massive stars already form in the system centre, and (2) dynamical mass segregation, where the most massive stars migrate towards the system centre with time due to gravitational interactions (Bonnell

& Davies, 1998; McMillan et al., 2007; Allison et al., 2009). It is important to note that, whether mass segregation is found by observations or in simulations strongly depends on the definition of mass segregation, as well as of the method of its measurement (see Olczak et al., 2011; Parker et al., 2015, and references therein). For example, whether the ONC, which was taken as a model, is (partially) mass segregated is still under debate (Bonnell & Davies, 1998; Olczak et al., 2011; Huff & Stahler, 2006; Allison et al., 2009; Moeckel & Bonnell, 2009).

In the simulations, the associations/clusters were not primordially mass segregated, but mass segregation did take place to some degree during cluster evolution. General predictions about the influence of mass segregation on the association/cluster dynamics and the protoplanetary disc sizes can be made:

1. gravitational focussing due to the massive stars in the system centre would lead to an overall enhanced fly-by rate;
2. the discs around the most massive stars would become even smaller, as they would be born in the dense system centre;
3. the stellar mass loss due to gas expulsion in associations would be smaller, yielding a more massive remnant.

Duration of embedded phase and gas expulsion

In the simulations, the embedded phase after star formation was modelled to last between 0 and 2 Myr. Observations are not conclusive on how long this phase lasts, and to which extent it depends on the mass and density of the cluster. The duration of the embedded phase in associations only has a minor effect on the protoplanetary discs, as most fly-bys occur within the first half of the modelled embedded phase (Vincke & Pfalzner, 2016).

For stellar clusters, the duration of the embedded phase is not very well constrained by observations, but young, massive clusters like Arches or Westerlund 2 contain very little gas. The clusters modelled here expel their gas after 1 Myr (model C1), or right at the beginning of the simulations ("after 0 Myr", model C0); the latter is representative for a very short embedded phase $t_{emb} \ll 1$ Myr. The duration of the embedded phase significantly influences the protoplanetary disc sizes in clusters, the median disc sizes differ from roughly 20 AU (instant gas expulsion) to about 10 AU (gas expulsion after 1 Myr, Vincke & Pfalzner (2018)). For this reason, it is necessary to further constrain the duration of the embedded phase for clusters by observations, to make more accurate predictions about the disc sizes.

The duration of the gas expulsion usually lasts a few dynamical timescales. For the most massive associations and stellar clusters, the dynamical timescales are very short

($\approx 0.01 - 0.1$ Myr), so an approximation of instantaneous gas expulsion as made above is reasonable.

In the less dense associations, however, the gas expulsion would happen 'slowly', giving the system time to adjust to the mass loss. Therefore, fewer stars would become unbound and larger remnant associations would survive compared to the simulations presented here. Additionally, the stellar density would remain higher for a longer period, so fly-bys which further reduce the disc sizes would be more frequent.

Binaries

In all simulations above it was assumed that all stars were, at least initially, single. However, it is well known that a large fraction of stars is part of a binary or higher-order multiple system. The multiplicity, that is the fraction of stars in binaries and higher-order systems divided by the total number of stars/systems, increases with stellar mass (Köhler et al., 2006; Raghavan et al., 2010; Duchêne & Kraus, 2013).

In the simulations presented in this work, primordial binaries were not included initially, but within the simulation time of each association/cluster, binary systems formed through capture. The interaction of wide binaries with the protoplanetary discs were treated as repeated fly-bys, which is an acceptable approximation for wide binaries. However, the case of close binaries is more complicated, as (1) the influence of the components on the discs is stronger, (2) the discs of the binary companions might interact with each other, and (3) effects like accretion might come into play, which are not considered here.

On the one hand, binary and higher-order systems are significantly influenced by their association/cluster environment. Due to dynamical interactions with other association or cluster members, they can be either formed or destroyed, become *hardened* or *softened*, that is become bound stronger/weaker respectively, or individual stars can be exchanged (see e.g. Pfalzner & Olczak, 2007; Kaczmarek et al., 2011; Parker & Goodwin, 2011; Parker et al., 2011). On the other hand, the presence of binaries also influences the dynamical cluster evolution: Kaczmarek (2012) pointed out that the presence of binaries in a cluster accelerates its expansion on timescales of a few Myr.

The present day binary fractions in Galactic globular clusters can be reproduced by starting with a high initial binary fraction, a large fraction of soft binaries, and a high initial cluster density (Leigh et al., 2015). The binaries in such clusters usually reside in the cluster centre (Milone et al., 2012), which could be a result of gravitational focussing.

However, in the much younger ONC, the binary fraction in the outskirts is slightly higher than in the centre, pointing to (1) a low initial binary fraction or (2) a higher initial cluster density, and thus more dynamical interactions destroying binary systems (Köhler et al., 2006). For an overview of (massive) binary formation scenarios and their evolution, see e.g.

Moeckel & Bally (2007); Zinnecker & Yorke (2007).

In terms of close fly-bys, the rates in the embedded phase considered in this work are lower limits, because gravitational focussing due to binaries would lead to more and stronger fly-bys. The accelerated expansion of clusters after gas expulsion, however, should not affect the results significantly, as it was shown that most disc-shaping fly-bys happen in the embedded phase.

How do binaries or multiple systems influence their protoplanetary discs and/or planetary systems? Until today, about 730 exoplanets in and around binaries have been found[1], but there is an ongoing debate whether multiplicity stimulates (e.g. Boss, 2006) or constrains (e.g. Mayer et al., 2005) planet formation. Observations of star-forming regions and sparse associations found that close binaries are less likely to host protoplanetary discs than wide binaries (see e.g. Cieza et al., 2009; Daemgen et al., 2013; Mohanty et al., 2013; Akeson & Jensen, 2014). Therefore, the disc lifetime in close binaries is assumed to be a factor of ten shorter than in wide binaries or around single stars (Cieza et al., 2009).

In the binary system HK Tau, observations found both stars being surrounded by protoplanetary discs, which are misaligned by $60° - 68°$ (Jensen & Akeson, 2014), meaning that one or both discs are inclined with respect to the orbital plane of the binary. The interaction between the binary stars and the discs could have caused this inclination (cf. e.g. Zanazzi & Lai, 2018), similar to the process described by Xiang-Gruess (2016) for repeated stellar fly-bys. The misalignment between the disc and the binary orbit mostly affects the outer density structure and the truncation radius of the disc, whereas the innermost part remains almost unperturbed (see also Cyr et al., 2017).

4.1.2 Discs

Disc-size simulations

The protoplanetary-disc simulations performed by Breslau et al. (2014), Bhandare et al. (2016), and for Vincke & Pfalzner (2018) include some assumptions:

- All fly-bys were assumed to be *parabolic*, meaning that their eccentricity is $e = 1$. However, as shown for example in Figure 8 in Vincke & Pfalzner (2016), especially in the very dense associations, the fly-bys are highly hyperbolic. Such hyperbolic fly-bys have a weaker effect on the protoplanetary discs (e.g. Pfalzner et al., 2005b; Winter et al., 2018b), therefore, the shown disc-sizes represent lower limits.
- In the simulations above, only one star is surrounded by a protoplanetary disc (*star-disc fly-by*). However, most – maybe all – stars are initially surrounded by such discs, so the discs would interact with each other, for example, by exchanging material.

[1] Number of confirmed exoplanets and Kepler candidates which are part of a binary system taken from `http://exoplanets.org/` as of 22 May, 2018.

Pfalzner et al. (2005a) simulated fly-bys between two stars surrounded by low-mass discs (0.01 $M_\odot$) and found that they indeed exchange material, but that this is mostly transported to the inner regions of the discs. Therefore, the discs' size should not be affected much by the assumption of star-disc fly-bys.

- In the publications presented here, *photoevaporation* was not included. It is capable of shaping and destroying protoplanetary discs (see e.g. Störzer & Hollenbach, 1999; Scally & Clarke, 2002; Johnstone et al., 2004; Adams et al., 2006; Alexander et al., 2006; Ercolano et al., 2008; Gorti & Hollenbach, 2009; Drake et al., 2009; Winter et al., 2018b). During the embedded phase, the discs are at least partly shielded from the radiation of the most massive stars. Therefore, the discs most probably undergo two phases of external influence: (1) the *fly-by phase*, where the system is still embedded and the discs' sizes are changed by fly-bys (embedded phase of a few Myr), and (2) the *photoevaporation phase*, where fly-bys become less important and the external photoevaporation shapes the discs (a few Myr after gas expulsion with timescales of $0.1 - 10$ Myr). Recent studies argue, that photoevaporation always has a stronger effect on discs than fly-bys (Winter et al., 2018b). However, the stars would have to remain in a region of $G_0 \approx 3000$ for this period of time, which might not be the case especially in associations when the gas is expelled after 2 Myr and the stars move away from each other. For a more detailed discussion, see Sect. 1.2.1.
- The disc particles were assumed to be massless, therefore, no *self-gravity* was included. Self-gravity between the disc particles leads to disc fragmentation, the formation of spiral arms (see e.g. Meru & Bate, 2011; Dong et al., 2015) and can even enhance planet formation (Dong et al., 2016; Vorobyov, 2016, and references therein). A fly-by would increase the surface density in certain areas within the disc favouring (further) fragmentation. However, self-gravity is most important in very massive discs, therefore, the discs studied above should not be affected much.
- Another process, which was not included in the disc simulations, is *viscosity*. Rosotti et al. (2014) investigated the influence of fly-bys on viscous discs using combined SPH/Nbody simulations. They found that the median disc size at the end of their simulation only depends on the distance of the closest fly-by (see Rosotti et al., 2018, for a re-evaluation of their data). Viscosity is most important in the inner parts of very massive discs, so it could play a role when such discs become very small.

Initial disc size

At the beginning of the simulations, all stars were surrounded by protoplanetary discs of the same artificial sizes of 10^5 AU (Vincke et al., 2015), 10^4 AU (Vincke & Pfalzner, 2016) and 200 AU (Vincke & Pfalzner, 2018). In the first two cases, the discs are part

of numerical experiments to quantify the effect of fly-bys on discs in associations. Based on these studies, a more physically reasonable initial size of 200 AU was chosen to study stellar clusters.

In all publications presented here, any dependence of the initial disc size on its host's mass has been neglected (cf. Hillenbrand et al., 1998; Vicente & Alves, 2005; Eisner et al., 2008; Vorobyov, 2011; Andrews et al., 2013; Mohanty et al., 2013). Simulations of discs around Class 0 and Class I stars found disc sizes of roughly ≈ 100 AU for low-mass stars and $\gtrsim 1\,000$ AU for solar-mass stars, respectively (Vorobyov, 2011). This means that, especially for higher-mass stars, the initial disc size would be much larger than assumed in Vincke & Pfalzner (2018). However, the simulations show that the discs around more massive stars finally become much smaller than 1 000 AU, such that choosing the initial disc size smaller than this is reasonable. However, for the overall disc-size distribution, a more realistic initial disc-size distribution would be preferable.

4.2 Sizes of protoplanetary discs and planetary systems

Protoplanetary disc-sizes in associations and clusters

Observations found a number of protoplanetary discs in associations, as well as in stellar clusters. A compilation of a few examples is shown in Table 1 of Vincke et al. (2015) (associations) and Table 1 in Vincke & Pfalzner (2018) (clusters). It is evident that the median disc size in clusters is more than a factor of ten smaller than the one in less dense associations – $11 - 20$ AU compared to ≈ 400 AU (Vincke & Pfalzner, 2016, 2018). This is in very good agreement with the discs found by observations in the very dense cluster centres. In the Trapezium, for example, the majority of discs (60%) were found to be smaller than 50 AU (Vicente & Alves, 2005). In contrast, discs in the ONC were found to be as large as 500 AU, which is very close to the median disc size found here.

Influence of the environment on exoplanets – theory and observations

Eventually, planetary systems form from protoplanetary discs, provided that those contain enough mass. The planet formation itself is rather complicated and influenced by a number of internal and external processes. For an overview see, for example, the reviews by Mordasini et al. (2009); Morbidelli et al. (2012) and Winn & Fabrycky (2015).

The birth environment can influence the growth (timescale) of planets (Furlan et al., 2009; Mordasini et al., 2012) and already formed planetary systems (see e.g. Malmberg et al., 2011; Cai et al., 2017). The work above can be applied to evolved discs, and even to planetary systems, to quantify these effects.

However, there are a few things which have to be carefully taken into account:

- If a planetary system undergoes a fly-by and the planetary orbits are disturbed, this can lead to follow-up planet-planet scattering (Malmberg & Davies, 2009; Malmberg et al., 2011). Previously unperturbed planetary orbits can be altered by this scattering, and in extreme cases, planets can be ejected from the system several Myr after the fly-by (Malmberg et al., 2011). This long-term development is not covered by the work presented here.
- The planet masses have to be much smaller than the host star masses (Breslau et al., 2014; Bhandare et al., 2016; Breslau et al., 2017). For very massive planets around low-mass stars, an application of such simulations might not be reasonable.
- The disc sizes provide only *upper limits* for the sizes of planetary systems.
- The discs have to contain enough mass at the onset of planet formation, and the total mass after the fly-bys and the mass-density distribution within are crucial for the position(s) and mass(es) of forming planet(s).
- Fly-bys do not only hinder planet formation, they can also cause mass-density bumps, which can favour planet formation (see Fig. 1 in Breslau et al. (2014) and Bitsch et al. (2015)).
- Planets or planetesimals can be captured by the perturbing star during a fly-by (Belbruno et al., 2012; Jílková et al., 2015; Mustill et al., 2016). The new orbital properties of the planet around the perturber can be approximated with the help of the plots in the appendix of Breslau et al. (2017), under the assumption that the interacting stars are much more massive than the planet.

A recent study of Cai et al. (2017) investigated the planet survivability (within a planetary system) in associations of different densities. Their models contain 2 000, 8 000 and 32 000 stars, respectively, with an initial virial radius of 1 pc. In contrast to the studies presented here, they did not simulate the gas expulsion or the following expansion. Instead, they included two-body relaxation, stellar evolution, and the galactic field. The outer planets in their systems resided on orbits with $a \approx 40$ AU and $a \approx 206$ AU. They found that the planet survivability depends on the density of the environment. In the least dense model, about 95% of all planets survive, which means that they remain almost unperturbed. In a different study of substructured, dissolving clusters, it was found that, as long as the planets are within a few tens of AU from their host star, they will not be significantly perturbed by fly-bys (Craig & Krumholz, 2013). This is in line with our findings that the median disc size in such an environment remains rather large (≈ 750 AU, see Fig. 4 in Vincke & Pfalzner (2016)), meaning that bodies close to the host star will remain (almost) pristine.

In the denser environment, Cai et al. (2017) found that still more than half of the

planets survive in their systems (60%). The models in Vincke & Pfalzner (2018) showed that the median disc size in a comparable environment is close to 120 AU, which means that, depending on the initial set-up, more than half of the systems of Cai et al. might indeed remain (almost) unperturbed. Ejections of planets from their systems play a minor role, as only about 3% of all fly-bys are strong enough to excite the planetary orbits to a high degree. Rather, cumulative interactions are necessary to destabilise the outer planets (Cai et al., 2017).

However, in denser systems, where moderately close fly-bys are more frequent, they can excite exoplanet orbits to higher eccentricities and/or inclinations, which, in turn, can lead to follow-up interplanetary perturbations and ejections (see e.g. Spurzem et al., 2009). Such ejected planets remain part of their birth cluster as *free-floating planets*, as were found, for example, in σ Orionis (Lucas et al., 2001; Zapatero Osorio et al., 2001).

A compilation of all 23 exoplanets found in stellar clusters by observations so far is presented in Table 1.1. Among the listed exoplanets are two planetary systems: one in Praesepe containing two planets and one in Hyades consisting of three planets. The system in Praesepe has a very close-in planet with an almost circular orbit, a semi-major axis of $a_{pl} = 0.03$ AU, and a mass of approximately two Jupiter masses. The second planet is heavier (≈ 7.8 $M_{\oplus}$) and resides on a very eccentric orbit ($e = 0.71$) at $a_{pl} = 5.5$ AU (Malavolta et al., 2016). Simulations of Praesepe-like clusters – based on the simulations presented in this work – show that about $12-20\%$ of all stars similar to the host star Pr 0211 undergo fly-bys, which could lead to such systems during the lifetime (roughly 600 Myr) of Praesepe (Pfalzner et al., 2018). The fly-bys do not only cut down protoplanetary discs, but are also capable of exciting matter – for example planets – initially on circular orbits to more distant and eccentric orbits.

4.3 The solar system

It is very likely that our solar system formed in an association or a stellar cluster, see Section 1.3. The effect of fly-bys on protoplanetary discs was analysed and it was found that the most probable type of birth environment is a very dense association or even a stellar cluster, see Section 3.

However, the exact properties of this birth environment are still under debate. It is not only a question of stellar (cluster) dynamics, protoplanetary disc and planetary evolution, stability, and fly-bys, but also of geology, chemistry and biology. In each of those fields, a large body of research has been conducted to restrain properties of the birth environment, but due to the complexity of the problem, it is not possible to give a definite answer yet

what kind of system the Sun was born in. It is beyond the scope of this thesis to analyse all these very diverse fields of science, rather, an overview of the findings in astronomy and astrophysics are given below and compared to the results obtained in the presented study (Section 3). For detailed reviews about the birth environment of the solar system, see for example Adams (2010), Pfalzner et al. (2015a), and Pfalzner et al. (2016).

Today, the Sun is no longer part of an association or a cluster, which indicates that (1) the birth association/cluster dissolved with time (Portegies Zwart, 2009) or (2) the Sun was ejected from its birth environment after the solar-system forming fly-by. However, there is no constraint on the time the Sun spent in its birth environment, and it is unclear whether the planets already formed during this phase.

Fly-by probability

Previous studies of associations ($\rho \approx 100$ pc^{-3}) showed that the probability of a fly-by which reduces the solar disc to about 30 AU is very small, about $10^{-4} - 10^{-2}$ fly-bys per million years (see e.g. Adams, 2010). Due to the very different set-up and assumptions, it is not possible to directly compare the results presented here to this frequency. However, (1) the birth environment was assumed to be an association where strong fly-bys are naturally less frequent than in dense clusters and (2) it was previously assumed that the solar system was cut down to 30 AU (the orbit of Neptune) by a fly-by of 100 AU, which is only true if the perturbing star has almost the same mass as the Sun. The masses of stars within stellar clusters follow an IMF (Kroupa, 2002), so equal-mass fly-bys are rather an exception. Breslau et al. (2014) and the follow-up study by Bhandare et al. (2016) showed that the mass ratio between the stars is crucial for the final disc size, so a much larger parameter space of fly-by distances and mass ratios between the interacting stars has to be taken into account. Although the majority of solar-system forming fly-bys in the here modelled associations and clusters have mass ratios smaller than unity, the SSF fly-by rate is comparably quite high, for example 10^3 SSF fly-bys per solar-like star and per Myr in the ONC. This is due to the gas mass, which was added directly to the cluster mass and which caused a higher velocity dispersion.

Previous numerical simulations of fly-bys in stellar clusters have shown that the interactions between their members are too frequent and destructive, such that solar-system-sized planetary systems would be destroyed (Pfalzner, 2013). However, they also used the fly-by restrictions by Adams (2010) and thus assumed all fly-bys closer than 100 AU to be destructive. In reality, this is not necessarily the case because very close interactions with a low-mass star can still leave a solar-system-like disc unperturbed. Furthermore, their associations and clusters were in virial equilibrium, whereas the ones in the presented study expanded after gas expulsion, which leads to significant drops in stellar density and thus

changes in the systems' dynamics (Vincke & Pfalzner, 2018). As a result, the destructive events are less common after $t_{\rm sim} = 2$ Myr. In addition, in this study, the orientation of the fly-bys was taken into account. In contrast, Pfalzner (2013) only looked at the more destructive coplanar fly-bys.

In summary, it can be concluded, that the parameter space of fly-bys shaping the solar system was much too restricted in previous studies. Especially coplanar, equal-mass fly-bys systematically overestimated the influence of gravitational interactions in different associations and clusters on discs. Therefore, clusters and dense associations were disregarded as possible birth environments of the Sun. However, the present work clearly shows that this needs to be re-evaluated.

Outer planets and Planet Nine

If the solar system was still in the association/cluster after the planets had formed, a fly-by could have affected the already formed outer planets. Studies of solar-like systems show that, as a result of fly-bys, planets are ejected in $5 - 15\%$ of the cases investigated 10 Myr after the fly-by in a typical open cluster (Malmberg et al., 2011). The ejection rate in less dense associations is much smaller, because the survivability of a solar-system like planetary systems depends on the association/cluster density (Cai et al., 2017).

However, planet-formation theory suggests that the gas giants formed much closer to the Sun, with Neptune originally located at ≈ 15 AU, and eventually migrated outwards due to angular momentum exchange with the outer planetesimals (Fernandez & Ip, 1984; Hahn & Malhotra, 1999; Batygin & Brown, 2010). Therefore, the outer planets on their current orbits would only have been disturbed if the Sun resided long enough in its birth environment for the planets to form *and* for them to migrate outwards. The timescales for planet formation and migration are of the order of tens of millions of years (Lissauer, 2001; Pfalzner et al., 2016; Batygin & Brown, 2010). Most of the solar-system forming fly-bys happen within the first few Myr after the end of star formation, so it is unlikely that the planets were already on their current orbits. The inner parts of the discs remain almost undisturbed (see e.g. Breslau et al., 2014), so the gas giants would not have been influenced.

Recent studies of the orientation of Kuiper belt objects (KBOs) suggest that there might be a yet undetected ninth planet in the solar system influencing the KBOs (Trujillo & Sheppard, 2014; Batygin & Brown, 2016a,b; Holman & Payne, 2016a,b; Becker et al., 2017). It has been suggested that this *Planet Nine* resides at $a \approx 150 - 250$ AU with an eccentricity of 0.6 and a mass of ≈ 10 $M_\oplus$ (Batygin & Brown, 2016a). It is still under debate whether such a planet could have formed in-situ (Kenyon & Bromley, 2016) or if it formed closer to the Sun and was then scattered onto its current (hypothesised) orbit

(Bromley & Kenyon, 2016; Li & Adams, 2016), which could be a result of a close fly-by. There are also studies suggesting that it was captured by the Sun during a close fly-by with another star in its birth environment (Li & Adams, 2016; Mustill et al., 2016), but it is still under discussion whether such an event is probable (see Parker et al., 2017).

Independent of the actual formation mechanism, as the outermost planet in the solar system, Planet Nine would be prone to orbit perturbations or ejection due to fly-bys, even in environments with a *mean* density of 100 pc^{-3} (Li & Adams, 2016). The systems studied in this work are much denser within their half-mass radius, where most of the fly-bys happen. It is thus probable that Planet Nine's orbit was excited to such a high eccentricity through a fly-by if it was already formed, because the cross section for such disturbing fly-bys strongly depends on the velocity dispersion of the environment (Li & Adams, 2015) and its density (Vincke et al., 2015; Vincke & Pfalzner, 2016, 2018). Therefore, a very dense birth environment like the one found in our work can explain the unusual orbit of Planet Nine (for orbital properties of particles/planets after fly-bys see Breslau et al., 2017).

Kuiper belt objects

Today's structure of the Kuiper belt suggests that the solar system was dynamically active in the past. Objects on extreme orbits, for example the *extreme scattered disc objects (ESDOs)*, including Sedna (Brown et al., 2004) and 2012 VP_{113} (Trujillo & Sheppard, 2014), were probably influenced by a fly-by, either directly or indirectly through follow-up planet-planet scattering (Pfalzner et al., 2015a). In the systems, which were investigated in the presented study, the solar-like stars underwent strong fly-bys, which could have either disturbed the KBOs directly or caused planet-planet scattering leading to KBO-perturbations.

Similar to the case of Planet Nine, small objects like meteoroids could have been captured during a fly-by. There have also been suggestions that through such a captured meteoroid, life could have been brought into the solar system (Belbruno et al., 2012). However, further studies about capture rates and the composition of the affected objects are necessary at this point.

The Oort cloud

The Oort cloud is a still hypothesised structure which is supposed to expand to several 10^4 AU – 10^5 AU and which might be the origin of some short-period comets (Morbidelli, 2005). In very strong fly-bys in dense stellar systems, such a cloud would be strongly perturbed, if not even completely stripped away. In the present studies, only the sizes of protoplanetary discs and/or planetary systems were investigated, while the particles outside

were not analysed. However, there could be a lot of widely distributed material outside of the disc size as defined here (Breslau et al., 2014; Bhandare et al., 2016; Breslau et al., 2017). In addition, material can also be captured during fly-bys, so it is impossible to say, whether the solar-like systems would be able to form an Oort cloud with the presented simulations.

Studies of small stellar groups ($50 - 1\,000$ stars) showed that the probability to form an Oort Cloud is $\approx 1.5\%$ (Brasser et al., 2012). It is important to note that (1) these systems are *much* less dense than the systems investigated in this study and (2) the authors were not able to determine a dependence of the Oort-cloud-formation probability on the number of stars N within the cluster, because they chose the cluster sizes r_t according to $r_t \propto N^{1/3}$, making them all equally dense. As explained above, the interaction rate and the strength of fly-bys strongly depends on the density of the environment.

A recent study investigated much denser systems, including a large, high-mass cluster ($N = 36\,000$, $r_{hm} = 4.0$ pc, $\rho_{hm} \approx 10$ M$_\odot$ pc^{-3}) and an intermediate mass cluster ($N = 2\,000$, $r_{hm} = 1$ pc, $\rho_{hm} \approx 10$ M$_\odot$ pc^{-3}). The authors found that only an inner part of the Oort could would survive, and that it is probable, that the Oort cloud formed after the Sun left its birth environment (Nordlander et al., 2017).

In summary, additional studies with clusters of different densities and a detailed investigation of the material far outside the solar-system disc would be necessary to verify whether the presented solar-like systems could form and retain Oort-cloud-like structures.

Isotopic abundances

The so-called *short-lived radionuclides (SLRs)* like ^{60}Fe and ^{26}Al were most probably injected into the solar system in the early phases of its formation. It is still under debate where the SLRs originated from, how exactly the material was injected, and how probable such a scenario is (cf. e.g. Williams & Gaidos, 2007; Lichtenberg et al., 2016)

^{60}Fe most probably originates from a supernova (SN) explosion in the vicinity of the young solar system. In the past, it has been assumed that a star cluster ($> 1\,000$ members) is necessary to get a sufficiently high injection probability. This is in line with the systems which were found most probable as a birth place of the solar system in the present investigation.

However, in recent studies it was found that less massive associations with only a few massive stars are also able to implant enough ^{60}Fe to reproduce today's isotopic abundances in the solar system (see e.g. Nicholson & Parker, 2017). Therefore, it is hard to constrain the birth environment with the help of the ^{60}Fe origin alone. In addition, investigations showed that the abundance of ^{60}Fe is only slightly elevated with respect to the galactic background (Moynier et al., 2011; Tang & Dauphas, 2012), therefore, a single SN in the molecular birth

cloud of the Sun would suffice to explain the slight elevation in ^{60}Fe (Gounelle et al., 2009).

Aluminium-26 is also produced in supernova explosions, however, its abundance relative to ^{60}Fe is too low for a SN to be its only origin. Recent studies suggest that it stems from wind-shells around massive stars in which stars – including the Sun – formed as a result of sequential star formation (Gounelle & Meynet, 2012). Such an event is most probable in systems which contain roughly 1 200 (second generation) stars, which in turn stems from a star complex of several tens of thousands of (generation 0) stars.

The simulations in this work start at the end of the star formation process and do not include sequential star formation. However, if the Sun was indeed born $5 - 10$ pc away from a very massive cluster, it could have gravitationally interacted with these 0-generation stars, leading to (1) the enrichment of ^{26}Al through an already exploded SN and (2) to a small disc through fly-bys with other cluster members.

In summary, there are many indications that the Sun might indeed have been born in a very dense association or a cluster environment, although most previous studies suggested that dense clusters are too hostile to host a solar-system analogue. It is often argued that it is very unlikely that planetary systems survive in clusters, because there is a lack of observed exoplanetary systems in dense clusters compared to associations and field stars. However, this could very well be a consequence of observational constraints due to the very high stellar density and dynamical activity of the environment. Future observations, for example with the *Atacama Large Millimeter/submillimeter Array (ALMA)* might close the gap between the number of planets around stars in the field and around stars in clusters. Dense clusters should therefore not be excluded from future solar-system studies a priori. More detailed planet formation analysis, as well as investigations of the influence of cluster members on protoplanetary discs or planets in such systems are necessary to further constrain the properties of the Sun's birth environment.

Bibliography

Aarseth, S.J. (1973), Vistas in Astronomy, **15**, 13
Aarseth, S.J. (2003), *Gravitational N-Body Simulations*, Cambridge University Press
Adachi, I., Hayashi, C., & Nakazawa, K. (1976), Progress of Theoretical Physics, **56**, 1756
Adams, F.C. (2000), ApJ, **542**, 964
Adams, F.C. (2010), ARA&A, **48**, 47
Adams, F.C., Proszkow, E.M., Fatuzzo, M. et al. (2006), ApJ, **641**, 504
Akeson, R.L. & Jensen, E.L.N. (2014), ApJ, **784**, 62
Alexander, R., Pascucci, I., Andrews, S. et al. (2014), Protostars and Planets VI, 475
Alexander, R.D., Clarke, C.J., & Pringle, J.E. (2005), MNRAS, **358**, 283
Alexander, R.D., Clarke, C.J., & Pringle, J.E. (2006), MNRAS, **369**, 229
Alibert, Y., Mordasini, C., Benz, W. et al. (2005), A&A, **434**, 343
Allison, R.J., Goodwin, S.P., Parker, R.J. et al. (2009), ApJ, **700**, L99
Andrews, S.M., Rosenfeld, K.A., Kraus, A.L. et al. (2013), ApJ, **771**, 129
Andrews, S.M. & Williams, J.P. (2007), ApJ, **659**, 705
Andrews, S.M., Wilner, D.J., Hughes, A.M. et al. (2009), ApJ, **700**, 1502
Andrews, S.M., Wilner, D.J., Hughes, A.M. et al. (2010), ApJ, **723**, 1241
Balbus, S.A. & Hawley, J.F. (2002), ApJ, **573**, 749
Bastian, N. (2011), in *Stellar Clusters & Associations: A RIA Workshop on Gaia*, pp. 85–97
Bastian, N. & Goodwin, S.P. (2006), MNRAS, **369**, L9
Batygin, K. & Brown, M.E. (2010), ApJ, **716**, 1323
Batygin, K. & Brown, M.E. (2016a), AJ, **151**, 22
Batygin, K. & Brown, M.E. (2016b), ApJ, **833**, L3
Baumgardt, H. & Kroupa, P. (2007), MNRAS, **380**, 1589
Baumgardt, H., Parmentier, G., Gieles, M. et al. (2010), MNRAS, **401**, 1832
Becker, A.C., Arraki, K.S., Rest, A. et al. (2007), Minor Planet Electronic Circulars, **2007**
Becker, J.C., Adams, F.C., Khain, T. et al. (2017), AJ, **154**, 61
Belbruno, E., Moro-Martín, A., Malhotra, R. et al. (2012), Astrobiology, **12**, 754
Bhandare, A., Breslau, A., & Pfalzner, S. (2016), A&A, **594**, A53
Binney, J. & Tremaine, S. (1987), *Galactic dynamics*
Bitsch, B., Johansen, A., Lambrechts, M. et al. (2015), A&A, **575**, A28
Boily, C.M. & Kroupa, P. (2003a), MNRAS, **338**, 665
Boily, C.M. & Kroupa, P. (2003b), MNRAS, **338**, 673
Bonnell, I.A. & Davies, M.B. (1998), MNRAS, **295**, 691
Boss, A.P. (2006), ApJ, **641**, 1148
Braiding, C. (2011), *Star Formation and the Hall Effect*, Ph.D. thesis, PhD Thesis, 2011
Brandt, T.D. & Huang, C.X. (2015a), ApJ, **807**, 58
Brandt, T.D. & Huang, C.X. (2015b), ApJ, **807**, 24
Brasser, R., Duncan, M.J., & Levison, H.F. (2006), ICARUS, **184**, 59

Brasser, R., Duncan, M.J., Levison, H.F. et al. (2012), ICARUS, **217**, 1
Brasser, R. & Schwamb, M.E. (2015), MNRAS, **446**, 3788
Breslau, A., Steinhausen, M., Vincke, K. et al. (2014), A&A, **565**, A130
Breslau, A., Vincke, K., & Pfalzner, S. (2017), A&A, **599**, A91
Brinch, C. & Jørgensen, J.K. (2013), A&A, **559**, A82
Bromley, B.C. & Kenyon, S.J. (2016), ApJ, **826**, 64
Brown, M.E., Trujillo, C., & Rabinowitz, D. (2004), ApJ, **617**, 645
Brucalassi, A., Pasquini, L., Saglia, R. et al. (2014), A&A, **561**, L9
Brucalassi, A., Pasquini, L., Saglia, R. et al. (2016), A&A, **592**, L1
Busso, M., Gallino, R., & Wasserburg, G.J. (2003), Publications of the Astronomical Society of Australia, **20**, 356
Cai, M.X., Kouwenhoven, M.B.N., Portegies Zwart, S.F. et al. (2017), MNRAS, **470**, 4337
Cassen, P. & Moosman, A. (1981), ICARUS, **48**, 353
Chen, Y.T., Kavelaars, J.J., Gwyn, S. et al. (2013), ApJ, **775**, L8
Chevalier, R.A. (2000), ApJ, **538**, L151
Cieza, L.A., Padgett, D.L., Allen, L.E. et al. (2009), ApJ, **696**, L84
Clark, P.C., Bonnell, I.A., Zinnecker, H. et al. (2005), MNRAS, **359**, 809
Clarke, C.J., Gendrin, A., & Sotomayor, M. (2001), MNRAS, **328**, 485
Clarke, C.J. & Owen, J.E. (2015), MNRAS, **446**, 2944
Clarke, C.J. & Pringle, J.E. (1993), MNRAS, **261**, 190
Clarkson, W.I., Ghez, A.M., Morris, M.R. et al. (2012), ApJ, **751**, 132
Craig, J. & Krumholz, M.R. (2013), ApJ, **769**, 150
Cyr, I.H., Jones, C.E., Panoglou, D. et al. (2017), MNRAS, **471**, 596
Da Costa, G.S., Grebel, E.K., Jerjen, H. et al. (2009), AJ, **137**, 4361
Daemgen, S., Petr-Gotzens, M.G., Correia, S. et al. (2013), A&A, **554**, A43
Davies, M.B., Adams, F.C., Armitage, P. et al. (2014), Protostars and Planets VI, 787
de Juan Ovelar, M., Kruijssen, J.M.D., Bressert, E. et al. (2012), A&A, **546**, L1
Delorme, P., Collier Cameron, A., Hebb, L. et al. (2011), MNRAS, **413**, 2218
Dong, R., Hall, C., Rice, K. et al. (2015), ApJ, **812**, L32
Dong, R., Vorobyov, E., Pavlyuchenkov, Y. et al. (2016), ApJ, **823**, 141
Drake, J.J., Ercolano, B., Flaccomio, E. et al. (2009), ApJ, **699**, L35
Duchêne, G. & Kraus, A. (2013), ARA&A, **51**, 269
Dukes, D. & Krumholz, M.R. (2012), ApJ, **754**, 56
Dunham, M.M., Stutz, A.M., Allen, L.E. et al. (2014), Protostars and Planets VI, 195
Eisner, J.A., Plambeck, R.L., Carpenter, J.M. et al. (2008), ApJ, **683**, 304
Elmegreen, B.G. (1985), in D.C. Black & M.S. Matthews (eds.), *Protostars and Planets II*, pp. 33–58
Elmegreen, B.G. (1993), in E.H. Levy & J.I. Lunine (eds.), *Protostars and Planets III*, pp. 97–124
Elmegreen, B.G. (2007), ApJ, **668**, 1064
Elmegreen, B.G. (2008), ApJ, **672**, 1006-1012
Elmegreen, B.G. & Lada, C.J. (1977), ApJ, **214**, 725
Ercolano, B., Drake, J.J., Raymond, J.C. et al. (2008), ApJ, **688**, 398
Fall, S.M. & Chandar, R. (2012), ApJ, **752**, 96
Fang, M., van Boekel, R., Bouwman, J. et al. (2013), A&A, **549**, A15

Fellhauer, M. & Kroupa, P. (2005), ApJ, **630**, 879
Fernandez, J.A. & Ip, W.H. (1984), ICARUS, **58**, 109
Figer, D.F. (2008), in F. Bresolin, P.A. Crowther, & J. Puls (eds.), *IAU Symposium*, vol. 250 of *IAU Symposium*, pp. 247–256
Font, A.S., McCarthy, I.G., Johnstone, D. et al. (2004), ApJ, **607**, 890
Furlan, E., Watson, D.M., McClure, M.K. et al. (2009), ApJ, **703**, 1964
Gerdes, D.W., Sako, M., Hamilton, S. et al. (2017), ApJ, **839**, L15
Geyer, M.P. & Burkert, A. (2001), MNRAS, **323**, 988
Gladman, B., Holman, M., Grav, T. et al. (2002), ICARUS, **157**, 269
Gomes, R.S., Matese, J.J., & Lissauer, J.J. (2006), ICARUS, **184**, 589
Goodwin, S.P. (1997a), MNRAS, **284**, 785
Goodwin, S.P. (1997b), MNRAS, **286**, 669
Goodwin, S.P. (2009), Ap&SS, **324**, 259
Gorti, U., Dullemond, C.P., & Hollenbach, D. (2009), ApJ, **705**, 1237
Gorti, U. & Hollenbach, D. (2009), ApJ, **690**, 1539
Gounelle, M. (2015), A&A, **582**, A26
Gounelle, M. & Meibom, A. (2008), ApJ, **680**, 781-792
Gounelle, M., Meibom, A., Hennebelle, P. et al. (2009), ApJ, **694**, L1
Gounelle, M. & Meynet, G. (2012), A&A, **545**, A4
Gritschneder, M., Lin, D.N.C., Murray, S.D. et al. (2012), ApJ, **745**, 22
Gutermuth, R.A., Pipher, J.L., Megeath, S.T. et al. (2011), ApJ, **739**, 84
Hahn, J.M. & Malhotra, R. (1999), AJ, **117**, 3041
Haisch, Jr., K.E., Lada, E.A., & Lada, C.J. (2001), ApJ, **553**, L153
Hall, S.M. (1997), MNRAS, **287**, 148
Hall, S.M., Clarke, C.J., & Pringle, J.E. (1996), MNRAS, **278**, 303
Han, E., Wang, S.X., Wright, J.T. et al. (2014), PASP, **126**, 827
Harsono, D., Jørgensen, J.K., van Dishoeck, E.F. et al. (2014), A&A, **562**, A77
Hénault-Brunet, V., Evans, C.J., Sana, H. et al. (2012), A&A, **546**, A73
Hillenbrand, L.A. & Hartmann, L.W. (1998), ApJ, **492**, 540
Hillenbrand, L.A., Strom, S.E., Calvet, N. et al. (1998), AJ, **116**, 1816
Hills, J.G. (1980), ApJ, **235**, 986
Hollenbach, D., Johnstone, D., Lizano, S. et al. (1994), ApJ, **428**, 654
Holman, M.J. & Payne, M.J. (2016a), AJ, **152**, 80
Holman, M.J. & Payne, M.J. (2016b), AJ, **152**, 94
Huff, E.M. & Stahler, S.W. (2006), ApJ, **644**, 355
Ida, S., Larwood, J., & Burkert, A. (2000), ApJ, **528**, 351
Janes, K., Barnes, S.A., Meibom, S. et al. (2013), AJ, **145**, 7
Jensen, E.L.N. & Akeson, R. (2014), Nature, **511**, 567
Jílková, L., Portegies Zwart, S., Pijloo, T. et al. (2015), MNRAS, **453**, 3157
Jiménez-Torres, J.J., Pichardo, B., Lake, G. et al. (2011), MNRAS, **418**, 1272
Johnstone, D., Hollenbach, D., & Bally, J. (1998), ApJ, **499**, 758
Johnstone, D., Matsuyama, I., McCarthy, I.G. et al. (2004), in G. Garcia-Segura, G. Tenorio-Tagle, J. Franco, & H.W. Yorke (eds.), *Revista Mexicana de Astronomia y Astrofisica Conference Series*, vol. 22 of *Revista Mexicana de Astronomia y Astrofisica Conference Series*, pp. 38–41

Kaczmarek, T. (2012), *The Evolution of Binary Populations in Young Star Clusters: From the ONC to OB associations.*, Ph.D. thesis, Universität zu Köln
Kaczmarek, T., Olczak, C., & Pfalzner, S. (2011), A&A, **528**, A144
Kant, I. (1755), *Allgemeine Naturgeschichte und Theorie des Himmels oder Versuch von der Verfassung und dem mechanischen Ursprunge des ganzen Weltgebudes nach Newtonischen Grundstzen abgehandelt.*, Knigsberg und Leipzig
Kenyon, S.J. & Bromley, B.C. (2004), Nature, **432**, 598
Kenyon, S.J. & Bromley, B.C. (2016), ApJ, **825**, 33
King, I. (1962), AJ, **67**, 471
Klahr, H.H. & Bodenheimer, P. (2003), ApJ, **582**, 869
Kobayashi, H. & Ida, S. (2001), ICARUS, **153**, 416
Köhler, R., Petr-Gotzens, M.G., McCaughrean, M.J. et al. (2006), A&A, **458**, 461
Kraus, A.L. & Hillenbrand, L.A. (2007), AJ, **134**, 2340
Kroupa, P. (2002), Science, **295**, 82
Kroupa, P., Aarseth, S., & Hurley, J. (2001), MNRAS, **321**, 699
Kroupa, P., Petr, M.G., & McCaughrean, M.J. (1999), New Astronomy, **4**, 495
Krumholz, M.R., Bate, M.R., Arce, H.G. et al. (2014), Protostars and Planets VI, 243
Krumholz, M.R. & McKee, C.F. (2005), ApJ, **630**, 250
Krumholz, M.R. & Tan, J.C. (2007), ApJ, **654**, 304
Kuhn, M.A., Feigelson, E.D., Getman, K.V. et al. (2014), ApJ, **787**, 107
Lada, C.J. & Lada, E.A. (2003), ARA&A, **41**, 57
Lada, C.J., Margulis, M., & Dearborn, D. (1984), ApJ, **285**, 141
Lamers, H.J.G.L.M. & Gieles, M. (2008), in A. de Koter, L.J. Smith, & L.B.F.M. Waters (eds.), *Mass Loss from Stars and the Evolution of Stellar Clusters*, vol. 388 of *Astronomical Society of the Pacific Conference Series*, p. 367
Larson, R.B. (1969), MNRAS, **145**, 271
Larson, R.B. (2003), Reports on Progress in Physics, **66**, 1651
Lee, J.E., Bergin, E.A., & Lyons, J.R. (2008), Meteoritics and Planetary Science, **43**, 1351
Leigh, N.W.C., Giersz, M., Marks, M. et al. (2015), MNRAS, **446**, 226
Li, G. & Adams, F.C. (2015), MNRAS, **448**, 344
Li, G. & Adams, F.C. (2016), ApJ, **823**, L3
Lichtenberg, T., Parker, R.J., & Meyer, M.R. (2016), MNRAS, **462**, 3979
Lissauer, J.J. (2001), Nature, **409**, 23
Livingston, J.H., Dai, F., Hirano, T. et al. (2018), AJ, **155**
Lovis, C. & Mayor, M. (2007), A&A, **472**, 657
Lucas, P.W., Roche, P.F., Allard, F. et al. (2001), MNRAS, **326**, 695
Lüghausen, F., Parmentier, G., Pflamm-Altenburg, J. et al. (2012), MNRAS, **423**, 1985
Luu, J.X. & Jewitt, D.C. (2002), ARA&A, **40**, 63
Lynden-Bell, D. & Pringle, J.E. (1974), MNRAS, **168**, 603
MacPherson, G.J., Davis, A.M., & Zinner, E.K. (1995), Meteoritics, **30**, 365
Malavolta, L., Nascimbeni, V., Piotto, G. et al. (2016), A&A, **588**, A118
Malmberg, D. & Davies, M.B. (2009), MNRAS, **394**, L26
Malmberg, D., Davies, M.B., & Heggie, D.C. (2011), MNRAS, **411**, 859
Mamajek, E.E. (2009), in T. Usuda, M. Tamura, & M. Ishii (eds.), *American Institute of Physics Conference Series*, vol. 1158 of *American Institute of Physics Conference Series*,

pp. 3–10
Mann, A.W., Gaidos, E., Mace, G.N. et al. (2016a), ApJ, **818**, 46
Mann, A.W., Newton, E.R., Rizzuto, A.C. et al. (2016b), AJ, **152**, 61
Martínez-Barbosa, C.A., Brown, A.G.A., Boekholt, T. et al. (2016), MNRAS, **457**, 1062
Matsuyama, I., Johnstone, D., & Hartmann, L. (2003), ApJ, **582**, 893
Matzner, C.D. & McKee, C.F. (2000), ApJ, **545**, 364
Mayer, L., Wadsley, J., Quinn, T. et al. (2005), MNRAS, **363**, 641
Mayor, M. & Queloz, D. (1995), Nature, **378**, 355
McCaughrean, M.J. & O'dell, C.R. (1996), AJ, **111**, 1977
McCaughrean, M.J. & Stauffer, J.R. (1994), AJ, **108**, 1382
McKee, C.F. & Ostriker, E.C. (2007), ARA&A, **45**, 565
McMillan, S.L.W., Vesperini, E., & Portegies Zwart, S.F. (2007), ApJ, **655**, L45
Meibom, S., Torres, G., Fressin, F. et al. (2013), Nature, **499**, 55
Melioli, C. & de Gouveia dal Pino, E.M. (2006), A&A, **445**, L23
Melita, M.D., Larwood, J., Collander-Brown, S. et al. (2002), in B. Warmbein (ed.), *Asteroids, Comets, and Meteors: ACM 2002*, vol. 500 of *ESA Special Publication*, pp. 305–308
Mengel, S. & Tacconi-Garman, L.E. (2007), A&A, **466**, 151
Meru, F. & Bate, M.R. (2011), MNRAS, **410**, 559
Milone, A.P., Piotto, G., Bedin, L.R. et al. (2012), A&A, **540**, A16
Moeckel, N. & Bally, J. (2007), ApJ, **656**, 275
Moeckel, N. & Bonnell, I.A. (2009), MNRAS, **400**, 657
Mohanty, S., Greaves, J., Mortlock, D. et al. (2013), ApJ, **773**, 168
Morbidelli, A. (2005), ArXiv e-prints: astro-ph/0512256
Morbidelli, A., Brown, M.E., & Levison, H.F. (2003), Earth Moon and Planets, **92**, 1
Morbidelli, A. & Levison, H.F. (2004), AJ, **128**, 2564
Morbidelli, A., Lunine, J.I., O'Brien, D.P. et al. (2012), Annual Review of Earth and Planetary Sciences, **40**, 251
Mordasini, C., Alibert, Y., & Benz, W. (2009), A&A, **501**, 1139
Mordasini, C., Alibert, Y., Benz, W. et al. (2012), A&A, **541**, A97
Moynier, F., Blichert-Toft, J., Wang, K. et al. (2011), ApJ, **741**, 71
Mustill, A.J., Raymond, S.N., & Davies, M.B. (2016), MNRAS, **460**, L109
Nicholson, R.B. & Parker, R.J. (2017), MNRAS, **464**, 4318
Nordlander, T., Rickman, H., & Gustafsson, B. (2017), A&A, **603**, A112
O'dell, C.R. (1998), AJ, **115**, 263
O'dell, C.R., Wen, Z., & Hu, X. (1993), ApJ, **410**, 696
Olczak, C., Kaczmarek, T., Harfst, S. et al. (2012), ApJ, **756**, 123
Olczak, C., Pfalzner, S., & Eckart, A. (2008), A&A, **488**, 191
Olczak, C., Pfalzner, S., & Eckart, A. (2010), A&A, **509**, A63
Olczak, C., Pfalzner, S., & Spurzem, R. (2006), ApJ, **642**, 1140
Olczak, C., Spurzem, R., & Henning, T. (2011), A&A, **532**, A119
Ouellette, N., Desch, S.J., & Hester, J.J. (2007), ApJ, **662**, 1268
Owen, J.E., Clarke, C.J., & Ercolano, B. (2012), MNRAS, **422**, 1880
Parker, R.J. & Dale, J.E. (2016), MNRAS, **456**, 1066
Parker, R.J., Dale, J.E., & Ercolano, B. (2015), MNRAS, **446**, 4278
Parker, R.J. & Goodwin, S.P. (2011), MNRAS, **411**, 891

Parker, R.J., Goodwin, S.P., & Allison, R.J. (2011), MNRAS, **418**, 2565
Parker, R.J., Lichtenberg, T., & Quanz, S.P. (2017), MNRAS, **472**, L75
Parmentier, G. & Pfalzner, S. (2013), A&A, **549**, A132
Paulson, D.B., Cochran, W.D., & Hatzes, A.P. (2004), AJ, **127**, 3579
Pelupessy, F.I. & Portegies Zwart, S. (2012), MNRAS, **420**, 1503
Perryman, M.A.C., Brown, A.G.A., Lebreton, Y. et al. (1998), A&A, **331**, 81
Pfalzner, S. (2004), ApJ, **602**, 356
Pfalzner, S. (2009), A&A, **498**, L37
Pfalzner, S. (2011), A&A, **536**, A90
Pfalzner, S. (2013), A&A, **549**, A82
Pfalzner, S., Bhandare, A., & Vincke, K. (2018), A&A, **610**, A33
Pfalzner, S., Davies, M.B., Gounelle, M. et al. (2015a), Physica Scripta, **90**, 6, 068001
Pfalzner, S. & Kaczmarek, T. (2013a), A&A, **555**, A135
Pfalzner, S. & Kaczmarek, T. (2013b), A&A, **559**, A38
Pfalzner, S., Kirk, H., Sills, A. et al. (2016), A&A, **586**, A68
Pfalzner, S. & Olczak, C. (2007), A&A, **462**, 193
Pfalzner, S., Olczak, C., & Eckart, A. (2006), A&A, **454**, 811
Pfalzner, S., Steinhausen, M., & Menten, K. (2014), ApJ, **793**, L34
Pfalzner, S., Umbreit, S., & Henning, T. (2005a), ApJ, **629**, 526
Pfalzner, S., Vincke, K., & Xiang, M. (2015b), A&A, **576**, A28
Pfalzner, S., Vogel, P., Scharwächter, J. et al. (2005b), A&A, **437**, 967
Pietrinferni, A., Cassisi, S., Salaris, M. et al. (2004), ApJ, **612**, 168
Plummer, H.C. (1911), MNRAS, **71**, 460
Porras, A., Christopher, M., Allen, L. et al. (2003), AJ, **126**, 1916
Portegies Zwart, S.F. (2009), ApJ, **696**, L13
Portegies Zwart, S.F. (2016), MNRAS, **457**, 313
Portegies Zwart, S.F., McMillan, S.L.W., & Gieles, M. (2010), ARA&A, **48**, 431
Proszkow, E.M. & Adams, F.C. (2009), The Astrophysical Journal Supplement Series, **185**, 486
Quinn, S.N., White, R.J., Latham, D.W. et al. (2012), ApJ, **756**, L33
Quinn, S.N., White, R.J., Latham, D.W. et al. (2014), ApJ, **787**, 27
Raghavan, D., McAlister, H.A., Henry, T.J. et al. (2010), ApJS, **190**, 1
Richer, H.B., Fahlman, G.G., Rosvick, J. et al. (1998), ApJ, **504**, L91
Rickman, H., Froeschlé, C., Froeschlé, C. et al. (2004), A&A, **428**, 673
Rosotti, G.P., Dale, J.E., de Juan Ovelar, M. et al. (2014), MNRAS, **441**, 2094
Rosotti, G.P., Dale, J.E., de Juan Ovelar, M. et al. (2018), MNRAS, **473**, 3223
Salpeter, E.E. (1955), ApJ, **121**, 161
Sarajedini, A., Dotter, A., & Kirkpatrick, A. (2009), ApJ, **698**, 1872
Sato, B., Izumiura, H., Toyota, E. et al. (2007), ApJ, **661**, 527
Scally, A. & Clarke, C. (2001), MNRAS, **325**, 449
Scally, A. & Clarke, C. (2002), MNRAS, **334**, 156
Scally, A., Clarke, C., & McCaughrean, M.J. (2005), MNRAS, **358**, 742
Schwamb, M.E., Brown, M.E., Rabinowitz, D.L. et al. (2010), ApJ, **720**, 1691
Schweizer, F. (2006), ArXiv Astrophysics e-prints
Scilla, D. (2016), in *Journal of Physics Conference Series*, vol. 703 of *Journal of Physics*

Conference Series, p. 012002
See, T.J.J. (1909), Proceedings of the American Philosophical Society, **48**, 191, 119, URL http://www.jstor.org/stable/983817
Shankman, C., Kavelaars, J.J., Lawler, S.M. et al. (2017), AJ, **153**, 63
Shu, F.H., Adams, F.C., & Lizano, S. (1987), ARA&A, **25**, 23
Smith, R., Fellhauer, M., Goodwin, S. et al. (2011), MNRAS, **414**, 3036
Soares, J.S. & Gomes, R.S. (2013), A&A, **553**, A110
Spurzem, R. (1999), Journal of Computational and Applied Mathematics, **109**, 407
Spurzem, R., Giersz, M., Heggie, D.C. et al. (2009), ApJ, **697**, 458
Steinhausen, M., Olczak, C., & Pfalzner, S. (2012), A&A, **538**, A10
Steinhausen, M. & Pfalzner, S. (2014), A&A, **565**, A32
Stolte, A., Morris, M.R., Ghez, A.M. et al. (2010), ApJ, **718**, 810
Störzer, H. & Hollenbach, D. (1999), ApJ, **515**, 669
Swedenborg, E. (1734), *Principia Vol. 1 - Opera Philosophica et Mineralia*, Royal Swedish Academy of Science, Stockholm
Tang, H. & Dauphas, N. (2012), Earth and Planetary Science Letters, **359**, 248
Testi, L., Birnstiel, T., Ricci, L. et al. (2014), Protostars and Planets VI, 339
Trujillo, C.A. & Sheppard, S.S. (2014), Nature, **507**, 471
Tutukov, A.V. (1978), A&A, **70**, 57
Vicente, S.M. & Alves, J. (2005), A&A, **441**, 195
Vincke, K., Breslau, A., & Pfalzner, S. (2015), A&A, **577**, A115
Vincke, K. & Pfalzner, S. (2016), ApJ, **828**, 48
Vincke, K. & Pfalzner, S. (2018), ApJ, **868**, 1, 1
Vorobyov, E.I. (2011), ApJ, **729**, 146
Vorobyov, E.I. (2016), A&A, **590**, A115
Weidenschilling, S.J. (1977), MNRAS, **180**, 57
Whipple, F.L. (1972), in A. Elvius (ed.), *From Plasma to Planet*, p. 211
Williams, J.P., Blitz, L., & McKee, C.F. (2000), in *Protostars and Planets IV (Book - Tucson: University of Arizona Press; eds Mannings, V., Boss, A.P., Russell, S. S.), p. 97*, p. 97
Williams, J.P. & Gaidos, E. (2007), ApJ, **663**, L33
Winn, J.N. & Fabrycky, D.C. (2015), ARA&A, **53**, 409
Winter, A.J., Clarke, C.J., Rosotti, G. et al. (2018a), MNRAS, **475**, 2314
Winter, A.J., Clarke, C.J., Rosotti, G. et al. (2018b), MNRAS, 949
Wolszczan, A. & Frail, D.A. (1992), Nature, **355**, 145
Xiang-Gruess, M. (2016), MNRAS, **455**, 3086
Yang, W., Bi, S., Meng, X. et al. (2013), ApJ, **776**, 112
Zanazzi, J.J. & Lai, D. (2018), MNRAS, **473**, 603
Zapatero Osorio, M.R., Béjar, V.J.S., Martín, E.L. et al. (2001), in R.J. Garcia Lopez, R. Rebolo, & M.R. Zapaterio Osorio (eds.), *11th Cambridge Workshop on Cool Stars, Stellar Systems and the Sun*, vol. 223 of *Astronomical Society of the Pacific Conference Series*, p. 70
Zheng, X., Kouwenhoven, M.B.N., & Wang, L. (2015), MNRAS, **453**, 2759
Zinnecker, H. & Yorke, H.W. (2007), ARA&A, **45**, 481
Zwicky, F. (1953), PASP, **65**, 205

5 Summary

The work presented herein investigates the influence of the association and cluster environment on the disc size reduction, and in extreme cases on the disc destruction, by stellar fly-bys. Therefore, different types of young, massive ($10^2 - 10^5$ $M_\odot$) associations and stellar clusters of different densities were simulated to quantify their effect on protoplanetary discs. The trajectories of each star were modelled using the code NBody6++ GPU, and the gravitational interactions between the stellar members were recorded. In contrast to previous studies, the simulations included the mass of the residual gas within the system, the gas expulsion, and the following expansion phase. Therefore, it was possible to study the importance of the dynamical evolution of the environment for the development of protoplanetary discs. The fly-by history was used to calculate the resulting size of protoplanetary discs around the stars after each interaction. Here, not only coplanar and prograde, but also randomly orientated fly-bys were considered.

The key findings are the following:

- Fly-bys in young, massive associations and clusters leave an imprint on the protoplanetary discs and planetary systems of their members: a denser association/cluster yields smaller discs.
- In principle, the median disc size in stellar clusters could be more than a factor of *ten* smaller than in less dense associations: $\approx 10 - 20$ AU versus ≈ 400 AU for the ONC, if the disc size was initially larger than 400 AU. The small discs in compact clusters and the much larger ones in associations are in very good agreement with observed discs and planetary systems in such environments.
- Fly-bys are capable of destroying discs completely, leaving behind very small structures (≤ 10 AU) with only little mass, which do not resemble discs, but rather cones or spheres. In dense stellar clusters, up to about half of all discs (47%) are reduced to such a state by fly-bys, compared to 6% in the densest investigated association.
- Discs in the environment's core are generally smaller than in the outskirts.
- Based on the assumption that the drop in mass density in the solar system was induced by a fly-by, it was found that the Sun was most probably part of either a very dense association, containing at least 10 000 stars, or a dense stellar cluster,

containing between 10 000 and 32 000 stars. These environments produce most solar-system analogues, which are discs surrounding solar-like stars ($0.8 - 1.2$ $M_\odot$) with sizes between 30 and 50 AU.

6 Conclusion

The lifetime of protoplanetary discs – and thus the formation timescale of planetary systems – is usually determined by looking at observed disc fractions in stellar groups. However, it is crucial to carefully distinguish between disc fractions in associations and in clusters, because the environment significantly influences the number of discs which survive the first few Myr of cluster evolution.

Protoplanetary discs in clusters are prone to destruction through stellar fly-bys: almost half of them do not survive the first few Myr of cluster development. In contrast, only very few discs are destroyed in the most massive associations ($\approx 6\%$), which makes them more suitable sites for planet formation. Therefore, restricting planet-formation timescales by compiling data from both types of environments is problematic, because discs in associations are less prone to externally induced destruction, see also Fig. 1.6 and Pfalzner et al. (2014). In addition, protoplanetary discs in clusters are reduced to considerably smaller disc sizes ($10 - 20$ AU) than in associations due to gravitational interactions alone. This changes the structure of eventually forming planetary systems.

The presented simulations show that in stellar clusters few but strong fly-bys are sufficient to reduce the disc size to a few tens of AU. Therefore, predictions can be made that planetary systems forming in such environments are most likely smaller than 10 AU. Systems as large as 100 AU should be extremely rare.

This is in very good agreement with observations, as all planetary systems found in open clusters (the successors of young, massive clusters) are smaller than 10 AU, see Table 1.1. However, the statistics are still rather low, as only 23 planets have been detected in open clusters so far. Future observations with, for example, ALMA should be tested against this hypothesis.

In the case of associations, the majority of fly-bys influencing protoplanetary discs take place in the first $1 - 2$ Myr. After that, planets can form almost unperturbed by the environment, because the cluster density drops significantly after gas expulsion and thus only few close fly-bys happen. The size of discs in associations is more than a factor of ten larger than in dense clusters, thus, planetary systems with sizes of up to a few hundreds of AU seem probable. As a result, field stars should often be surrounded by planetary systems that extend to 100 AU or more, in contrast to planetary systems in clusters.

In summary, the gravitational interactions between stars in their birth environment, to some extent, determine how many planetary systems can form and they are decisive for the size of the planetary system: clusters yield systems of a few tens of AU at most, whereas much larger systems of several hundreds of AU are likely common in associations. Although additional effects, like for example photoevaporation, play an important role, the disc sizes provided in this work are in very good agreement with observationally found disc sizes and sizes of planetary systems, which underlines the importance of stellar fly-bys in planet formation. Future observations will yield better statistics for planetary systems in associations and clusters and can easily be tested against the data above.

Contribution

The body of this thesis are three publications, in all of which I acted as the first author: Vincke et al. (2015); Vincke & Pfalzner (2016), and Vincke & Pfalzner (2018). The basis of the work in all papers is a two-step approach. First, young, massive stellar associations and clusters were modelled, containing between 1 000 and 32 000 stars. This was done with the help of the code NBody6++ GPU, which was extended by our group to track the properties of stellar fly-bys (Olczak et al., 2012). For each publication a different type of simulation was performed: first embedded associations (Vincke et al., 2015), followed by evolving associations including the gas mass (Vincke & Pfalzner, 2016), and finally evolving clusters (Vincke & Pfalzner, 2018). For each set of initial parameters described in the work here, I carried out a few up to several hundreds of simulations using the already existing NBody6++ GPU code and its extensions by Christoph Olczak and Manuel Steinhausen.

The data obtained from these simulations was carefully reviewed and then, in a second step, analysed with the help of a diagnostic tool. I extended the framework of this already existing tool, including the disc-size formula by Breslau et al. (2014). For each fly-by event recorded in the NBody simulations, the disc size was calculated. I added routines to the diagnostic tool for each problem and statistical statement discussed in the publications above, obtaining statistically meaningful and self-consistent results.

To determine the disc sizes after randomly orientated fly-bys in associations and clusters, I re-analysed the data of Bhandare et al. (2016). Additional disc-simulation data to the one of Bhandare et al. (2016) was provided by Asmita Bhandare, which I then evaluated, finding a new fit formula which provides a more accurate description of disc sizes after close and *distant* fly-bys. This fit formula is given in equation (3) of Vincke & Pfalzner (2018) and was also added to the diagnostic tool as described above. The newly obtained results were again analysed and put into context with cluster, stellar, and fly-by parameters using the added diagnostic described above.

All results were thoroughly described in each publication in order to present them in a self-consistent and comprehensible way. The final versions of those papers were then sent to the reputable journals *Astronomy and Astrophysics* (Vincke et al., 2015) and *The Astrophysical Journal* (Vincke & Pfalzner, 2016, 2018).

Acknowledgements

First of all, I would like to thank my supervisor, Prof. Dr. Susanne Pfalzner, for giving me the opportunity to join the SPG and to write this thesis. The support she has offered me and every member of our group has been extraordinary and I am grateful for her guidance and her commitment.

I also would like to thank Prof. Dr. Karl Menten, the Max Planck Institute of Radio Astronomy in Bonn, and the Max Planck Society for their hospitality and their financial support.

I would like to express my gratitude to the whole SPG for making me feel part of the group from day one: Christina Korntreff, Manuel Steinhausen, Andreas Breslau, Mai Xiang, and Asmita Bhandare. It was a pleasure to work with you and I appreciate all the help you offered and constructive discussions we had. A special thanks goes to Andreas Breslau, for teaching me all kinds of tricks, which made life with linux, latex, gnuplot, fortran, and computers in general a lot easier – and for reminding me to "kill my Valentine".

I had the pleasure to supervise the best Master students I can think of: Mai Xiang and Asmita Bhandare. Thank you for your many new ideas and different perspectives, as well as for the wonderful time we had outside the office.

I am indebted to Rebecca Boll, Asmita Bhandare, Andreas Breslau, and Dennis Kütemeier for proof-reading this thesis. Despite being very busy, they managed to find time to get rid of all my weird sentences and typos.

Thank you, Rebecca, for asking the right questions at the right time, no matter how uncomfortable they were. I am lucky to have a friend like you.

I would like to express my deepest gratitude to my family, who unconditionally supported me in the idea of studying physics and writing this thesis. Thank you for always believing in me and for having my back. Without you I would not be the person I am today.

Last, but not least, I would like to thank the person, who stood by my side from day one, went through all the ups and downs with me, and who always managed to make me smile. Thank you for believing in me. Always.

This research has made use of the Exoplanet Orbit Database and the Exoplanet Data Explorer at exoplanets.org.

Erklärung

Ich versichere, dass ich die von mir vorgelegte Dissertation selbständig angefertigt, die benutzten Quellen und Hilfsmittel vollständig angegeben und die Stellen der Arbeit – einschließlich Tabellen, Karten und Abbildungen –, die anderen Werken im Wortlaut oder dem Sinn nach entnommen sind, in jedem Einzelfall als Entlehnung kenntlich gemacht habe; dass diese Dissertation noch keiner anderen Fakultät oder Universität zur Prüfung vorgelegen hat; dass sie – abgesehen von angegebenen Teilpublikationen – noch nicht veröffentlicht worden ist, sowie, dass ich eine solche Veröffentlichung vor Abschluss des Promotionsverfahrens nicht vornehmen werde. Die Bestimmungen der Promotionsordnung sind mir bekannt. Die von mir vorgelegte Dissertation ist von Prof. Dr. Susanne Pfalzner betreut worden.

Schwerte, den 19.07.2019

(Kirsten Vincke)